

# **Modeling of OLED Degradation for Prediction and Compensation of AMOLED Aging Artifacts**

Dissertation  
zur Erlangung des Grades  
des Doktors der Ingenieurwissenschaften  
der Naturwissenschaftlich-Technischen Fakultät  
der Universität des Saarlandes

von  
Xingtong Jiang

Saarbrücken  
2018

Tag des Kolloquiums: 07.05.2019

Dekan: Univ.-Prof. Dr. rer. nat. G. Kickelbick

Mitglieder des Prüfungsausschusses:

Vorsitzender: Univ.-Prof. Dr.-Ing. Matthias Nienhaus

Berichterstattender: Univ.-Prof. Dr.-Ing. Chihao Xu

Berichterstattender: Univ.-Prof. Dr.-Ing. Michael Möller

Akademischer Mitarbeiter: Dr. Tillman Sauerwald

## Acknowledgements

I hereby express my sincere gratitude to all those, who have made contributions to this work, both academically as well as personally.

- **Prof. Dr.-Ing Chihao Xu** for giving me the opportunity to carry out this research, pursue my doctoral degree, and work as a science researcher in the Institute of Microelectronics (Lehrstuhl für Mikroelektronik, LME). I am wholeheartedly thankful for his continuous guidance, encouragement and support throughout this study, and great help in my daily life in Germany.
- **Prof. Dr.-Ing Michael Möller** for his willingness and patience to examine this dissertation.
- My colleagues also as my dear friends in LME: **Michael Grüning, Maxim Schmidt, Julian Ritter, Pascal Volkert, Daniel Schäfer, Qiang Fu, Santosh Palayam,** and **Shreeja Mani** (proofreading). Thank you all for the discussions and cooperation, kind understanding and support throughout my research period. Thanks for the enjoyable journey together in the last few years.
- Secretary in LME: **Mrs. Brigitte Vogel-Schendel, Mrs. Silke Maas** for their help when I encountered difficulties, such as interaction in German, during my study and living in Germany.
- **CSC** (China Scholarship Council) for providing a four-year scholarship and covering my living during this study.
- **My parents and my sisters** for their countless and endless support in my whole life. My dear **Xialin Wang** for being with me all the time.



## **Abstract**

Degradation is still the most challenging issue for OLED, which causes the image-sticking artifact on AMOLED displays and limits their lifetime. To overcome the demerit, OLED degradation is modeled in this thesis, and compensation based on the models is applied for AMOLEDs.

A data-counting model is firstly developed to quantitatively evaluate the degradation on OLEDs, with consideration of the accumulation stress during operation. An electro-optical model is further built, based on an equivalent circuit. It can simulate the electro-optical characteristic (I-V, Eff-V) and the degradation behaviors in aging process. Besides, the correlation model is aimed to derive the current efficiency decay with measurable electrical values, delivering more dependable results at strongly aged state.

The prediction and compensation are implemented based on developed models. The results show that the models exactly predict the efficiency decay during operation. The image-sticking aging artifact on AMOLED can be suppressed by applying compensation, so that the display lifetime is extended.

## **Zusammenfassung**

Durch das Einbrennen von Bildern in AMOLED Displays wird deren Lebensdauer verringert; dieser Qualitätsverlust stellt nach wie vor die größte Herausforderung für die OLED Technologie dar. In dieser Thesis wird die Degradation der OLEDs modelliert und eine Kompensierung anhand der Modelle erreicht.

Zunächst wurde ein Data-counting Modell entwickelt, um die Degradation von OLEDs unter Berücksichtigung der akkumulierten Belastung während des Betriebs quantitativ zu bewerten. Des Weiteren wurde ein elektro-optisches Modell entwickelt, das auf einem äquivalenten Schaltungsmodell basiert. Es kann die elektro-optischen Eigenschaft (I-V, Eff-V) und das Degradationsverhalten im Alterungsprozess simulieren. Außer den beiden Modellen wird noch ein Korrelationsmodell entwickelt, das darauf abzielt, die Abnahme der Stromeffizienz aus den messbaren elektrischen Werten abzuleiten. Dieses Modell liefert im stark gealterten Zustand zuverlässigere Ergebnisse.

Aufbauend auf die entwickelten Modelle wurden die Vorhersage und die Kompensierung implementiert. Die Ergebnisse zeigen, dass die Modelle den Effizienzverlust während des Betriebes genau vorhersagen. Das Einbrennen des Bildes in das AMOLED-Display kann durch das Anwenden der Kompensierung unterdrückt werden, so dass die Lebensdauer des Displays verlängert wird.



## Table of Contents

<b>1</b>	<b>Introduction .....</b>	<b>1</b>
1.1	Background .....	1
1.2	Motivation .....	2
1.3	Research goals.....	5
1.4	Outline of this thesis.....	5
<b>2</b>	<b>Theory and Basic principles .....</b>	<b>7</b>
2.1	Organic Light-emitting Diodes .....	7
2.1.1	Working principles.....	7
2.1.2	Light emission efficiency.....	10
2.2	OLED Degradation .....	12
2.2.1	Degradation in electrical characteristic.....	13
2.2.2	Degradation in optical characteristic .....	14
2.2.3	Differential aging .....	16
2.3	AMOLED Technology.....	17
2.3.1	Active matrix addressing .....	17
2.3.2	Digital driving scheme .....	17
<b>3</b>	<b>Characterization and Degradation behaviors.....</b>	<b>21</b>
3.1	Test Arrangements .....	21
3.1.1	OLED devices tested.....	21
3.1.2	Measurement setup .....	23
3.2	Electrical-optical Characterization.....	24
3.2.1	Electrical characteristic.....	24
3.2.2	Optical characteristic .....	25
3.2.3	Comparison of devices.....	27

## Table of Content

---

3.2.4	Chromaticity .....	30
3.2.5	Temperature dependency .....	31
3.3	Degradation Behaviors .....	35
3.3.1	Aging test procedure .....	35
3.3.2	Decay of electrical characteristic .....	36
3.3.3	Decay of optical characteristic .....	37
3.3.4	Dependency on driving conditions .....	39
3.3.5	Color shift .....	42
3.4	Conclusion.....	43
<b>4</b>	<b>Data-counting Model.....</b>	<b>45</b>
4.1	Degradation of current efficiency .....	45
4.2	Current-amplitude dependency of degradation .....	49
4.3	Thermal dependence of degradation .....	52
4.4	Unified degradation profile .....	55
4.5	Discussion .....	58
<b>5</b>	<b>Electro-optical Model.....</b>	<b>61</b>
5.1	Structure and equivalent circuit.....	61
5.2	Electrical and optical characteristic.....	64
5.3	Modeling of degradation behaviors.....	68
5.4	Analysis with simulation.....	73
5.5	Conclusion.....	75
<b>6</b>	<b>Correlation Model .....</b>	<b>77</b>
6.1	Correlation between efficiency decay and current drift .....	78
6.2	Linear correlation profile .....	79
6.3	Partial correlation .....	80

---

6.4	Correlation for aging parameter .....	82
6.5	Conclusion.....	84
<b>7</b>	<b>Prediction and Compensation .....</b>	<b>87</b>
7.1	Validation on OLED devices .....	87
7.1.1	Data-counting model.....	87
7.1.2	Electro-optical model.....	92
7.2	Compensation on digital AMOLED display.....	96
7.2.1	Digital AMOLED prototype and test setup .....	96
7.2.2	Compensation algorithm.....	100
7.2.3	Validation results .....	104
<b>8</b>	<b>Conclusion and Outlook.....</b>	<b>109</b>
8.1	Conclusion.....	109
8.2	Outlook.....	113
<b>9</b>	<b>Appendix.....</b>	<b>115</b>
<b>10</b>	<b>List of abbreviations.....</b>	<b>119</b>
<b>11</b>	<b>List of figures .....</b>	<b>121</b>
<b>12</b>	<b>References.....</b>	<b>127</b>
<b>13</b>	<b>Publications .....</b>	<b>133</b>



# 1 Introduction

## 1.1 Background

Nowadays, the electronic display is one of the most important and effective ways to access information. They are widely used on mobile phones, computers, automobiles, and manufacturing industries. We are living around with lots and kinds of displays in day to day life. The display technology has developed in several generations, from CRT display in the last century to LCD display in around 2000, to recently the OLED display. Other technologies such as ePaper, LED display, and LCoS projection also play their roles in some specialized applications. For example, ePaper is suitable for reading, and LED display is adopted for outdoor signage.

Organic Light Emitting Diode (OLED) is a promising technology and becoming mainstream in recent years. The OLED display fulfils our growing demands for high-quality, thin, and flexible displays. It is widely penetrating the market from small to large size application, such as wearable devices (VR/AR or Smartwatch), Mobile phones, and TVs. Figure 1-1 shows some OLED display applications. In history, OLED technology experienced several stages of development: Tang and Van Slyke firstly developed the basic organic electroluminescent diodes in 1987 [Tang1987]; in around 2000, the passive matrix OLED product was developed for specialized applications (e.g. Pioneer for car); after 2010, Active-Matrix OLED display entered into the massive commercial stage (Samsung, LG). At present and looking into the future, OLED displays with high resolution, high luminance, a flexible substrate and longer lifetime are in demand. It is expected to have more potentials for near-eye displays (VR /AR), automotive (instrument cluster / central information display) or flexible/foldable smartphones.

To go far beyond LCD technology and dominate more markets, the OLED display should further improve its performance and reduce cost comparatively. A higher yield can help cut down the shipment price. Novel inkjet printing also provides the possibility to produce panels cost-effectively. For OLED performance, the adoption of phosphorescence or TADF materials can significantly improve device efficiency (IQE reach 100% in theory). To date, red and green

## 1. Introduction

---

Phosphorescence-OLED has been commercialized by UDC. Fluorescence blue OLED is adopted in displays for a longer lifetime.



Figure 1-1 OLED display applications including mobile phones, TVs, autos, VR/AR. (Photos from Reuters, OLED-info, and engadget.com)

### 1.2 Motivation

Besides efficiency, the lifetime is crucial for device performance. Unfortunately, OLED suffers from serious lifetime issue, compared to LCD or inorganic LEDs. OLED materials are unstable during operation. Over time, luminance on OLEDs will gradually decrease. The so-called image-sticking artifact is then observable, similar to the CRTs or plasma display. To solve the degradation issue, considerable effort has been taken in research over the last decades. With successive research and development of new materials and structures, the lifetime has been dramatically improved, as shown in figure 1-2. The fluorescent OLEDs achieved an acceptable lifetime ( $T_{1/2}$ ). The lifetime of red/green phosphorescent devices has also been comparable to fluorescent devices.

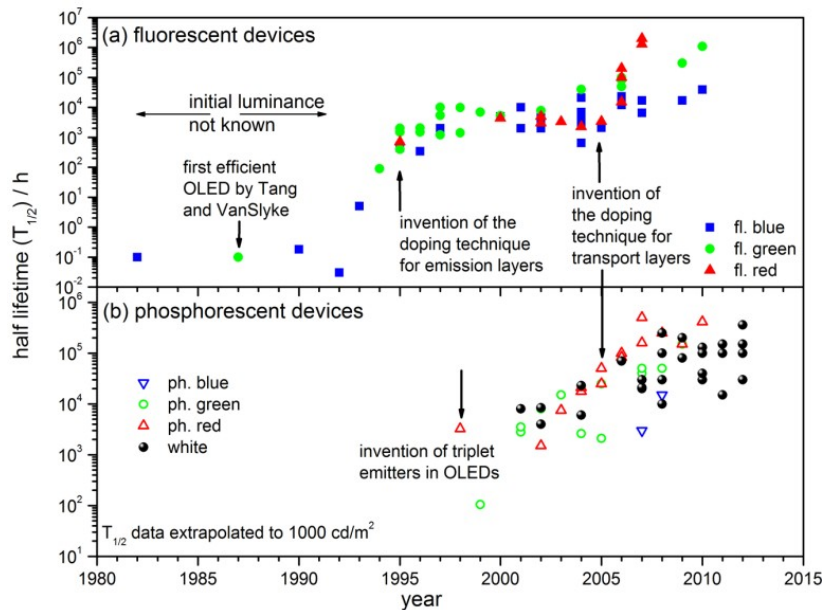


Figure 1-2 Lifetime improvement of OLEDs over the last decades: (a) fluorescent and (b) phosphorescent, including red, green, blue, and white OLEDs [Scholz2015].

### **Image-sticking problem**

Although OLED has been dramatically improved, it is still far away to fulfil our expectation for long lifetime, which is highly required for more application scenarios, such as automobile, TV, AR, or manufacturing industry. As we know, the lifetime of an OLED device is greatly influenced by its driving conditions. If devices are operated at higher luminance level (e.g. 500 nits) or high ambient temperature (e.g. 40°C), the lifetime will decline significantly. Thus, a tradeoff between lifetime and brightness have to be made in practice. Seriously, blue OLED has a very short lifetime among the three primary colors (phosphorescence is even worse than fluorescence). Differential degradation on pixels is then fatal to display. It is worth mentioning that the lifetime should be defined as  $T_{95}/T_{97}$ , instead of half lifetime  $T_{1/2}$ , due to the high sensitivity of human eyes to non-uniformity (just 3-5% tolerance). The lifetime of OLED panels today is still extremely low in this definition.

Due to differential aging on pixels, the well-known image-sticking artifact (also known as image retention or burn-in effect), commonly occurs on active emitting display, while an LCD, a passive emitting display technology, does not show such an artifact. This phenomenon was early found on CRT and plasma display, and now is visible on OLED display, as serious

drawback. The image-sticking artifact arises on display due to the differential aging of pixels. Some pixels are more stressed than others during usage, resulting in non-uniformity performance of pixels on panel, as described in figure 1-3. When an image is displayed on panel, the visible patterns formed by aged pixels will be observed.

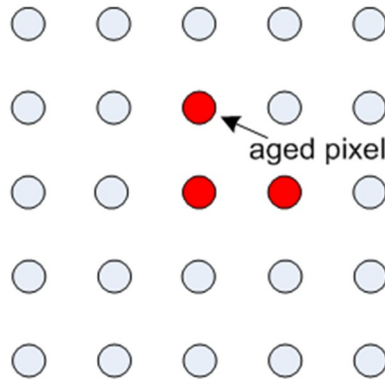


Figure 1-3 The differential aging of pixels on OLED panel. Red dots denote aged pixels (more stressed), and gray dots are pristine pixels (or less stressed).

For smartphones, the pixels for icons such as call, contact or message are overused, compared to others on the panel. After a period of operation, these patterns will stay on display, whatever image content is displayed. The image sticking artifact on AMOLED is as shown in figure 1-4. The panel, provided by Visionox, was stressed with some specific pattern (i.e. square/triangle) in our aging test to simulate the burn-in process.

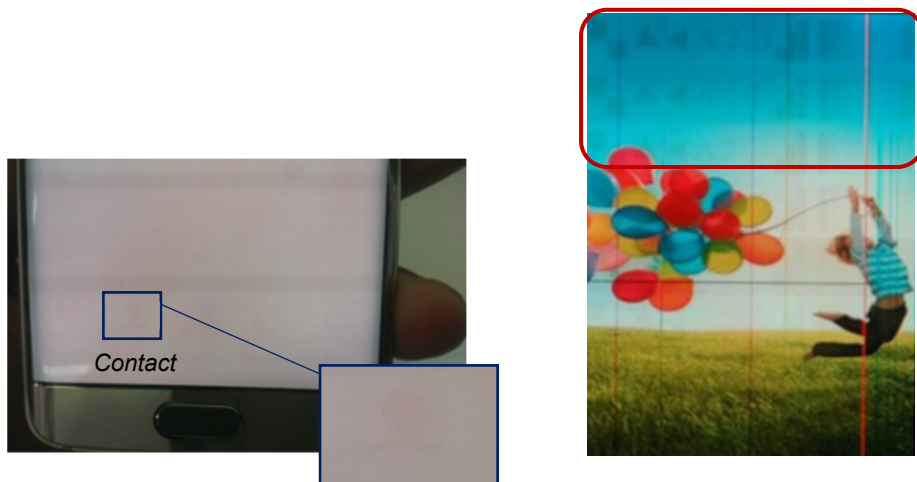


Figure 1-4 Image sticking artifact on Samsung Galaxy S6 (left) and on Visionox AMOLED panel (right).

### 1.3 Research goals

Thus, degradation is still the most challenging issue for OLED, which causes the image sticking artifact on AMOLED displays. To overcome this demerit, one method is to work on the chemical/physical front to improve the OLED lifetime. New materials/ structures should be developed continuously. However, the progress is modest. It is limited by the lack of understanding of the degradation mechanisms.

Another solution is the so-called aging compensation [Anton2004, Chen2012, Mats2008 and Lee2014]. Based on current OLED devices, the luminance loss of pixels will be compensated during operation, with compensation algorithm. The pixel-wise compensation can be implemented by optimizing driven data on pixels in controllers. The differential aging among pixels is alleviated, and image sticking artifact is thus suppressed.

For compensation, modelling of OLED degradation is necessary. It is required to predict the efficiency loss in operation. While the electrical values can be measured by an electronic unit within the display electronics, the luminance cannot be measured. The efficiency loss is indeed an indirectly measurable value in products. The challenge is how to build feasible models for degradation. The comprehensive physical model is still not available, due to limited understanding of internal degradation mechanisms, and complex dependence/interaction. The factors such as the driving-conditions, or the operation-point dependency, also impact the evaluation of degradation and should be considered in modeling.

In this thesis, modeling of OLED degradation is made for prediction and compensation of aging artifact on AMOLED display. Firstly, the experiments are carried out to characterize OLEDs and analyze the degradation behaviors. Based on these analyses, potential feasible models for degradation are developed. Finally, the proposed models are validated. Prediction and compensation based on these models are implemented.

### 1.4 Outline of this thesis

The thesis is organized to systematically present research procedurals for achieving the objectives. The outline is described as following. In chapter 2, the basic theory and principles regarding OLEDs and AMOLED display are presented. Chapter 3 shows the characterization

and degradation behaviors of OLEDs in the experiments. Subsequently, three modeling approaches for OLED degradation are proposed, including the data-counting model in chapter 4, the electro-optical model in chapter 5, and the correlation model in chapter 6. In chapter 7, prediction and compensation based on developed models are implemented on OLED devices and AMOLED display. Chapter 8 briefly summarizes the entire work and outlooks the continuous research in the future.

## 2 Theory and Basic principles

In this chapter, the theory and basic principles concerning organic light-emitting diodes and AMOLED are presented. Firstly, the working principles, as well as the light emission efficiency of OLEDs will be described. Subsequently, the OLED degradation in electrical and optical characteristic will be discussed. Thereafter, AMOLED technology will be introduced, including the active-matrix addressing and digital driving scheme.

### 2.1 Organic Light-emitting Diodes

#### 2.1.1 Working principles

Organic light-emitting diodes are electroluminescent organic semiconductor devices, in which the emission layer is an organic compound film that emits light in response to an electric current [Wik2018]. A basic OLED device consists of one organic layer sandwiched between two electrodes, all deposited layer by layer on a glass substrate, as shown in figure 2-1 (a). The indium tin oxide (ITO) which has electrical conductivity and optical transparency is commonly used as the anode film, while the metal with low working function is as the opaque cathode. With applying voltage, the flowing operation is resulted in the device, as figure 2-1 (b) shows: 1) Holes and electrons are injected from the electrodes, respectively, 2) the charge carriers are transported under electric field, 3) the excitons are formed with electron-hole pairs in the emission layer, 4) the excitons relax under the radiation of light. Holes and electrons from the anode and cathode are injected across the barrier into the adjacent organic film. Recombination on exciton spontaneously emits specific wavelength photon (light color), which correlates with the energy gap between the lowest unoccupied molecular orbital (LUMO) and the highest occupied molecular orbital (HOMO) level.

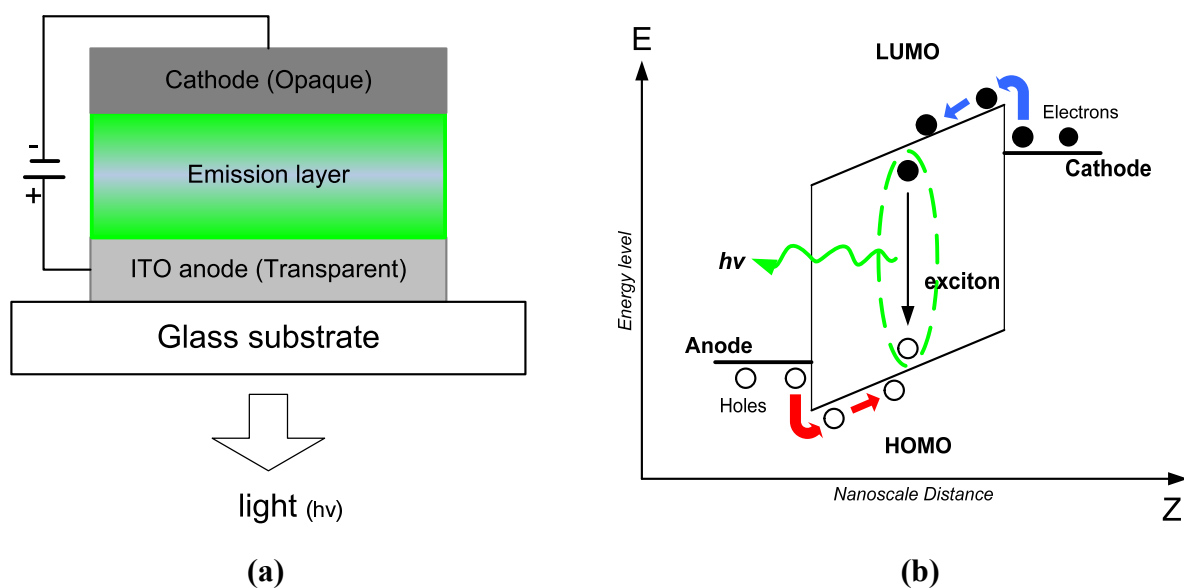


Figure 2-1 (a) Basic sandwich structure of an OLED device; (b) Simplified diagram of OLED device operation.

### The light emission mechanism

If an organic molecule is at the lowest possible energy with all electrons filled in bonding orbitals, it is in the ground state; at a higher energy level with any electron filled in antibonding orbitals, it is said to be in excited state [Wik.E2018]. The excited state is unstable. Through the recombination of a pair of hole and electron, in spontaneously emitting a photon, the organic molecule relaxes back to ground state.

The basic energy level and energy conversion process for organic molecules are shown in figure 2-2.  $S_0$  is the ground state of an organic molecule, with two  $\pi$ -electrons with opposite spin.  $S_1$  denotes the first excited singlet state ( $S_2$ : second).  $T_1$  is the first excited triplet state, with pairwise parallel oriented electron spins. Typically, the excited molecules relax their energy by one of the following ways [Tsuji2017]: the fluorescence, the phosphorescence, as heat (e.g. internal conversion) or chemical reaction. The emission of light from a singlet state  $S_1$  to ground state  $S_0$  is fluorescence (Green arrows); the radiative decay from triplet state  $T_1$  to ground state  $S_0$  is phosphorescence (Red arrows) [Schm2013].

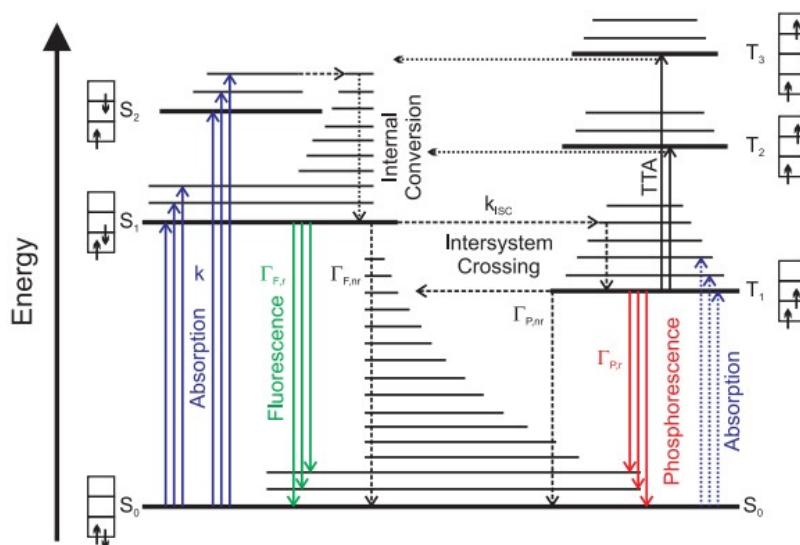


Figure 2-2 Energy level and energy conversion process diagram of an organic molecule [Schm2013].

In fluorescent emitting materials, only the decay of singlet state is radiative; in phosphorescent emitting materials, whereas, the decay of both singlet and triplet are radiative. Therefore, the phosphorescent OLEDs are more efficient than fluorescent ones, with respect to the similar emission spectra [Temp2014]. No further details will be given, with respects to more complex energy transfer mechanisms, such as internal conversion ( $S_2 \rightarrow S_1$ ), or intersystem crossing ( $S_2 \rightarrow T_1$ ). For absorption, it is a converse process compared to energy loss—with a molecule absorbing a photon, an electron changes its energy level from the ground state to excited states.

### Multi-layer OLEDs

In fact, OLEDs are commonly designed with multiple organic layers. This is done primarily to enhance the electron-hole recombination efficiency, compared to a device with single layer. Figure 2-3 illustrates an example of the multi-layer structure and schematic energy level for OLED devices. The layers include injection layers (electron-injection layer EIL, hole-injection layer HIL), transport layers (electron-transport layer ETL, hole-transport layer HTL), and the emission layer (EML). In the emissive layer, the excitons are formed by electron-hole pairs and decay under the radiation of light.

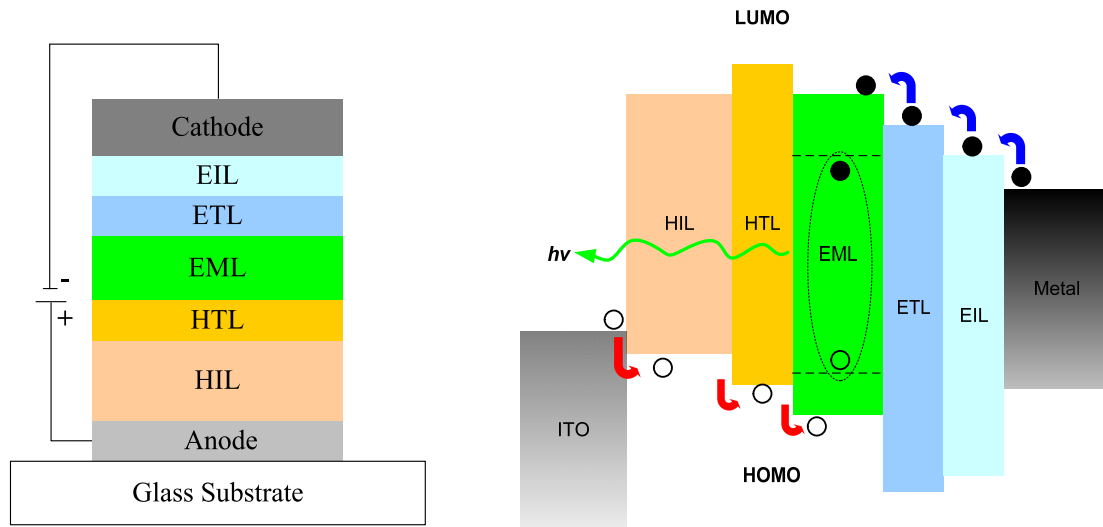


Figure 2-3 An example of multi-layer structure (left) and schematic energy level (right) for OLED devices. (Based on [Tsuji2017])

Due to the energy gap between two layers (electrodelorganic, or organiciorganic), holes and electrons have to cross the barrier from one layer to the adjacent film. Hole blocking layer (HBL) may be as an option in some devices, which is used to improve recombination and also adjust the location where the excitons formed [Tsuji2017].

### 2.1.2 Light emission efficiency

The light emission efficiency is a critical value to quantify how effectively an OLED device is emitting light, which depends on the light emission process and energy loss factors in this process. As the light emission efficiency, the external quantum efficiency (EQE) is commonly evaluated, which denotes the ratio of the emitted photons outside and the amount of injected charge. The EQE of an OLED can be calculated as following [Schm2013, Naka2014, and Gasp2015],

$$EQE = \gamma \cdot \eta_r \cdot q \cdot \eta_{out} \quad (2.1)$$

where the first factor  $\gamma$  in this equation is the charge-carrier balance (electron-hole balance); the second factor  $\eta_r$  represents the efficiency of radiative exciton production; the third factor  $q$  as the intrinsic radiative quantum efficiency; the last factor  $\eta_{out}$  is the so-called out-coupling factor.

Correspondingly, the light emission process and key factors for the external quantum efficiency of OLEDs are shown in figure 2-4.

With an external voltage applied, the charge carriers from the electrodes successively cross the injection barriers and into the organic layers. Only a fraction of holes and electrons form excitons in the emission layer. The factor of charge-carrier balance  $\gamma$  represents the proportion of the formed excitons to the injected charge carriers. Indeed, an amount of injected electrons and holes can reach the opposite electrode without forming excitons in the organic layer—these charge carriers are lost and do not contribute to light emission. By using appropriate injection and block layers in OLEDs, the balance in the amount of holes and electrons can be improved [Schm2013], and therewith the device efficiency is increased. It is worth mentioning that imbalance of bi-charges may happen in low operation point, due to asynchronous injection of holes and electrons; also, the imbalance may occur at the high operation point, due to the differential mobility of hole and electron within an organic molecule.

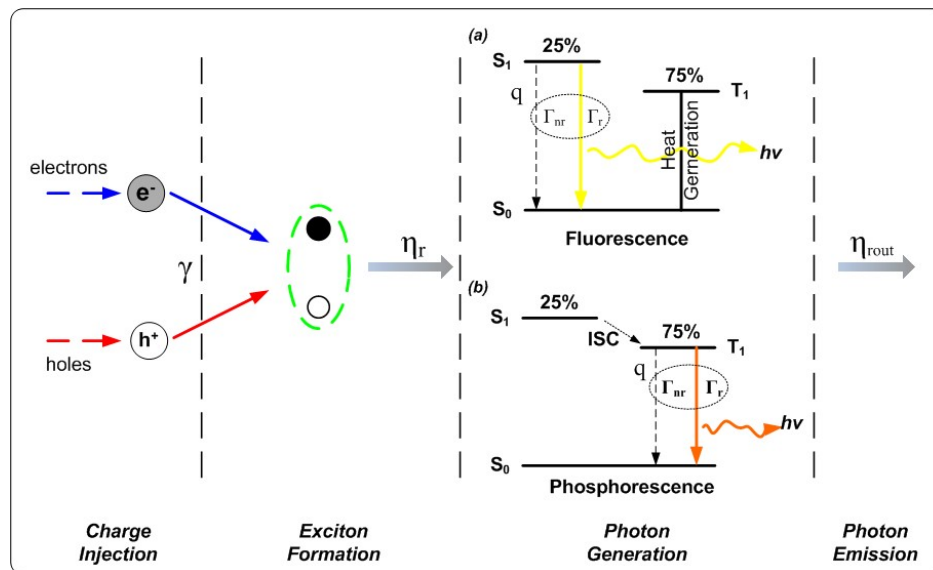


Figure 2-4 Schematic diagram of the light emission process and key factors for the external quantum efficiency of OLEDs. (Based on [Schm2013, Tsuji2017])

In the stage of exciton formation, the various species of excitons (singlets and triplets) are generated in organic film. The yield of the produced excitons which relax under the radiation of light is represented by the efficiency of radiative exciton production  $\eta_r$  [Naka2014]. In the formation of excitons, the ratio of produced triplets and singlets is three to one. For the

fluorescent devices, the relaxation of singlet exciton—transition from a singlet state to ground state, induces light emission; whereas the triplet excitons ( $T_1 \rightarrow S_0$ ) decay in the form of heat generation, not in light [Tsuji2017]. For the phosphorescent devices, due to internal system crossing ISC ( $S_1 \rightarrow T_1$ ), both singlets and triplets eventually relax their energy under the radiation of light.

In the stage of photogeneration, the intrinsic radiative quantum efficiency factor  $q$  (RQE) contributes to the external quantum efficiency. It depends on the radiative decay  $\Gamma_r$  and non-radiative decay rate  $\Gamma_{nr}$ , given as equation 2.2 [Schm2013]. This factor is strongly influenced by quenching effects (e.g. TTA).

$$q = \frac{\Gamma_r}{\Gamma_r + \Gamma_{nr}} \quad (2.2)$$

The out-coupling efficiency  $\eta_{out}$  is also a necessary factor in external quantum efficiency, considering the proportion of generated light which reflected and absorbed inside the device—some photons couldn't escape outside. This factor is impacted by the refractive indices and thicknesses of all used organic and inorganic layers [Schm2015]. When three previous factors are only considered (without  $\eta_{out}$ ), the emission efficiency is termed as IQE (internal quantum efficiency)—the proportion of injected electrons generates photons.

### 2.2 OLED Degradation

Degradation is still one of the most challenging issues for organic light-emitting diodes. The internal physical mechanisms are in complex dependence/interaction [Scholz2015, So2010, and Nowy2009], and many are still not fully understood. The degradation indeed depends on materials (small molecule/polymer), the light emission (fluorescence/phosphorescence), as well as device structures (multiple layers). Our intent in this thesis is not to present a unified/comprehensive theory on device degradation, but rather to analyze some common potential degradation effects on the electrical-optical characteristic. The degradation in electrical characteristic is illustrated firstly. Then, the contributions to degradation in optical property are analyzed, based on light emission efficiency presented in the previous section. Also, the correlation between electrical degradation and optical degradation is discussed.

### 2.2.1 Degradation in electrical characteristic

Deterioration of electrical characteristic is a common phenomenon for OLEDs during operation, as reported in many pieces of research [Gasp2015, Temp2014, and Scholz2015]. For example, the forward voltage rises or current-voltage curve shifts with aging. Multiple mechanisms contribute to aging behaviors. Considering current-flow generation on devices in operation as presented in the previous section, the degradation effects on electrical characteristic are discussed as follows:

#### I. Injection-barrier increase due to interface deterioration.

The injection barriers denote that, the charge carriers are injected from electrodes to organic films (Anode|Organic, Cathode|Organic), as well as from organic to organic film in multi-layer devices (e.g. HIL | HTL). The differential energy level at interface indeed contributes to the injection barriers. During operation, the interfaces might deteriorate with time, resulting in the injection barrier increasing. The rise of injection barrier then induces a voltage rise on the device. This effect has been reported in some publications [So2010, Scholz2015]. The internal reactions such as oxidation or ions migration might be responsible for the interface deterioration.

#### II. Conductivity decline caused by trap formation in transport layers.

Charge carriers (electrons, holes) do hopping transport inside the organic layers. The presence of traps states influences the charge carrier conductivity in organic thin films [Schm2013]. In reference [So2010], Franky So et al. discussed that the degradation in dual-carrier devices is related to trap formation. It is observed that trap dopant in ETL (electron transport layer) causes a significant voltage rise of OLED device. And in [Nowy2009/ 2010], Stefan Nowy et al. reported that the resistance of HTL observably increased with aging time through IS (Impedance spectroscopy) measurement, which is likely due to the trap formation in HTL. Even when injection barriers remain stable in degradation, it is demonstrated that trap formation may also lead to the voltage rise.

III. Additional contribution to voltage rise because of the accumulation of traps in the emission zone.

Another contribution is the accumulation of traps at or near emission layer/interface (e.g. HTL|EML). The increase of immobile charge density due to traps would typically result in a significant voltage rise [Scholz2015]. It is noteworthy that another effect induced by accumulation of traps may be the formation of the non-radiative recombination centers, which leads to a decrease of light emission efficiency. Further discussion will be described in the next section.

It is worth mentioning that the current-flow generation might be described by the equations such as drift-diffusion equation [Schm2013], space-charge-limited current (SCLC) equation [Tsuji2017], or current-flow equation considering injection-transport-recombination process [Niu2016]. Based on these equations, the degradation factors might be further derived and analyzed.

### 2.2.2 Degradation in optical characteristic

Indeed, the degradation of optical characteristic is a more critical issue, beyond the decay of electrical property. The current efficiency, the ratio between the luminance and current density, decreases with operation time, defining the lifetime of OLED devices. In considering the working process of OLED devices and the external quantum efficiency equation, the potential degradation effects on optical characteristic are discussed as follows:

#### I. Deterioration of charge-carrier balance.

In the light emission process, the balance in the amount of holes and electrons influences the exciton formation, and then the photons emitted from the device. With operation time, the charge-carrier balance may deteriorate due to some effects, such as the injection barrier increase, as well as transport properties of charge carriers are modified [Schm2015]. In reference [So2010], it is reported that charge balance becomes worse in aged device because of the declined hole-injection efficiency.

### II. Non-radiative recombination centers.

The recombination current flow comprises of both radiative (Langevin) and non-radiative recombination [Niu2016]. It has been identified that device operation results in accumulation of the charge traps in the emission zone, and longer operation will lead to a higher concentration of traps [Gasp2015]. The concentration of charge trap can make the operation voltage rise. More seriously, it induces a higher probability of recombination between free mobile carriers and charge traps. This is the so-called trap-assisted recombination (TAR), which acts as non-radiative recombination centers inside OLEDs (Shockley-Read-Hall, SRH recombination) [Niu2017, Kuik2012, and Nowy2010]. TAR may be originated from the recombination between free electrons and trapped holes, or between free holes and trapped electrons. The usage of AC waveform is suggested to alleviate accumulation effects, or reverse bias improve the recovery to some extent by de-trapping process [Van1996].

### III. Exciton quenching.

The decreasing radiative quantum efficiency in the emitting system is attributed to the weakened radiative rate and/or enhanced non-radiative rate, which may be caused by the exciton quenching effect. A well-known exciton quenching is triplet-polaron-quenching (TPQ) induced by deep traps [Schm2015]. In operation, deep carrier traps are created with internal chemical reactions [So2010]. With operation time, the previous accumulation of traps will influence the successive emitting behavior (exciton quenching). It is noteworthy that another possible explanation for decreasing radiative quantum efficiency can be luminance quenchers, which is formed by degraded organic molecule during operation [Gasp2015].

### IV. Decreasing out-coupling factor.

In the external quantum efficiency equation, the out-coupling factor also plays a role. In the aging process, the factor might decrease due to a shift of the position of the emission zone or reorientation of the transition dipole moments of the emitting species [Schm2015]. If the emission spectrum (emission zone) unlikely changes during operation, the factor remains stable and might be excluded as one possible degradation mechanism.

The potential degradation effects in electrical and optical characteristic have been listed above. It is found that some degradation effects contribute to both properties, while some solely impact on one of them. For the trap formation in emission zone, two effects on device operation are induced: traps create the non-radiative recombination centers, and also cause an operation voltage rise. From this perspective, the current efficiency loss and voltage rise are linked phenomena. Nonetheless, it is incorrect to assume that there is a deterministic relationship between the current efficiency loss and voltage rise phenomena. It can be identified with AC aging test. In the aging test, the AC driving scheme improves decay in electrical property dramatically, whereas it negligibly impacts on the efficiency decay [So2010]. This suggests that the optical decay has mechanistically its own degradation roots, except the shared degradation causes with the electrical decay. Therefore, it is indeed a partial correlation between the decay in electrical and optical characteristic.

### 2.2.3 Differential aging

In operation, OLEDs gradually lose the luminance under driven stress. OLED decay has the two-fold meaning: one is a long-term degradation effect on each pixel; the other is the differential aging effect, which denotes non-uniform luminance performance on pixels during operation [Anton2005].

For display, some pixels are overstressed than others on the panel during operation. For example, the pixels in icons are more often lighted on compared to others. The differential aging state among pixels induces the well-known image sticking aging artifact. With respects to luminance, 3-5% difference is the tolerance for human eyes.

Besides the luminance loss, the chromaticity of an OLED may also variate with operation. It is called color shift. It is also necessary to specify the allowable limitation to color shift in applications. Additionally, three primary subpixels (red, green, and blue) are degraded in operation asynchronously. The white point on display may shift in color coordinates, if three primary OLED pixels are degraded [Tsuji2017].

## 2.3 AMOLED Technology

### 2.3.1 Active matrix addressing

Two addressing schemes are usually used for OLED displays: the passive matrix and active matrix addressing [Temp2014]. The passive matrix addressing adopts simple control scheme, in which each row is driven sequentially. Active matrix organic light-emitting diode display (AMOLED) is driven with a thin-film-transistor (TFT) array, which controls the current flowing to each pixel. Each pixel is integrated with a circuit of transistor and capacitor [Wik.M2018]. The pixel state is maintained when other pixels are being addressed. A conventional active-matrix OLED display is shown in figure 2-5.

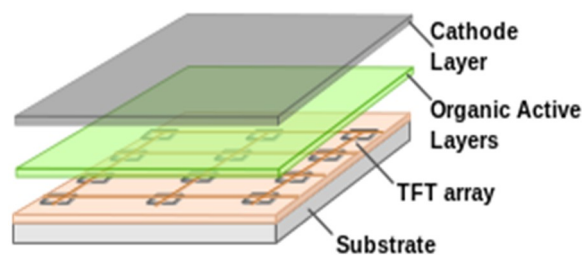


Figure 2-5 Active-matrix OLED display (AMOLED) [Wik.D2018].

On account of the low power consumption, high resolution and longer lifetime, the active matrix OLED technology (AMOLED) is applied for the mainstream displays nowadays. The passive addressed OLED display are easy and cheap to fabricate, but in size restrictions—generally for small size applications. Active matrix technology supports larger displays, such as smartphones or TVs.

### 2.3.2 Digital driving scheme

Typically, an OLED display has the pixel circuit with two TFTs and one capacitor (2T1C), as shown in figure 2-6 (a). One TFT is used to charge and discharge storage capacitor, and the other is to provide power for pixel. With pixel circuit, the analog and digital driving scheme can be applied to drive OLEDs, as shown in figure 2-6 (b) and (c).

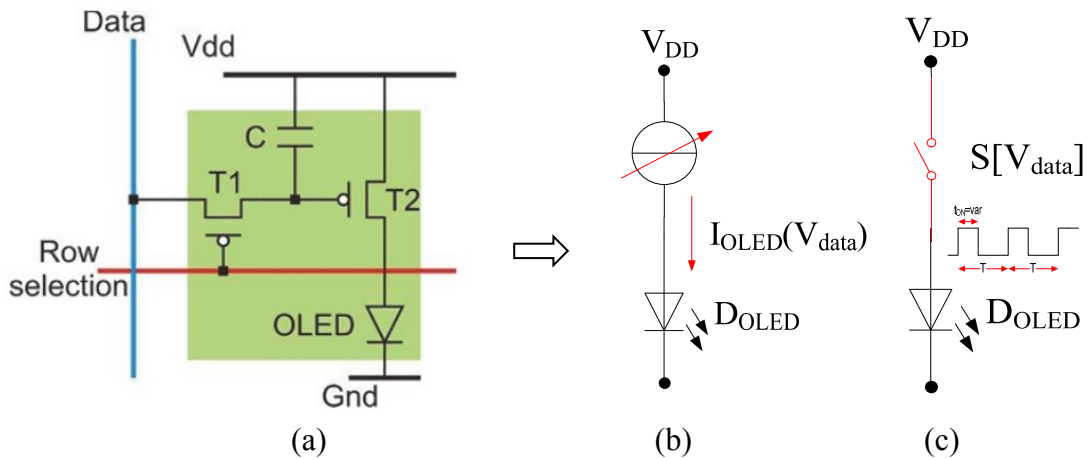


Figure 2-6 (a) 2T1C Pixel circuit [Ko2011] (b) analog driving (c) digital driving scheme.

In the analog driving scheme, the driver transistor T2 is used as a current source (in saturation region). The luminance gray values are modulated by current flows in DAC. In the digital driving scheme, the driver transistor T2 is used as a switch, which controls the OLED in on/off state. OLED is driven at a fixed voltage. The luminance gray values are modulated with the duty ratio in PWM (time).

In the digital AMOLED system, an input image-frame is decomposed into several subframes (binary), as shown in figure 2-7. Each subframe is given a duration time. In each subframe, every pixel is switched according to binary subframe. All subframes are subsequently displayed on the panel with time. Finally, sub images are accumulated as one single frame in human eyes [Volk2014].

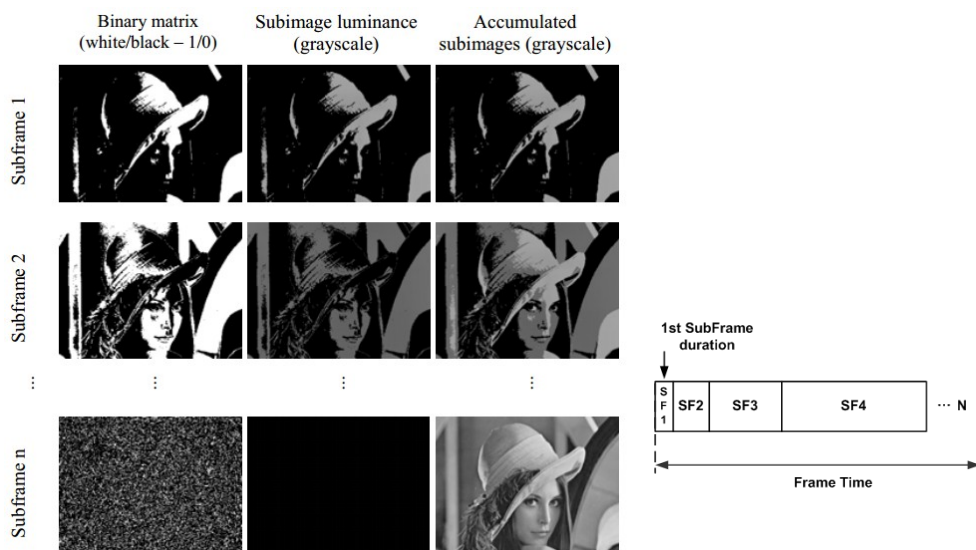


Figure 2-7 An image is decomposed into several subframes in digital driving scheme [Xu2012].

With respects to the analog driving scheme, a high requirement for uniformity of driver transistor ( $V_t$ ) in manufacture results in a low yield of panels. Complex compensation pixel circuit further decreases aperture ratio and pixel density. Seriously, the analog driving scheme has a low power efficiency, due to high power dissipation in driver TFT. In comparison, the digital driving scheme can overcome these issues. It has a low requirement for uniformity of  $V_t$ , and also saves power consumption with operating driver transistor in a linear region. However, some challenges are also encountered. Higher addressing speed is needed for multiple subframes. Moreover, OLED is susceptible to aging, manufacturing and temperature variation, due to voltage driven. Artifacts such as non-uniformity or contours may be induced. Some issues have been solved or compensated, whereas some are still not addressed/solved [Volk2017].



## 3 Characterization and Degradation behaviors

AMOLED display contains millions of pixels and each pixel is an organic light-emitting diode (OLED). Through the experiments on OLED devices, we can investigate the characteristic and degradation of OLED (for single pixel). The findings should allow the applications on display panel.

In experiments, OLED devices from Novaled and Merck are adopted as test samples. Both companies are supplying materials to the leading display producers (Samsung and LG). On these devices, an analysis of electrical-optical characteristic and degradation behaviors in aging is made via IVL measurement (current-voltage-luminance). After each aging interval, the IVL measure is performed to analyze the degraded characteristic of devices. The aging of the devices was established by an accelerated stress with consideration of the multiple driving conditions. The influence of driving condition such as current flow, temperature, or AC for degradation behaviors can be then analyzed.

Based on these investigation in experiments, the model of OLED degradation can be developed in further and will be presented in the next few chapters.

### 3.1 Test Arrangements

#### 3.1.1 OLED devices tested

OLEDs with generic multi-layer structure (anode|HIL|HTL|EML|ETL|cathode) were fabricated on the glass substrate. The indium tin oxide (ITO) is used as a transparent anode, and the low working function metal (Al) is as an opaque cathode. Between electrodes, the multiple organic thin films are fabricated one by one, using the standard vacuum deposition process. The OLED device is finally seal encapsulated using glue and an additional glass. Figure 3-1 shows some photos regarding Novaled and Merck OLED devices. For Novaled OLED devices, the glass substrate has the size of 2.5x2.5 cm<sup>2</sup>. Four identical OLED lights are fabricated in one row on substrate, with each active emitting area of 6.7 mm<sup>2</sup>. All four OLEDs

### 3. Characterization and Degradation behaviors

share a common cathode wire, whereas each one has its individual anode wire. For Merck OLED devices, the glass substrate is 3.0x3.0 cm<sup>2</sup>. On substrate, four identical OLED lights are fabricated with each active emitting area of 4.0 mm<sup>2</sup>. The OLEDs have their own individual cathode and anode wires. Each OLED on both devices can be controlled and light up, separately.



Figure 3-1 Photos of OLED devices from Novaled and Merck.

Table 3-1 shows the basic performance of OLED devices provided by Novaled and Merck. The Novaled samples are in red, blue and white color, and Merck samples are in blue and green color. The red and green devices are phosphorescent, and blue devices are fluorescent due to longer lifetime. The Novaled white OLED has hybrid multi-layer structure, using yellow phosphorescent emitters and blue fluorescent emitter. In table 3-1, the turn-on voltage  $V_{on}$  (generation of recombination current flow) shows the basic electrical performance for various samples. The luminance and efficiency indicate the optical performance of devices. Chromaticity (CIE1931) describes additional key features for OLEDs. The materials of samples are small molecules.

Table 3-1 OLEDs Performance

Devices	Color	Area [mm <sup>2</sup> ]	$V_{on}$ [V]	L [cd/m <sup>2</sup> ]	Max. Eff [cd/A]	CIE 1931 (x, y)	Emission
Novaled	B	6.7	2.3	2300 (4.0V)	6.8	0,13/0,12	FL
	R	6.7	1.8	1873 (3.5V)	20	0,66/0,34	PH
	W	6.25	5.2	10000 (9.2V)	91	0.35/0.45	PH
Merck	B	4	2.4	2600 (4.5V)	12	0,13/0,16	FL
	G	4	2.0	3000 (3.5V)	70	0.31/0.64	PH
Von= turn on voltage L= luminance Eff= efficiency FL= fluorescence PH= phosphorescence							

### 3.1.2 Measurement setup

The current-voltage-luminance (IVL) measurement is widely used to characterize the electrical-optical properties of OLED devices. When the applied voltage is scanned in an operation range (e.g. 0-6V) on device, the corresponding current flows and output luminance in this range can be depicted. It shows the OLED behaviors in the whole range, and indicates its internal operation mechanisms. The variation of characteristic in aging can be then evaluated, based on IVL data in each aging interval. OLED devices in experiments are placed in fixtures. Agilent E5270B applies voltage on devices and simultaneously senses the feedback current flow in high precision (fA). Spectra\_scan PR740 camera is used to obtain the optical information, such as luminance and chromaticity (e.g. CIE1931), when current flow through diode. The measurement is performed by the dual instruments, which are controlled via Matlab program on computer. It allows for stepwise applying voltage, and measuring the current flow and luminance from the device in a range. The measurements were taken in a dark room to exclude influence from the ambient light. And, room temperature is set constant due to the sensitivity of IVL on ambient temperature. The measurement setup for OLED devices is shown as a schematic diagram in figure 3-2 (a). Figure 3-2 (b) shows some measurement setup photos.

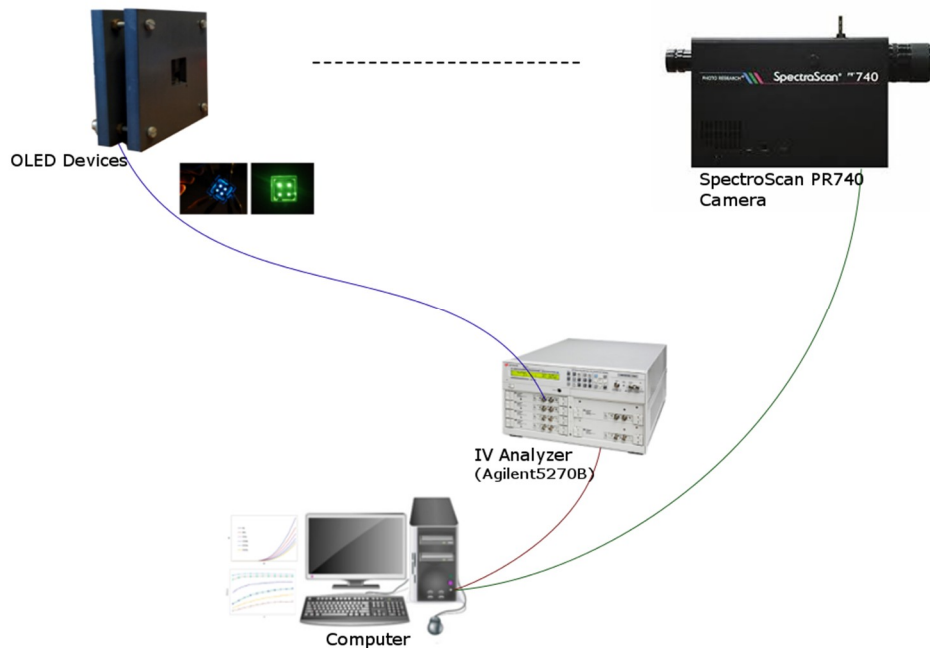


Figure 3-2 (a) The schematic diagram of measurement setup for OLED devices.



Figure 3-2 (b) the photos of measurement setup for OLED devices.

## 3.2 Electrical-optical Characterization

### 3.2.1 Electrical characteristic

The relation between the current flow through an OLED and the applied voltage is the current-voltage characteristic [Temp2014]. It depicts the electrical performance of an OLED, and indicates internal electrical mechanisms. The current-voltage (I-V) curve of an OLED is shown in figure 3-3. It is typical diode behavior. A leakage current flow through the organic light-emitting diode in the lower operation range. When the applied voltage surpasses turn-on voltage (e.g. 2.0V), the current flow through diode increases significantly (recombination). In this stage, the electrons are gradually injected and recombine with holes in the emission zone. From the slope of current-voltage curve in semi-log, the ideality factor can be extracted. Generally, the ideality factor is greater than 1 for an organic diode. In the high operation range, the rectification behavior occurs on the organic diode. The serial resistance of the device may play a key role in this stage. The organic light-emitting diodes commonly show the current-voltage characteristic, as reported in many publications [Nowy2009, Niu2017].

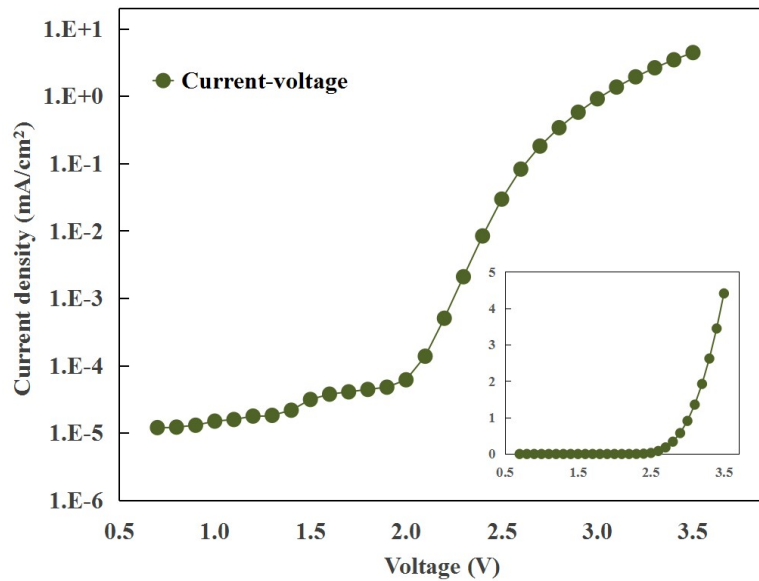


Figure 3-3 Current-voltage (I-V) curve in semi-log at room temperature. Data from Merck green OLED devices.

### 3.2.2 Optical characteristic

The relation between the luminance output from OLED and the applied voltage is luminance-voltage characteristic [Temp2014]. It describes the brightness performance of an emitting diode in operation range. Luminance is the luminous intensity at a unit area in a given direction [Wik.L2018], as one of the key features for display—it is used to evaluate the brightness level sensed by human eyes. The unit is the  $\text{cd/m}^2$  (candela per square meter), sometimes also called as nits. Figure 3-4 (a) shows the luminance-voltage (L-V) characteristic of an organic light-emitting diode. After turn-on voltage, the output luminance exponentially increases due to the sharply rising recombination of hole-electron pairs. The electroluminescent characteristic can also be described by the luminance-current (L-I) curve for an organic light-emitting diode, as shown in the subgraph of figure 3-4(a). The output luminance is proportional to current flow through the device, in approximately linear behavior. In the analog driving scheme, the brightness levels (gray levels) are modulated to corresponding current flows, according to the luminance-current curve in this figure.

### 3. Characterization and Degradation behaviors

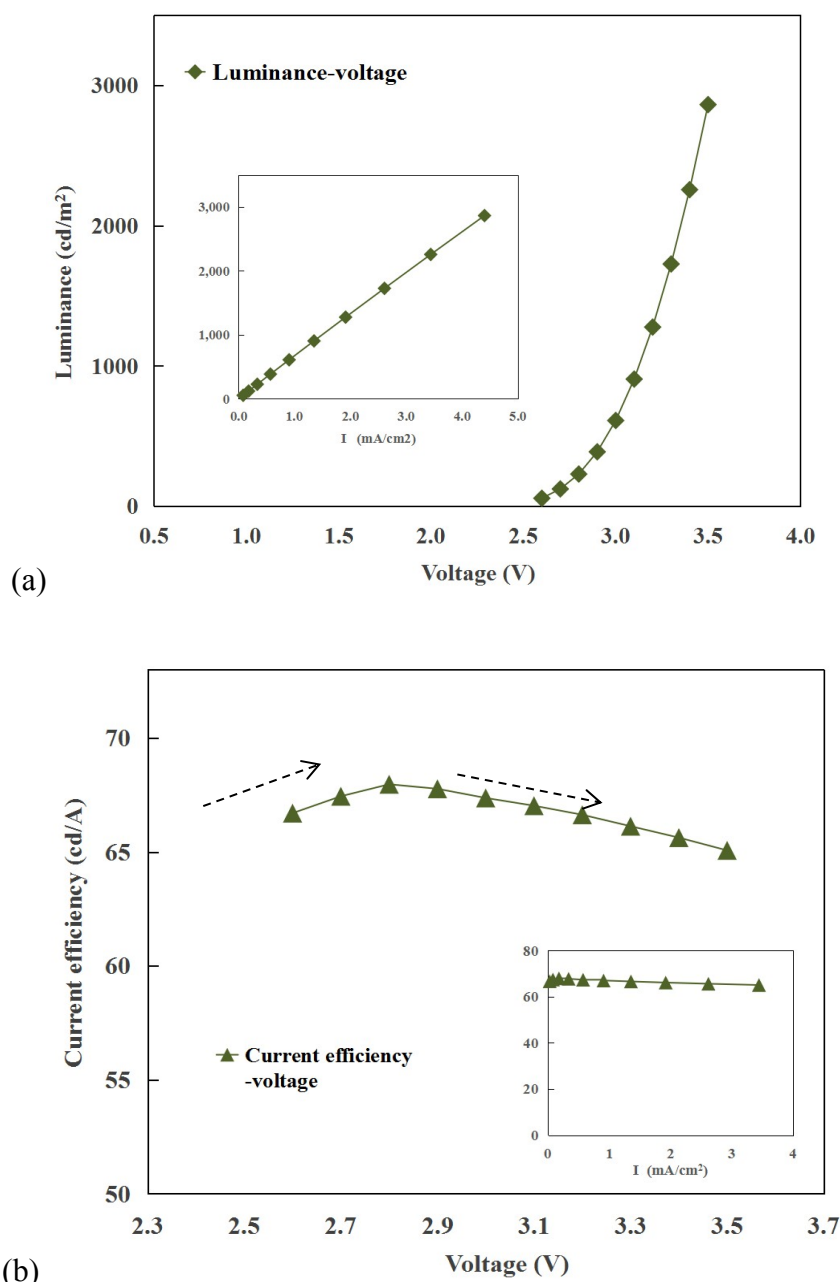


Figure 3-4 (a) Luminance-voltage (L-V) curve at room temperature (b) Current Efficiency-voltage (Eff-V) characteristic. Merck green OLED devices.

For organic light-emitting diodes, the current efficiency is a more crucial value. It reflects optical characteristic on OLED (internal radiative quantum mechanism). And its degradation determines the device lifetime. Luminance is attributed to current flow and efficiency. Current efficiency is the ratio between luminance and the current density. The current efficiency is thus solely analyzed, regardless of the electrical scale (current flow). The current efficiency in

operation range (versus voltage/current) for an OLED is plotted in figure 3-4 (b). The curve exhibits a rising stage, and a declining stage subsequently. This shows good agreement with the results published by other groups [So2010, Mahm2012]. No light is indeed emitted from OLED until at the turn-on voltage. With the radiative recombination of hole-electron pairs increasing, more photons are emitted from the device, resulting in the improvement of efficiency (the rising stage). After reaching a peak, the efficiency gradually reduces (the declining phase), indicating that an additional internal physical mechanism contributes to optical characteristic in this range. Accurately, the declining behavior is the so-called roll-off effect [Kali2002, Rein2007]. The mechanism for this effect might be lack of charge balance (holes-electrons) [Gieb2008], or exciton quenching process (e.g. triplet-polaron quenching TPQ, triplet-triplet annihilation TTA) in high operation range [Tsujii2017]. The efficiency characteristic can also be described by the curve of current efficiency versus current density, as shown in the subgraph of figure 3-4(b). The efficiency is observed approximately stable in major operation range—it shows less dependence on operation point in the current scale compared to voltage scale, especially in high operation range. This feature will be more considered in the analog driving scheme.

#### 3.2.3 Comparison of devices

For an OLED, the electrical and optical characteristic can be analyzed with IVL measurements, as presented in the previous section. Regarding various OLED samples (Merck and Novaled, colors), the characteristic for them can be depicted using the same method, as shown in figure 3-5. On the left column is experimental current-voltage (I-V) & luminance-voltage (L-V) curves, and on the right side is the current efficiency versus voltage (Eff-V) curves for various OLED devices. The current value is in logarithmical scale, and luminance curve in linear scale is plotted in the secondary axis. Current efficiency is displayed in a linear scale in the secondary graph.

Comparing the experimental results from various samples, it clearly shows that they exhibit approximately identical electrical-optical behaviors: a typical diode I-V curve with leakage, recombination and rectification stages; current efficiency depends on the operation point, with the rising and roll-off stages. There is a deviation for leakage current among various samples, likely due to the measurement errors in very low current. However, it would not be very

### 3. Characterization and Degradation behaviors

---

problematic in our case, since the characteristic in the light-emitting stage is more concerned where the diode is switched on, generating recombination current flow.

With respect to the electrical performance, the turn-on voltage for monochromic OLED of Merck and Novaled is similar (e.g. at around 2.5V). For white color, a higher value is observed (at around 5V), due to its hybrid emitting structure (two serial diodes). In the rectification region (high OP), a stronger limitation is applied to the current flow through Merck blue sample than Novaled blue sample.

Luminance level of Novaled blue is higher than that of Merck blue (approx. 2300 vs 1500 nits at 4V). This might be due to better electrical performance for Novaled device—higher current flow through devices. However, Merck blue sample achieves relatively higher current efficiency (Max. 12 vs 6.8 cd/A). Comparing Eff-V curves of both devices, Merck blue suffers serious roll-off effects on efficiency, which may make it encounter a challenge in the analog driving scheme.

With a comparison between blue and green color devices, the green device has achieved excellent efficiency, which is approximately five/six times as blue device. The Merck green sample is indeed phosphorescence, whereas the blue sample is fluorescence.

### 3. Characterization and Degradation behaviors

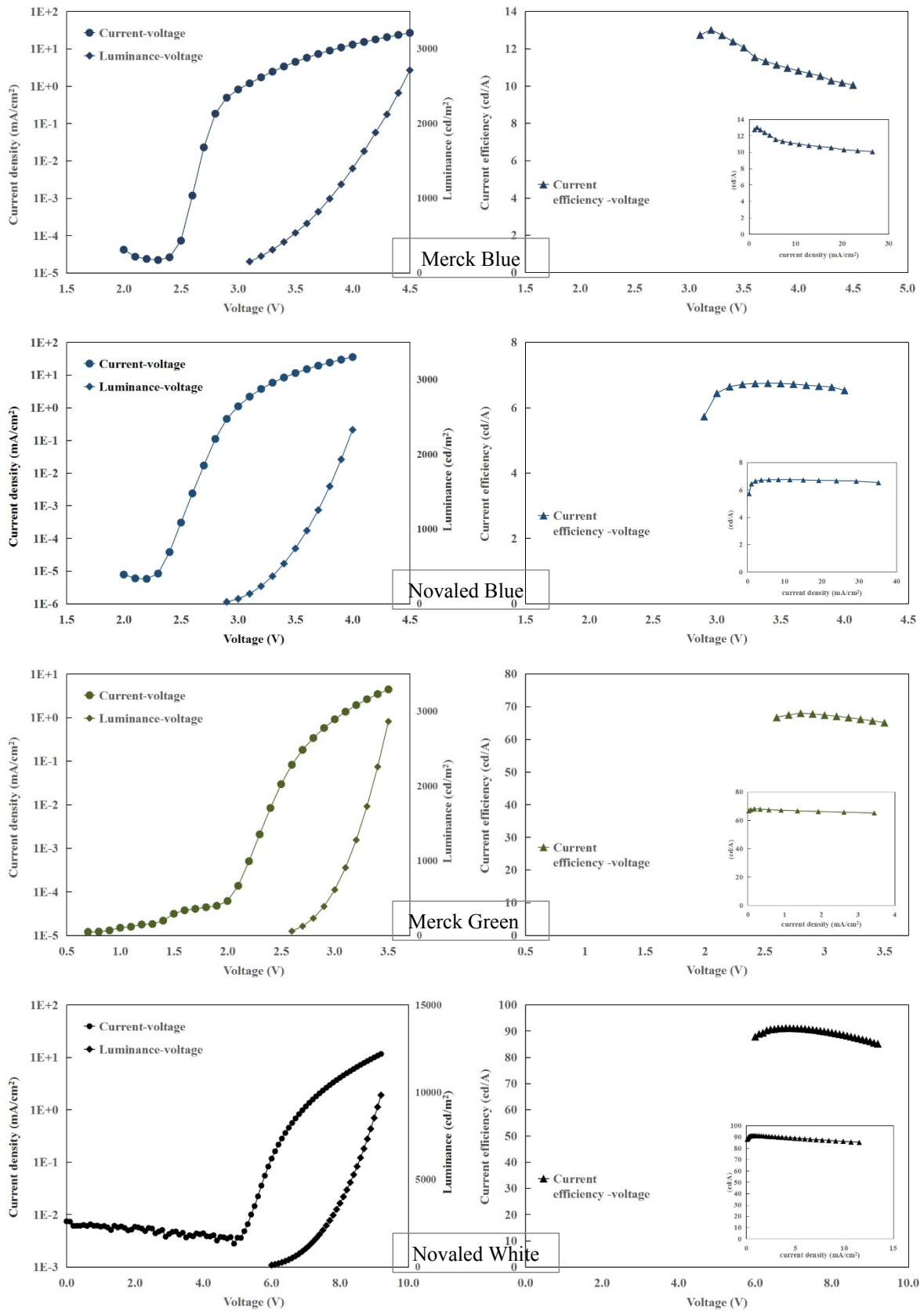


Figure 3-5 Experimental IVL curves (left) and current efficiency curves (right) for Merck and Novaled OLED samples.

### 3.2.4 Chromaticity

The chromaticity is an objective specification for the color quality regardless of its luminance [Wik.C2018], as one of the key features for a display panel. Three primary colors on organic light-emitting diodes determine the color space of a display panel. To satisfy the spectral sensitivity of human eyes, high-quality chromaticity on monochromatic OLEDs should be developed. Figure 3-6 shows the chromaticity of Merck and Novaled OLEDs in CIE1931. The Novaled blue OLED shows better chromaticity than the Merck device. However, both of them haven't achieved deep blue for Rec.709 primary chromaticity. It may be due to the fact that the development of blue OLED has to focus on lifetime. Efforts should also be taken to develop deep blue OLED for high-quality display. The Merck green sample achieves high-quality green color. Novaled red sample satisfy the Rec.709 standard. A Novaled white sample is more likely yellow in chromaticity (far from white point D65).

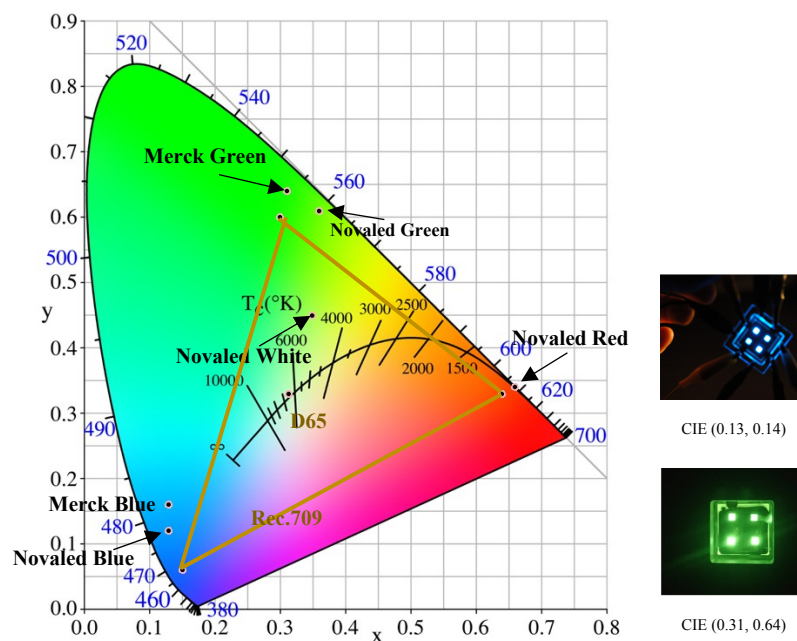


Figure 3-6 The chromaticity of OLEDs (Merck and Novaled) in CIE1931.

Figure 3-7 shows CIE coordinates of OLEDs at various operation points. It shows that Merck blue OLED has quite stable color in operation range (3.0-4.5V)—less dependence on the operation point. This will support high-quality performance in driving display, especially in the analog driving scheme. Merck green devices are also relatively stable at various operation

points. With respects to the chromaticity of Novaled blue OLED, CIE y strongly depends on the operation point. Novaled white sample is sensitive to operation points, too. Therefore, more stable organic light-emitting diodes in chromaticity should be developed for high-quality display. Additional feasible approaches for solving the issue of unstable color may be an adoption of the digital driving scheme (at a fixed operation point), or compensation algorithm.

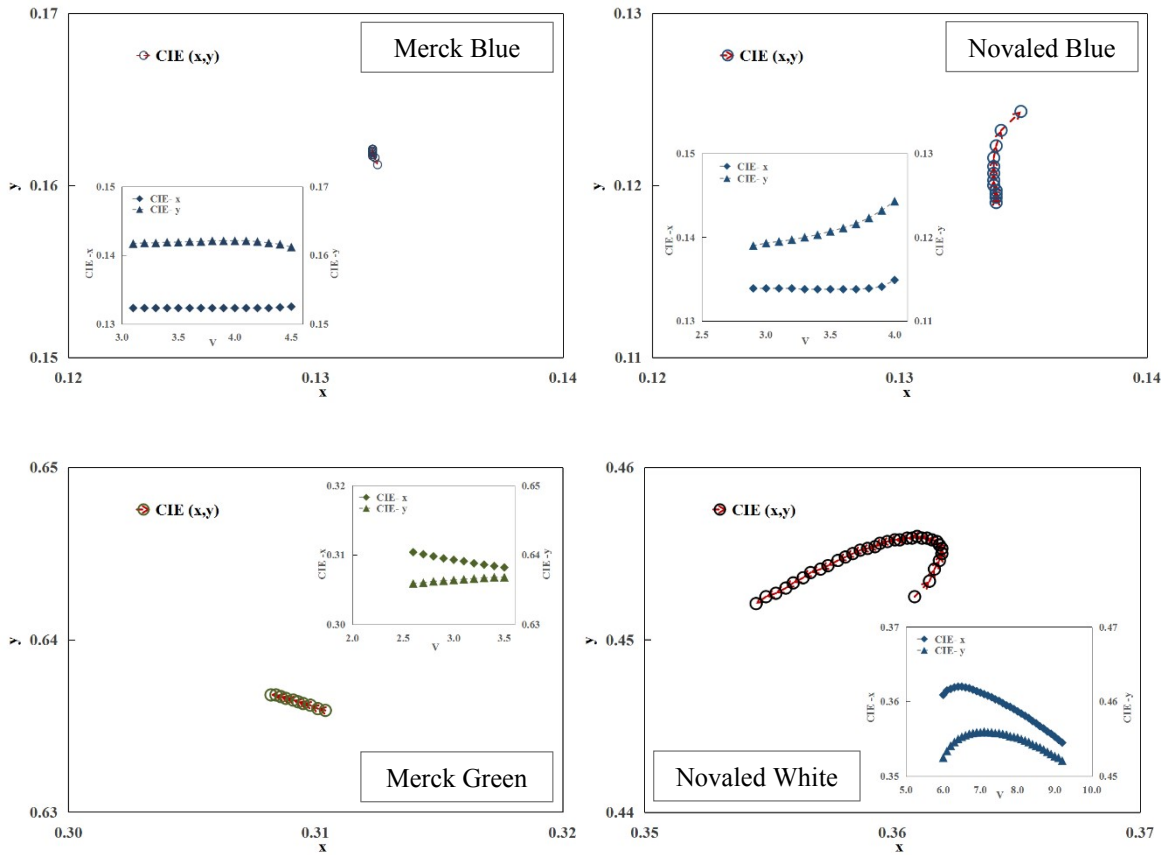


Figure 3-7 CIE coordinates of OLEDs at various operation points.

### 3.2.5 Temperature dependency

Organic light-emitting diode is a thermal dependent device. The hole and electron current flows are tuned since carrier mobility is a function of temperature [Tsuji2017, Temp2014]. OLED characteristic such as electrical-optical property or chromaticity might be dramatically influenced by temperature. In this section, we discuss how OLED behaviors are affected by the ambient temperature. It is noteworthy that the temperature doesn't refer to internal Joule

### 3. Characterization and Degradation behaviors

heating, which is induced by driving OLED at extremely high power dissipation (high current flow) [Scholz2015].

#### Electrical characteristic

With temperature increasing, the current-voltage (I-V) curve dramatically shift, as shown in figure 3-8. From temperature at 292 K to 344 K, I-V curve rises significantly. At a given operation point (e.g. 2.8V), the current flow through device exponentially increases, as the right graph shows. For each 10 degrees rise, the current flow is approximately elevated one to two-fold. Therefore, the OLED is unstable in terms of temperature sensitivity of electrical characteristic. Elevated temperature increase conductivity is also discussed in many publications [Suo2008, Baiju2011]. The injection barrier can be indeed lowered by increasing temperature (Schottky effect) [Tsuji2017]. According to the Richardson-Dushman equation, the saturation current depends on temperature, and thus current flow through device increases with temperature rising. Additionally, the electrical shift depends on the operation point, as the right figure shows. The temperature effect is stronger at lower operation voltage, compared to higher operation voltage (e.g. 2.8V versus 3.5V).

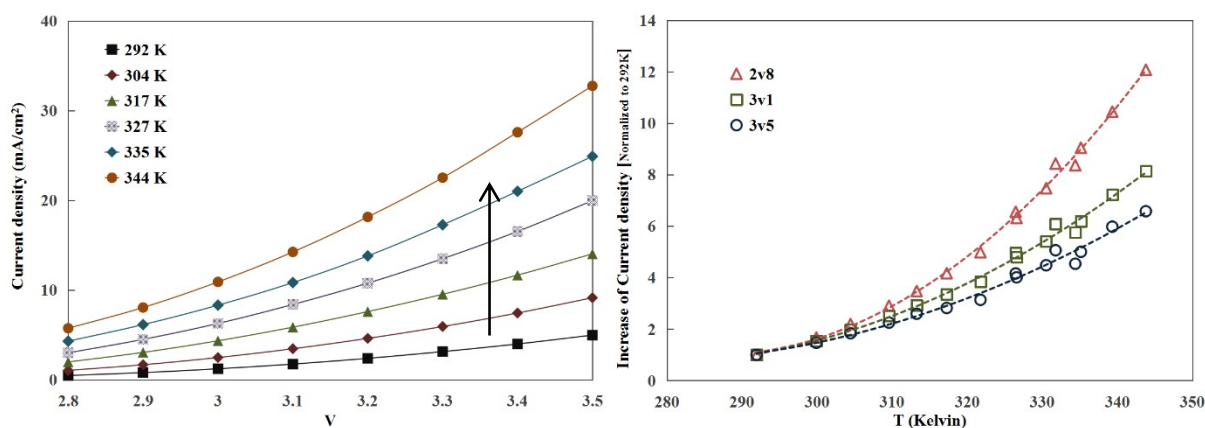


Figure 3-8 I-V curve shift with temperature (left); current flow at given operation points increases with temperature (right). Data from Merck green OLED devices.

#### Optical characteristic

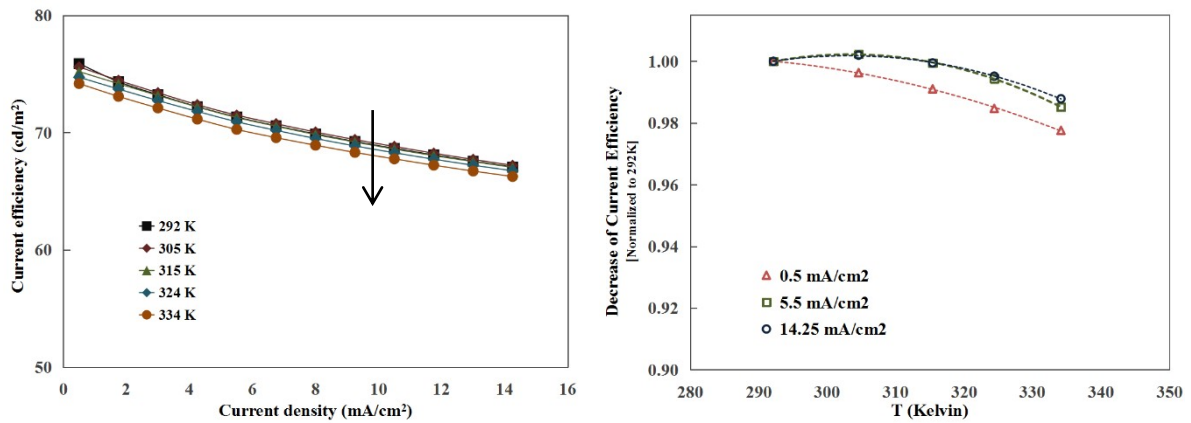
With temperature increasing, the current efficiency (Eff-I or Eff-V) curve also shift, as shown in figure 3-9. The current efficiency curve gradually sinks. The current efficiency at a given

operation point monotonously decreases as temperature increases (subfigure b). Additionally, the efficiency decrease with temperature depends on the operation point. The temperature effect is stronger at lower current than higher current point. Compared to temperature dependency of electrical characteristic (I-V), the efficiency of an OLED is relatively weaker in temperature dependence. The phenomenon that elevated temperature induces efficiency decline is also analyzed in some publications [**Baiju2011**, **Moraes2015**]. The quenching effect can be indeed strengthened by increasing temperature on devices, resulting in current efficiency drop as measured.

Figure 3-9 (c) shows current efficiency versus voltage (Eff-V) at various temperature. In a comparison of Eff-V and Eff-I (subfigure a) for temperature dependency, Eff-V curve encounters more severe decline. It is due to the current efficiency not only depends on temperature but also on operation point. The elevated temperature induces the current flow significantly increased (at a given voltage), and in further results in an additional efficiency drop— according to roll off effect, the efficiency declines with higher operation point. In the digital driving scheme, therefore, it will suffer more serious temperature issue, compared to the analog driving scheme (ref. Appendix 9-1). Considering the temperature dependency in both electrical and optical characteristic, the luminance output from devices will be significantly influenced by ambient temperature in the digital driving scheme. To alleviate the temperature effect on the digital driving AMOLED display, compensation may be implemented, through measuring electrical current flow and adopting supply voltage. This approach has been discussed in reference [**Kana2016**].

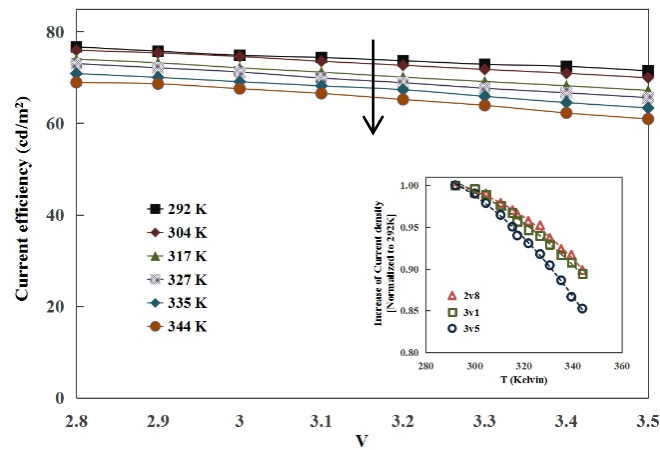
It is worth mentioning that the decrease of current efficiency in temperature experiments should not be attributed to the degradation in operation, because of very short measurement time on green OLED samples (less than five minutes). The same conclusion has also been made in the publication [**Moreos2015**].

### 3. Characterization and Degradation behaviors



(a)

(b)



(c)

Figure 3-9 (a) Current efficiency versus current density curve (Eff-I) shift with temperature (b) the current efficiency at given operation points decreases with temperature (c) Current efficiency versus voltage curve (Eff-V) shift with temperature. Merck green OLED devices.

### Chromaticity

In figure 3-10, the color coordinates of an OLED vary with temperature is shown. It is clearly seen that color shifts with temperature rising—chromaticity depends on temperature. This variation suggests the change in the emission of device. It might be attributed to the emission zone shift or molecular vibrations [Moreos2015]. Moreover, the temperature dependency of chromaticity may be varied for various color samples. More investigations are thus needed.

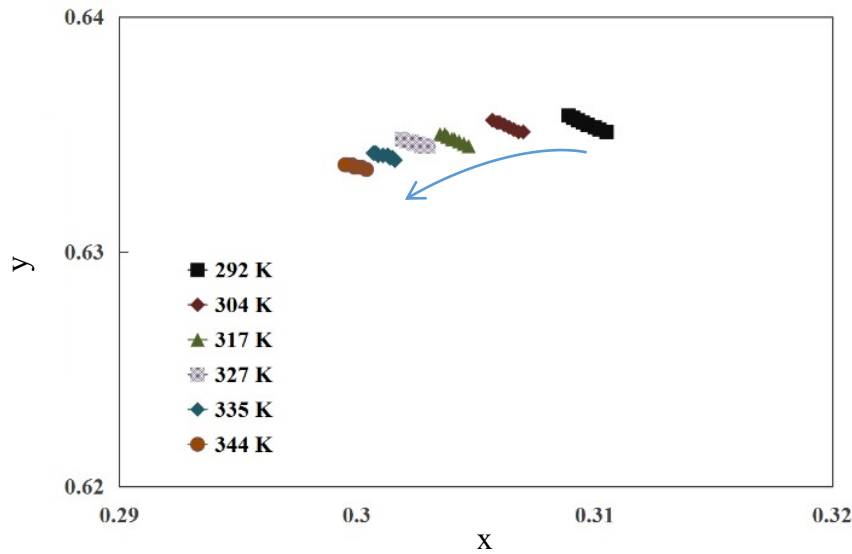


Figure 3-10 color shift with temperature rising. Data from Merck green OLED devices.

### 3.3 Degradation Behaviors

As we know, organic light-emitting diode suffers from severe degradation. Unstable OLEDs will gradually degrade during operation, resulting in the aging artifact such as image sticking on display panels. Indeed, multiple complex physical mechanisms potentially contribute to the degradation in both electrical and optical characteristic, as analyzed in chapter 2. To further learn the degradation behaviors, the electrical-optical characteristic in aging will be analyzed, and impact factors (driving conditions) for decay scale will be quantified. These findings in experiments will allow modeling of degradation on OLEDs.

#### 3.3.1 Aging test procedure

The aging tests on OLED samples are commonly continuous for thousands of hours. It is desirable to perform more aggressive stressing test to accelerate the decay rate on devices [Kobrin2003], especially for green or red OLED samples with longer lifetime. Accelerate stressing conditions, using higher luminance and higher temperature, are thus generally applied in the aging test.

For OLED aging, the tests were taken in a dark room and at constant room temperature. A number of OLED samples under multiple driving conditions, such as luminance (e.g. 800, 1500, 2500 nits), ambient temperature (e.g. 18, 32, 48°C, each device with individual heating system),

or AC/DC conditions, were stressed in the aging tests. Current-voltage-luminance (IVL) characteristic was measured after each aging interval (a period of aging time). At the beginning of aging process, the measurement was taken more frequently, because of sharply aging in the beginning stage. The measuring interval was then gradually extended in the long term. To simulate the digital driving conditions, diodes were switched on/off with frequency (e.g. 800 Hz) via PWM signals on a driving board. The atmospheric humidity is not considered in the test, due to high-quality capsulation on most devices today.

The degradation in characteristic will be discussed in the following sections. Also, the impact factors on degradation behaviors can be analyzed based on the aging experiments.

#### **3.3.2 Decay of electrical characteristic**

Figure 3-11 shows current-voltage (I-V) curves at various aging time in experiment. Curves are plotted in semi-log and line scale (secondary). In the aging test, OLED sample was stressed at 2500 nits for approximate 2200 hours. It clearly shows that I-V curve significantly drifts with aging time, identifying that the electrical characteristic of OLED is vulnerable to degradation. This is consistent with the finding in references [So2010, Schm2015]. I-V curve in linear scale shifts right in aging, as seen in secondary axis. At a given voltage point, the current flow would gradually drop with aging time. The electrical degradation behaviors is illustrated more details in log I-V curves.

As the degradation mechanisms analyzed in chapter 2, several potential causes may contribute to the degradation behavior. The interfaces such as anode|organic or cathode|organic may deteriorate in aging, resulting in a rise of injection barrier. Moreover, traps may be formed in the transport layers (e.g. hole-traps in HTL), inducing carrier mobility decreased. The declining conductivity then causes a drop of the current flow through device. Another possibility to explain this behavior would be accumulation of traps in the emissive layer, resulting in voltage rise/current decrease. For the leakage current flow, it slightly increases with aging. Indeed, it is the hole-leakage current flow increased, due to only holes are injected in this stage.

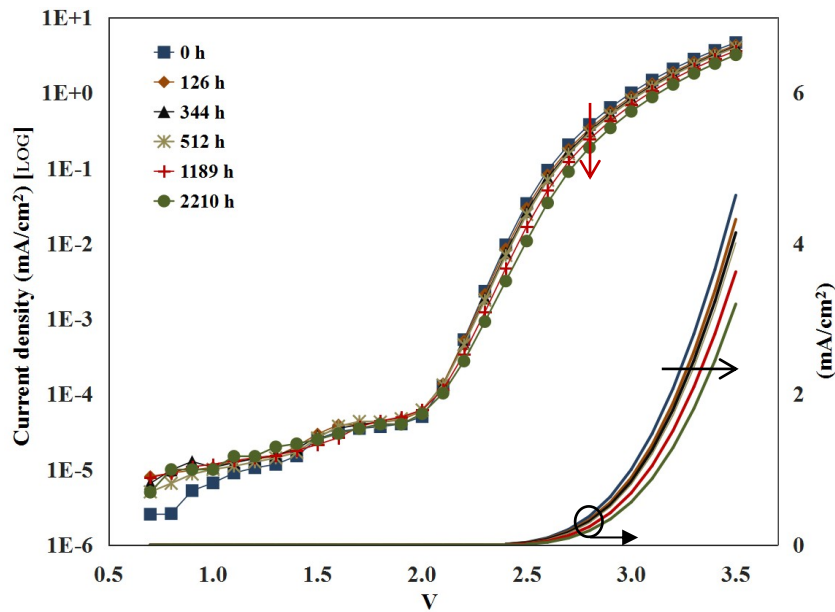


Figure 3-11 Current-voltage (I-V) curve drift with aging time. Primary axis in semi-log, and secondary axis in linear scale. Merck Green OLED sample is stressed at approx. 2500 nits at 32°C.

The experimental aging results for more samples could be found in Appendix 9-2. They show identical degradation behaviors as discussed above. The turn-on voltage for Novaled blue sample slightly become lower in aging, identifying the injection barrier increased in aging—increased injection barrier reduces work function difference between two electrodes [Niu2016].

### 3.3.3 Decay of optical characteristic

Besides the degradation in electrical characteristic, the optical degradation is a more pressing issue that requires understanding. In figure 3-12, current efficiency versus voltage at various aging states is shown. It clearly shows that current efficiency curve sinks with the aging time. It identifies that the optical characteristic of OLED is prone to degradation, in agreement with the analysis in references [So2010, Niu2016]. For current efficiency at a given voltage point, it would significantly drop with aging time (at 3.5V, there is approx. 23 % loss after 2200 hours). Furthermore, another fact shown in this figure is that the optical degradation depends on the operation point. As the figure shows, the decay in a lower operation point is stronger, compared to a higher operation point. For example, at 2.6 volts, the current efficiency decay is about 46% after 2200 aging hours, which is much bigger than it at 3.5 volts (i.e. 23%).

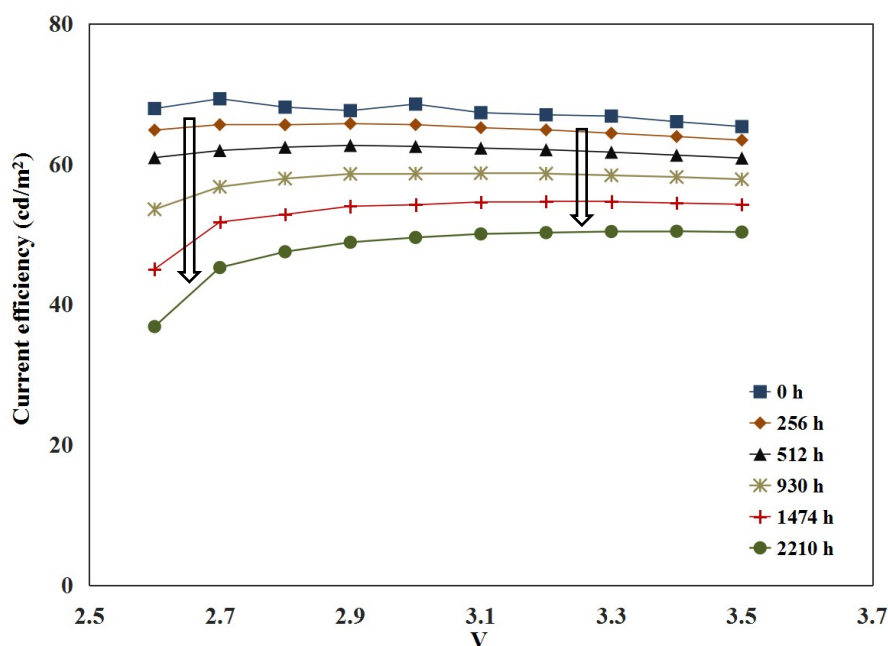


Figure 3-12 Current efficiency versus voltage at various aging states.

The degradation behavior in optical characteristic is probably attributed to multiple degradation mechanisms, as analyzed in chapter 2. In the aging process, charge traps may be gradually accumulated in emission zone. The concentration of charge traps more likely induces the recombination between free mobile carriers and charge traps (trap-assisted recombination effect TAR), which is known as non-radiative recombination centers. Furthermore, the exciton quenching effect is probably induced and gradually enhanced with operation time, such as the well-known triplet-polaron-quenching TPQ by deep traps. The exciton quenching results in the decline of radiative quantum efficiency, which is observed as the current efficiency loss in experiments. Additional possibility to explain the behavior is the deterioration of charge carrier balance. With operation time, the transport/injection for charge carrier (e.g. holes) declines, inducing the imbalance in the amount of dual carriers. The radiative recombination (Langevin) will thus decrease with operation. It is worth mentioning that the maximum efficiency (optimized charge balance) gradually shifts to higher operation voltage as shown in figure 3-12, identifying the variation of the charge balance in aging. The experimental results for more samples could be found in Appendix 9-3. They show the identical degradation behaviors as discussed above.

Figure 3-13 shows luminance-voltage (L-V) curves at various aging time. The L-V curve dramatically drifts in aging. At a given point, the luminance output from OLED will significantly drop. For example, the luminance at 3.5V decreased approx. 50% of its initial value after 2200 aging hours, as shown in the subgraph. Actually, the luminance loss is attributed to decreases in both current flow and current efficiency.

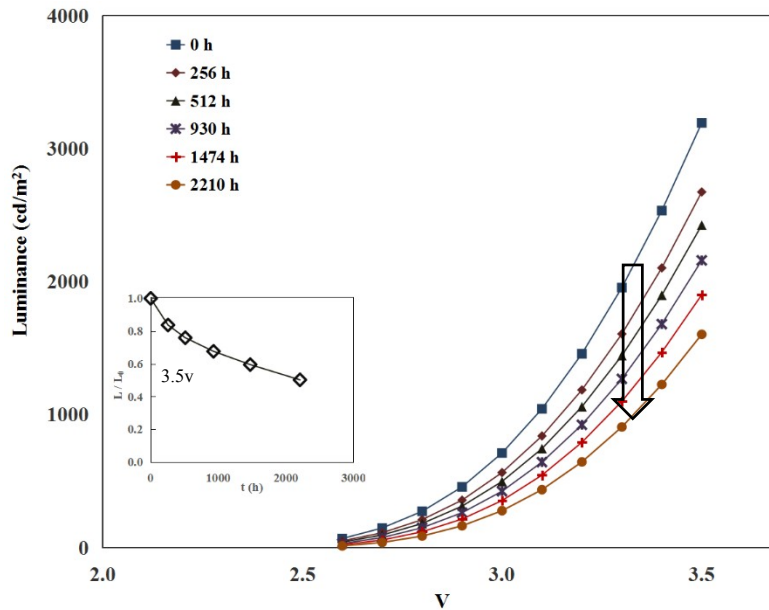


Figure 3-13 Luminance-voltage (L-V) curves at various aging states.

In fact, OLED sharply degrades in the beginning phase of aging process, and then enters into a smooth long-term decay. For the display application, a pre-aging in production may be applied to mitigate the first sharp aging regime. Additionally, compared to the analog driving scheme, display with the digital driving scheme will suffer more serious aging issue due to contributions of both electrical and optical decay. The luminance loss in the analog driving scheme is solely caused by the current efficiency decay. However, the dependence of degradation on operation point also makes the analog driving display vulnerable to degradation—in the digital driving, the operation voltage is fixed.

### 3.3.4 Dependency on driving conditions

In the aging process, the degradation on OLED device is inevitably influenced by driving conditions. It is necessary to investigate the potential factors which impact the degradation, and

### 3. Characterization and Degradation behaviors

---

also significant for modeling of OLED degradation in further. To investigate the impact factors, the OLED samples have been stressed under various driving conditions. Figure 3-14 (a) shows that current efficiency decays in aging, under various driving current flows—50, 100 and 200  $\mu\text{A}$  (i.e. initial luminance 800, 1500 and 2500 nits) at room temperature. It is observed that the decay profile strongly depends on driven current flow. Figure 3-14 (b) shows that current efficiency decays with aging time, under various ambient temperature—18, 32 and 48 $^{\circ}\text{C}$  at identical current flow. It shows that decay profile is highly dependent on the ambient temperature. Indeed, the organic light-emitting diode is a thermally unstable device. Thermal accelerating effect on degradation is induced by higher ambient temperature. This result is consistent with the analysis in references [Soh2006, Parker1999]. In figure 3-14 (c), it shows the current efficiency decays under multiple driving conditions, including various current flow and ambient temperature. In fact, both accelerating effects contribute to OLED degradation.

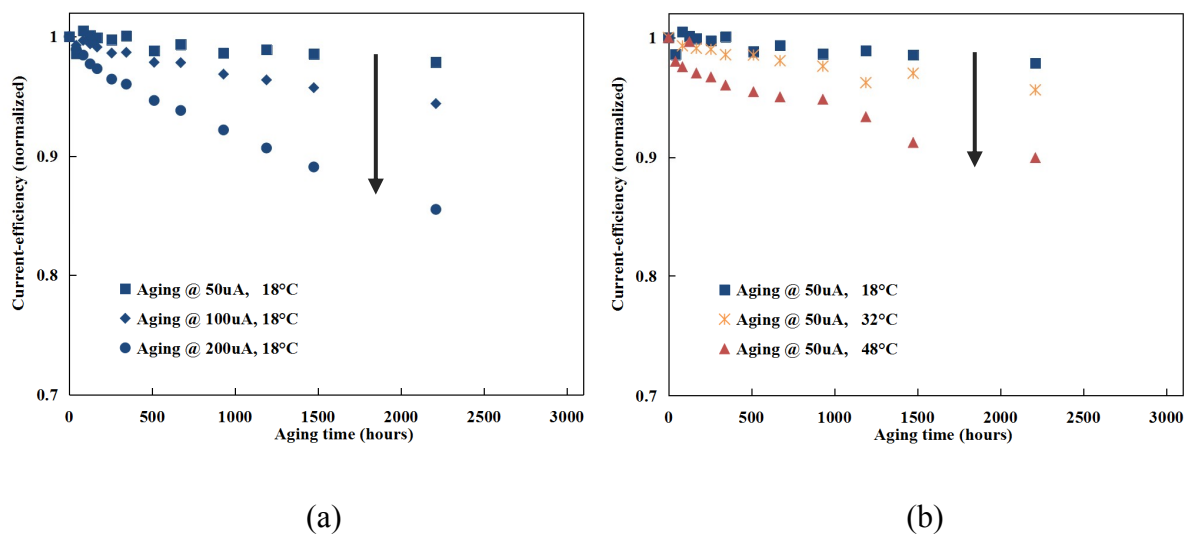
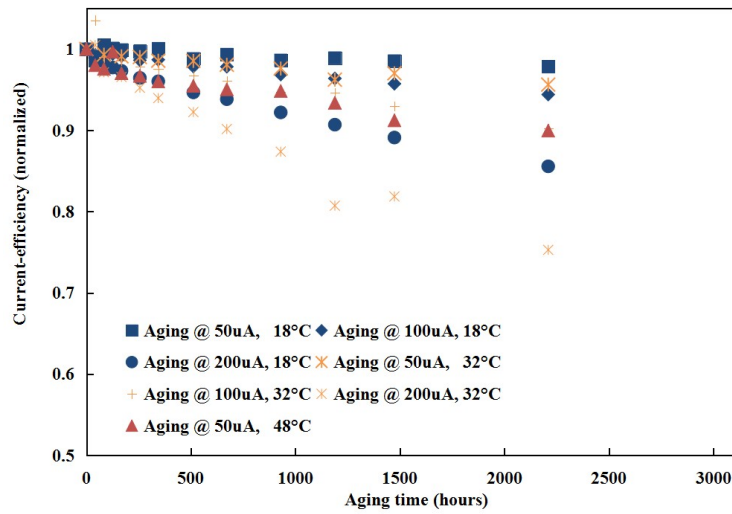


Figure 3-14 (a) Current efficiency of OLEDs decays with aging time under various driving current flows (b) current efficiency decays under various ambient driving temperature. Data from Merck green OLED devices.



(c)

Figure 3-14 (c) current efficiency decays with aging time under multiple driving conditions. Data from Merck green OLED devices.

These impact factors exert accelerating aging effects on both electrical and optical degradation. Since the electrical decay is measurable value in the practical applications, impacts on optical characteristic are mainly concerned.

### Dependency on AC driven condition

Besides the two impact factors above, AC driven condition may also play a role in the degradation. The study for the AC effect was early taken by Van and Tang et al. in publication [Van1996]. With an AC drive waveform, the issue of space-charge accumulation in the EL layer has been alleviated. In reference [Scholz2015], Scholz et al. discussed that there is a positive influence of the AC condition on degradation for small-molecule OLED.

To investigate the AC effect, we stressed OLED samples with identical luminance level (800nits), in various waveform, including DC driving scheme, AC pulse with 100 and 800 Hz (same duty cycle 50%). The experimental results are shown in figure 3-15. Figure 3-15 (a) shows current decrease with aging time under the AC and DC driven conditions. In a comparison of DC and AC condition, it clearly shows that AC driven condition improves the electrical degradation in operation—the lifetime is longer, confirming the positive AC effect. Additionally, comparing the 100 Hz AC and 800 Hz AC, it is observed that higher driving

### 3. Characterization and Degradation behaviors

frequency more likely suppresses the electrical degradation. Kim et al. reported the frequency dependency of electrical degradation in publication [Kim.H2007]. It identifies that electrical degradation (I-V drift) can be effectively suppressed with higher operating frequency.

In figure 3-15 (b), current efficiency drift in aging under AC/DC driving conditions is shown. It shows that AC/Frequency conditions have little impact on efficiency decay, compared to its impact on electrical degradation. The result is in good agreement with analysis in reference [Kim.H2012].

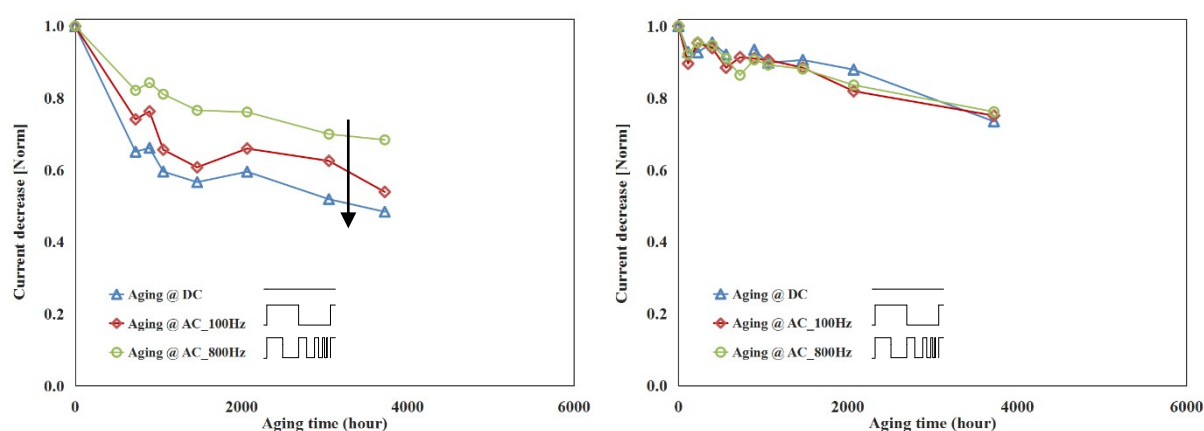


Figure 3-15 (a) Current decreases with aging time under DC and AC (100 and 800 hz) driven conditions (b) Current efficiency decreases with aging time under DC and AC driven conditions. Data from Merck green OLED devices.

In the display system with digital driving scheme, an AC pulse and higher operation frequency will improve the lifetime of OLEDs. Additionally, reverse bias driven pulse is also likely to improve (even recover) both electrical and optical degradation to some extent, as reported in some publication [Yahi2000, Scholz2015]. This reverse bias is presumably effective in “de-trapping” accumulated space charges during the reverse cycle. More investigations are needed.

#### 3.3.5 Color shift

In the aging process, the chromaticity of an OLED may variate with time. To investigate the color variation in degradation, the OLED sample from Novalled was stressed. The device was driven at 2200 nits for approx. 4000 hours. In figure 3-16, the CIE coordinates of OLEDs at various aging times are shown. It is observed that the color dramatically shifts with aging time.

In the subgraph, CIE-x / CIE-y versus voltage at pristine and aged states are plotted. As the graph shows, color shift depends on the operation point.

The color shift on OLEDs is likely attributed to variation in the recombination/emission zone during aging [Schm2015]. In fact, the blue OLED sample is vulnerable to color shift, compared to the other two primary colors (green and red). Differential variation for three primary colors would induce the shift of white point on display. Additionally, display with the analog driving scheme may suffer more serious color shift due to the dependency of chromaticity decay on operation point. The experimental results for more samples could be found in Appendix 9-4. It could be observed that the color of green samples is quite stable in the aging process.

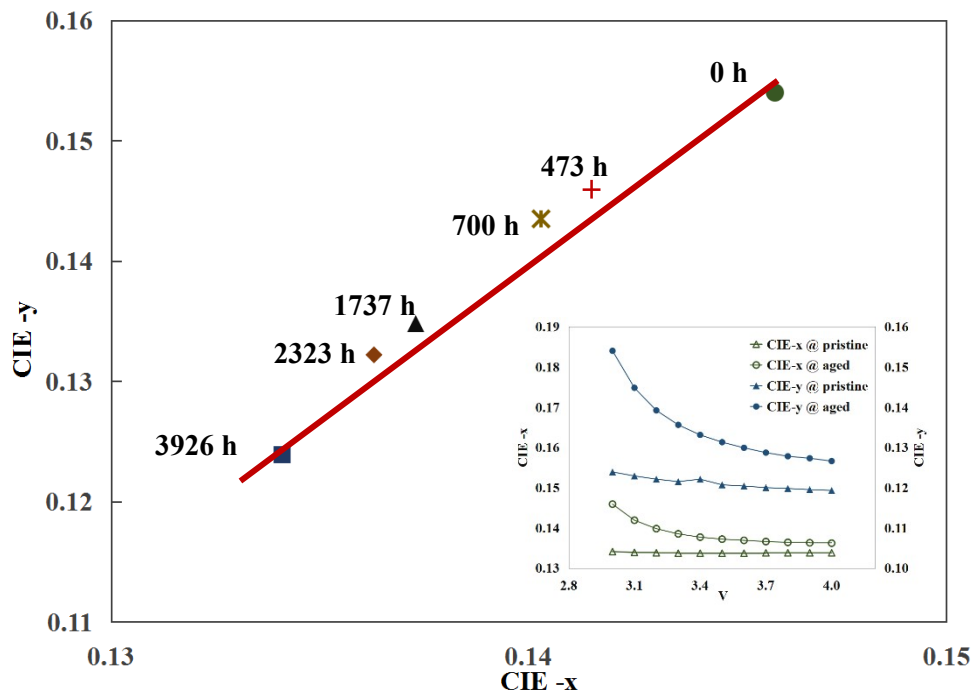


Figure 3-16 Color shifts with aging time. Novald blue OLED samples.

### 3.4 Conclusion

In this chapter, OLED devices (Merck & Novald, blue & green) and measurement setup were introduced. Based on the experimental results on these devices, the electrical-optical characteristic, chromaticity, temperature dependency has been characterized. Furthermore, the degradation behaviors were analyzed, including the decay in electrical-optical characteristic, impact factors on degradation (e.g. the accelerating effect and AC effect), as well as the color

### 3. Characterization and Degradation behaviors

---

shift. These findings would allow modeling of OLED degradation, which will be described in the following chapters.

## 4 Data-counting Model

To effectively compensate pixel-wise luminance loss, which induces the image sticking artifact on AMOLED display, analyzing and modeling the degradation behavior of OLED become necessary. Because of limited understanding and complex dependency of degradation mechanisms, it is not feasible to build a comprehensive physical model for OLED degradation. As discussed in chapter 2, for example, the degradation mechanisms depends on materials (Small molecular or polymer), the emission type (fluorescence or phosphorescence), as well as the device structure. Instead, a data-counting approach may provide a feasible means to quantify the degradation in operation. The decay curves are extracted from numbers of samples, and aging history on devices are counted for empirical prediction. The similar investigations were taken by some groups [**Anton2005**, **Soh2006**, and **Fan2017**]. In this chapter, a data-counting model for prediction and compensation of OLED degradation will be presented. The empirical model considers the OLED decay under multiple driving conditions, including various current amplitude and ambient temperature. Through the calculation of accumulated stress on devices during operation, the decay could be evaluated and the corresponding compensation can be implemented. It is worth mentioning that a unified degradation model will be derived by integrating multiple decay curves under various driving conditions—this makes the implementation of compensation more practical. The data-counting model has been discussed in the publication [**Jiang2016**].

### 4.1 Degradation of current efficiency

During operation, the luminance decays with operation time, as figure 4-1 shows. It exhibits the nonlinear monotonous decrease in a long term, which could be described by empirical equation. LT50—luminance drops to the half of its initial level, is usually defined as the lifetime of OLED devices.

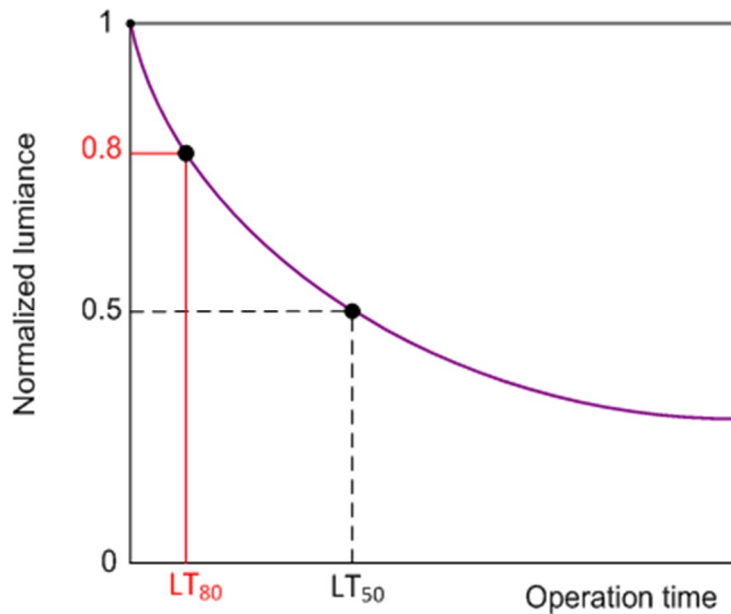


Figure 4-1 The luminescence decays with operation time.

An empirical equation was typically applied to describe the luminescence decay in many published works [Kobrin2003, Anton2005, and Soh2006], as shown in equation 4.1,

$$\frac{L(t)}{L(t_0)} = \frac{1}{1 + \left(\frac{t}{LT_{50}}\right)^\alpha} \quad (4.1)$$

Where  $L(t_0)$  is the initial luminescence value,  $LT_{50}$  is the time when the luminescence drops to one-half of its initial brightness at a given current/voltage.  $\alpha$  is the decay exponent.

Other alternative empirical equations were also introduced by some works. In reference [Fery2005, Scholz2015], a bi-exponential decay equation was introduced, interpreting the rapid short-phase initial decay and long-term smooth decay. Nevertheless, the equation might over/under-estimate the lifetime. In literature [Kobrin2003, Oh2015], a stretched exponential decay equation was discussed. It may also fit data but not well as equation 4-1. The equation 4-1 can generally well fit the luminescence decay, and simplify the model parameters as well.

The shape parameter,  $\alpha$ , for three primary colors, varied from 0.4 to 1.0 approximately [Kobrin2003]. As  $\alpha$  value decreases, the luminescence decay becomes less linear. It is worth mentioning that decay exponent  $\alpha$  is constant when changing the initial luminescence or

temperature, reducing the fit to one single parameter ( $LT_{50}$ ). This will improve the predictive nature of the fit, when extrapolating lower and more realistic degradation curves. More detail will be discussed in the following sections.

### Current efficiency decay

The decay in current efficiency, instead of luminance decay, is targeted to analyze optical degradation. In the analog driving scheme, the luminance loss is solely caused by decay in current efficiency due to current-source driving; in the digital driving scheme, decay in current efficiency is the key to estimate the luminance loss, besides the measurable current drift in applications.

The current efficiency of an OLED decays with operation time. In operation, the decay degree is influenced by the driving scheme and ambient driving conditions. The corresponding experiment results have been discussed in chapter 3. As simplified, the degradation is represented as a function of three impact factors including current  $I$ , operation time  $t$  and temperature  $T$ , described by  $Eff = f(I, t, T)$ . The current efficiency  $Eff$  could be normalized to 1, since just a relative value is needed for compensation.

Due to a high requirement for display, the LT80 is indeed preferred to evaluate lifetime. Considering the introduced degradation equation 4.1 and impact factors (current  $I$ , ambient temperature  $T$ ), the following equation may be established.

$$Eff = \frac{1}{1 + 0.25 \times \left( \frac{t}{LT_{80} |_{(I,T)}} \right)^\alpha} \quad (4.2)$$

$LT_{80} |_{(I,T)}$  is the lifetime when the current efficiency drops to 80% of its initial value. It depends on current (related to luminance), and ambient temperature due to the thermal instability of OLED. Here, the current efficiency  $Eff$  as the key is used to analyze optical degradation instead of luminance  $L$  for both analog and digital driving schemes.

### Coulombic degradation law

Aging caused by the active operation is a matter of time, the current as well as temperature. The total amount of charges which have been injected into OLED may be applied to quantify

the efficiency decay. In reference [Van1996], it was found that the luminance decay rate is directly proportional to the injection current density, implying that the degradation is coulombic. In reference [Parker1999], the OLED decay was described as an expression of total charge passed through the device. It can be termed as coulombic degradation law, as so-called in [Aziz2002]. Figure 4-2 shows a simple schematic diagram for this process, in which the OLED degrades with accumulation stress due to injected charge.

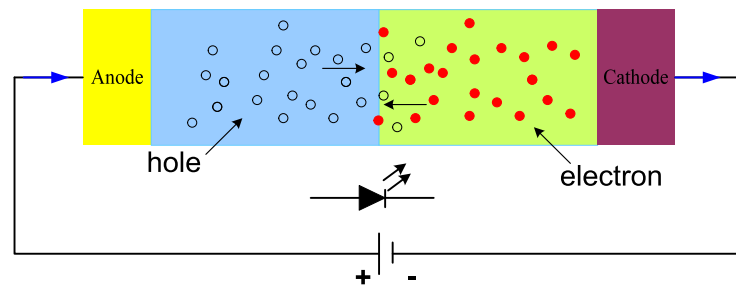


Figure 4-2 A simple schematic diagram that charge are injected into the device, which induces the OLED decay with accumulation in this process.

Considering the coulombic degradation law, analog to equation 4.2 presented above, the following expression equation 4.3 can be obtained,

$$Eff = \frac{1}{1 + 0.25 \times \left( \frac{Q}{Q_{80} |_{(I,T)}} \right)^\alpha} \quad (4.3)$$

with,

$$Q = \int I \cdot dt \propto \sum GV$$

$Q_{80} |_{(I,T)}$  is the accumulation quantity of injected charge when current efficiency drops to 80% of its initial value. The parameter depends on the current amplitude and temperature.  $Q$  is the total injected charge during operation. In an OLED display system, it is proportional to the gray values (GV) ever displayed on a pixel. Thus, this method is called data counting.

The electrical damage on an OLED device is proportional to the number of passing charges, which is also denoted as electric current. Nevertheless, the damage is indeed proportional to  $J^n$ , whose  $n$  is greater than one, implying that there remains an acceleration mechanism for OLED degradation [Tsuji2017]. The acceleration factor will be further discussed in the following section.

## 4.2 Current-amplitude dependency of degradation

Figure 4-3 shows that current efficiency decay versus total injected charge  $Q$  into devices at various stressing current amplitudes. Three Merck green OLED samples were stressed at 50, 100, 200 $\mu$ A respectively, at identical room temperature 18 °C. It shows that the decay curve shift with current amplitude change. This implies that the current amplitude exerts additional acceleration effect on OLED degradation, besides considering the coulombic effect (injected charge  $Q$ ). The decay curves are well-fitted by equation 4.3.  $Q_{80}$  solely depends on the current amplitude at a given temperature  $T_0$  in this case.

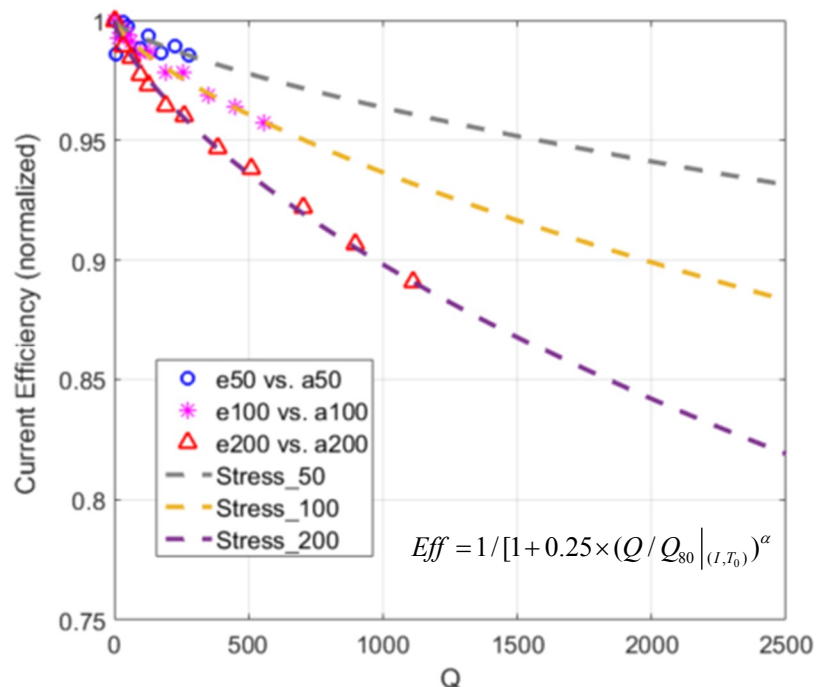


Figure 4-3 Current efficiency decay (normalized) versus total injected charge ( $Q$ ) into devices at various stressing current amplitudes. Decay exponent  $\alpha = 0.7926$ .

#### 4. Data-counting Model

---

To extract the acceleration effect of current amplitude on degradation, a well-known scaling law [Fery2005, Meer2006, and Scholz2015] is introduced, as shown in equation 4.4. It defines the relationship between the lifetime and initial luminance, quantified with the constant  $C$ .

$$L_0^\beta \times t_{1/2} = C \quad (4.4)$$

where  $t_{1/2}$  is the half-life time (also as  $LT_{50}$ ),  $\beta$  an acceleration factor, and  $L_0$  as the initial luminance.

In this acceleration function, the lifetime would decline by a factor  $\beta$ , if increase the initial luminance on device. The coefficient  $\beta$  is generally greater than one.

Luminance is approximately proportional to current flow over a wide operation range. Considering the scaling law, the following relation for  $Q_{80}$  in coulombic degradation equation 4.3, can be determined. At a given ambient temperature ( $T_0$ ),  $Q_{80}$  is a function of current amplitude.

$$Q_{80} \Big|_{(I, T_0)} \propto \frac{1}{I^{\beta-1}} \quad (4.5)$$

The higher is the applied current amplitude, the faster the current efficiency decays ( $Q_{80}$  is smaller). In figure 4-4, the  $Q_{80}$  quantities of Merck's green OLED devices are plotted with dependence on the current amplitude. The measurement data are fitted by the equation 4.5 with high quality (R-square 0.9993). The extracted  $\beta$  value in this case is  $2.122 \pm 0.2$ . In reference [Fery2005], the acceleration factor is around 1.7. The  $\beta$  here is comparable reasonable value. The acceleration factor is device and/or material-specific. It is worth mentioning that, degradation might be accelerated beyond the scaling law due to significant internal heating effects, at extremely high luminance and current densities, as reported in publication [Scholz2015]. Nevertheless, for devices under usual/reasonable driving conditions like in this case, the degradation would not exceed the law leading to an overestimation of device lifetime.

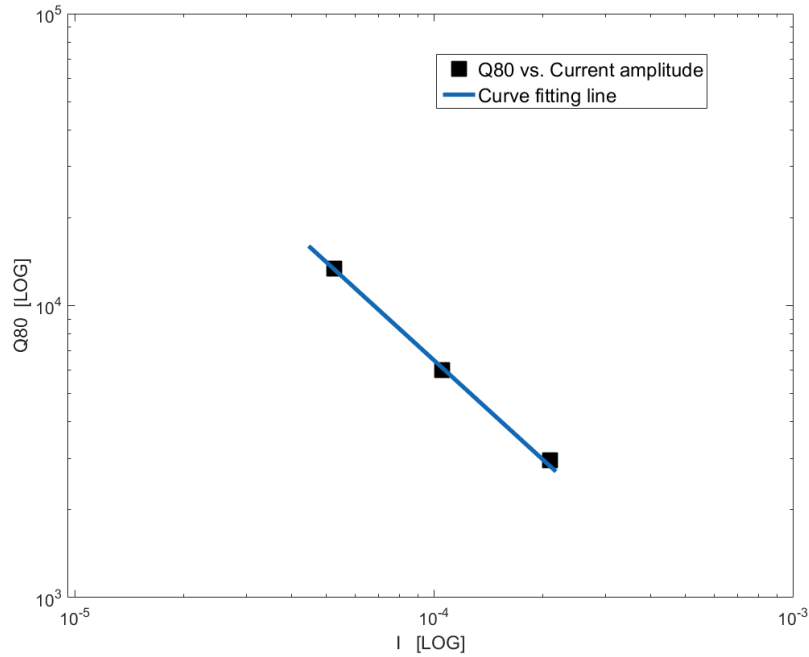


Figure 4-4 Q<sub>80</sub> versus Current amplitude in log scale.

When Q<sub>80</sub> is fixed at a reference current Q<sub>80</sub> | I=I<sub>ref</sub>, the following equation 4.6 could be in further established. Variable ACC(I) substituting Q in equation 4.3 describes the accumulated stress on OLED with dependence on current amplitude. The accumulation stress as a function of current amplitude is shown in equation 4.7, with ignoring temperature factor.

$$Eff = \frac{1}{1 + 0.25 \times \left( \frac{ACC(I)}{Q_{80} | I=I_{ref}} \right)^\alpha} \quad (4.6)$$

$$ACC(I) = Q \times \left( \frac{I}{I_{ref}} \right)^{\beta-1} \quad (4.7)$$

The data counting value Q is now amended to ACC. The acceleration effect of current amplitude in a wider range is considered in the accumulated stress function ACC (I). Based on the above analysis, degradation could be described by the unified equation. The accumulation stress ACC is hence as data counting value, which considers the acceleration effect of I. The calculation of accumulation stress, which considers the thermal acceleration effect, as well as the further unified degradation function, will be discussed in the following section.

### 4.3 Thermal dependence of degradation

Besides the current-amplitude dependence, the degradation still depends on ambient temperature, due to the thermal-induced process or thermal instability of OLED materials, as reported in some works [Parker1999, Soh2006]. The thermal acceleration effect on degradation can be observed in the measurement results, as shown in figure 4-5. OLED samples were stressed under identical current amplitude, but at various temperature (18, 32, 48 °C). The results identify that there is a relative contribution of ambient temperature to degradation, in addition to coulombic degradation law and current-amplitude acceleration effect. The decay curves are well-fitted by equation 4.3. At a given current amplitude, the  $Q_{80}$  predominately depends on the ambient temperature.

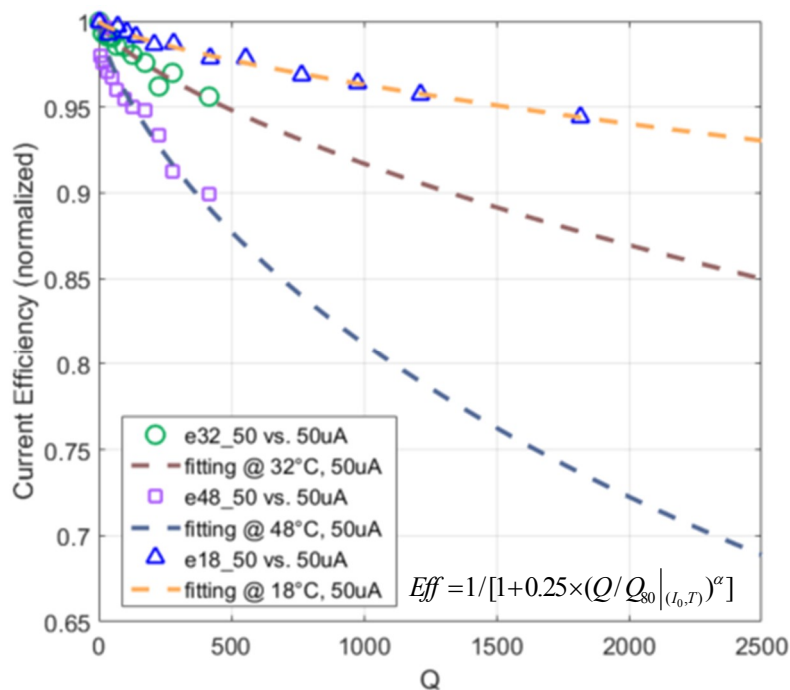


Figure 4-5 Current efficiency decay vs Q for OLEDs aged under various ambient temperature (18, 32, 48 °C). Decay exponent  $\alpha = 0.7926$ .

To quantify the thermal dependence of degradation, the Arrhenius law in physics is introduced, as shown in equation 4.8 [Wik.A2018, Parker1999]. This equation is commonly used to describe the rate of thermally-induced process/reaction, as an empirical relationship.

$$k = A e^{\frac{-E_a}{k_B T}} \quad (4.8)$$

$k$  is the rate of the thermally-induced process.  $A$  is the pre-exponential factor, a constant coefficient for this process.  $E_a$  is the thermal activation energy, which denotes a minimum amount of energy is required for process.  $k_B T$  is Boltzmann constant and absolute temperature.

Considering the thermally induced degradation process on OLED, the flowing relation regarding  $Q_{80}$  of coulombic degradation, can be established. At a given current amplitude ( $I_0$ ),  $Q_{80}^{-1}$  is attributed to ambient temperature. The higher temperature on device is applied, the stronger decay rate it would have ( $Q_{80}$  is smaller), without considering other acceleration factors.

$$Q_{80}^{-1} \Big|_{(I_0, T)} \propto e^{\frac{-E_a}{k_B T}} \quad (4.9)$$

$E_a$  describes the height of the potential barrier for degradation process, with respects to the HOMO-LUMO gap in OLED (eV). This coefficient is termed as the thermal activation energy. Increasing the activation energy would result in the improvement of device stability [Zoran2003].

In figure 4-6, the  $Q_{80}$  values of green OLED devices stressed at various temperatures are plotted. Based on the Arrhenius law above, the measurement data are fitted in high quality (R-square 0.9979). The result shows the sensitivity of degradation on the ambient temperature. The activation energy extracted in this case is 0.62 eV. In publication [Parker1999], the activation energy is  $0.67 \pm 0.06$ , which is in good agreement with the value achieved above. It is worth mentioning that, the degradation might be beyond this law at an extremely high temperature (e.g. 85°C).

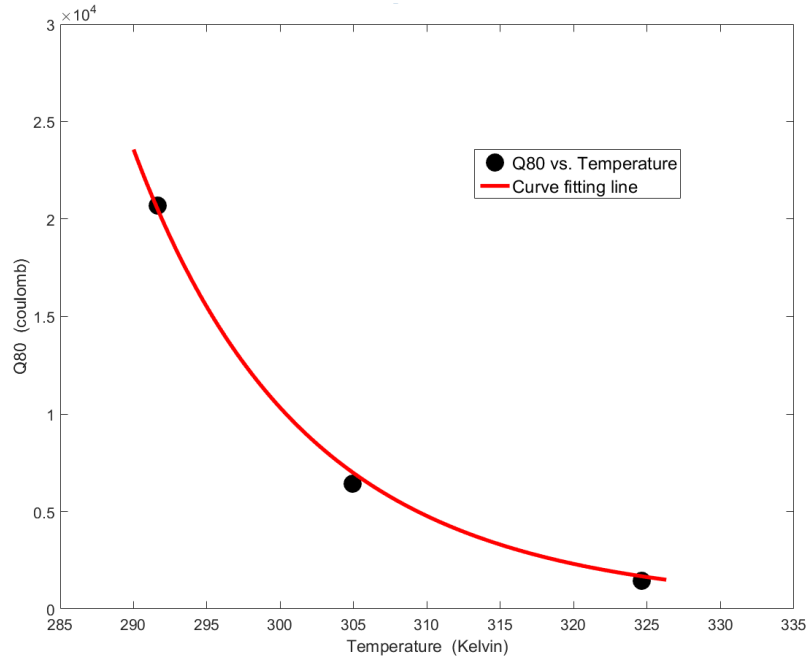


Figure 4-6  $Q_{80}$  versus temperature with  $E_a = 0.62$  eV.

When  $Q_{80}$  is fixed at a reference point  $Q_{80} \Big|_{T=T_{ref}}$ , the following equation 4.10 could be in further deduced. Here, the degradation is solely influenced by thermal acceleration effect, without considering current-amplitude acceleration effect (at a given point  $I_0$ ). Variable  $ACC(T)$  converted from  $Q$  in equation 4.3 describes the accumulated stress on OLED with the thermal dependence. The accumulation stress as a function of temperature is shown in equation 4.11.

$$Eff = \frac{1}{1 + 0.25 \times \left( \frac{ACC(T)}{Q_{80} \Big|_{T=T_{ref}}} \right)^\alpha} \quad (4.10)$$

$$ACC(T) = Q \times e^{\left( \frac{E_a}{k_B T_{ref}} - \frac{E_a}{k_B T} \right)} \quad (4.11)$$

The acceleration effect of ambient temperature in a wider range is thus considered in the thermal-induced accumulated stress function  $ACC(T)$ . Combined with the current-amplitude acceleration factor in the previous section, the accumulation stress considering all acceleration factors, as well as unified degradation function will be finally presented in the flowing section.

#### 4.4 Unified degradation profile

For current efficiency decay under various ambient driving conditions, they share the common shape—identical decay exponent  $\alpha$  ( $=0.7926$ ). The operation current and temperature do not change shape, but just affect the lifetime in scale/quantity. It is clearly shown in the previous sections. In reference [Ishii2002], it is identified that temperature and drive current do not change the relative contribution of degradation mechanisms. To practically implement the prediction in display system, a unified degradation profile merging various decay curves under multiple driving conditions should be established. The model could be then feasibly integrated into display application.

Figure 4-7 shows the unification of multiple decay curves into a single decay profile for OLEDs stressed under the various drive currents. The left figure shows multiple decay curves in experiment; the right figure is the unified decay profile based on equation 4.6 and 4.7, which consider the coulombic degradation law and current-amplitude acceleration effect. A single unified decay profile for flexible drive currents is thus achieved (at a given temperature  $T_0$ ). The parameters for the degradation curves are:  $\alpha = 0.7296$  and  $\beta = 2.122$ , respectively. For prediction, through calculation of the accumulated stress, the decay scale will be quantitatively derived from the unified decay profile.

Figure 4-8 shows the unification of multiple decay curves into a single decay profile for OLEDs stressed under various ambient temperatures. The unified decay profile in the right diagram is derived based on equation 4.10 and 4.11, which consider the coulombic degradation law and thermal acceleration effect. A single unified decay profile for flexible operation temperatures is obtained (at a given current  $I_0$ ). Here, the parameter  $E_a$  is equal to 0.62 eV.

## 4. Data-counting Model

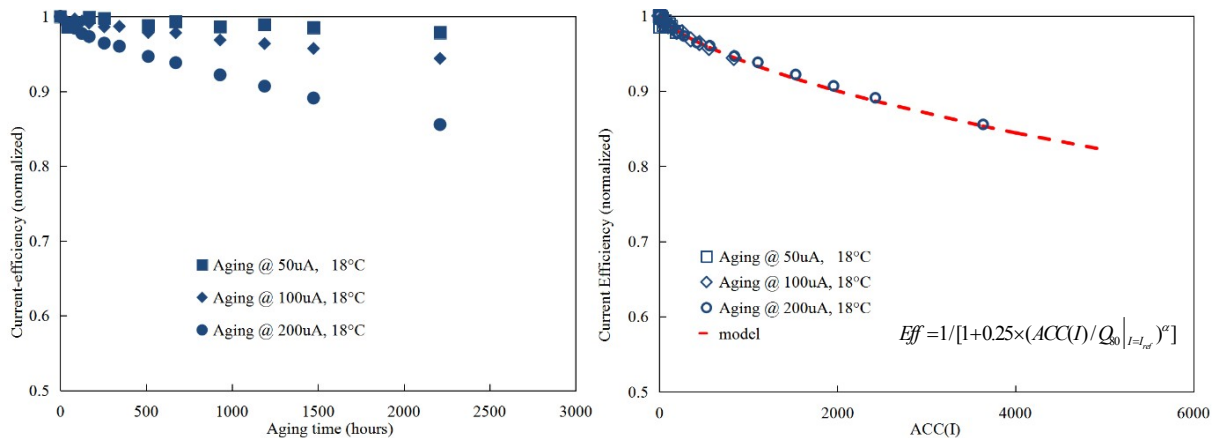


Figure 4-7 Multiple decay curves for OLEDs stressed under various drive currents in experiment (left); unified decay profile for various drive currents based on derivation in the model (right).

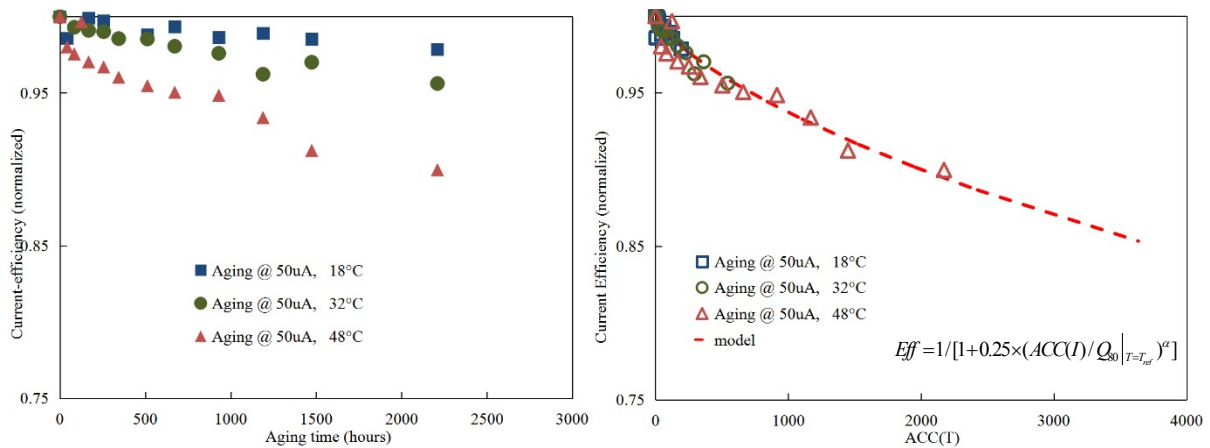


Figure 4-8 Multiple decay curves for OLEDs stressed under various ambient temperatures in experiment (left); unified decay profile for various ambient temperature based on derivation in the model (right).

### Data-counting model for multiple driving conditions

Considering both impact factors in terms of current amplitude and temperature for the degradation according to equation 4.7 and 4.11, the accumulated stress ACC could be derived, as shown in equation 4.12. The data counting model is established with consideration of the coulombic degradation law, the current-amplitude and thermal acceleration effects. The current

amplitude is known from operation and the temperature can be sensed. The accumulated stress on an OLED pixel under various driving conditions in a real operation can be thus counted.

Finally, the current efficiency decay with all impact factors can be established, as the following equation 4.13 shows.  $Q_{80} | I_{ref}, T_{ref}$  is given at one specific point of current amplitude and temperature degree (as reference).

$$\begin{aligned}
 ACC(I, T) &= Q \times \left( \frac{I}{I_{ref}} \right)^{\beta-1} \times e^{\left( \frac{E_a}{k_B T_{ref}} - \frac{E_a}{k_B T} \right)} \\
 &= \int \left[ \left( \frac{I}{I_{ref}} \right)^{\beta-1} \cdot e^{\left( \frac{E_a}{k_B T_{ref}} - \frac{E_a}{k_B T} \right)} \right] \cdot I \cdot dt
 \end{aligned} \tag{4.12}$$

$$Eff = \frac{1}{1 + 0.25 \times \left( \frac{ACC(I, T)}{Q_{80} | I_{ref}, T_{ref}} \right)^\alpha} \tag{4.13}$$

Figure 4-9 shows the unification of multiple decay curves to a single decay profile for OLEDs stressed under multiple driving conditions. The left figure shows multiple decay curves in the experiment; the right figure shows the unified decay profile with derivation from the equations above, which considers the coulombic degradation effect, current-amplitude and thermal acceleration effect. A data-counting model with unified degradation profile for flexible driving conditions is finally achieved. The model parameters for the degradation on OLEDs are:  $\alpha = 0.7296$ ,  $\beta = 2.122$ , and  $E_a = 0.62$  eV, respectively. Through the calculation of the accumulated stress, the decay scale can quantitatively be derived from the unified profile. Subsequently, Image sticking artifact can be suppressed with compensation based on the evaluation of accumulated stress.

## 4. Data-counting Model

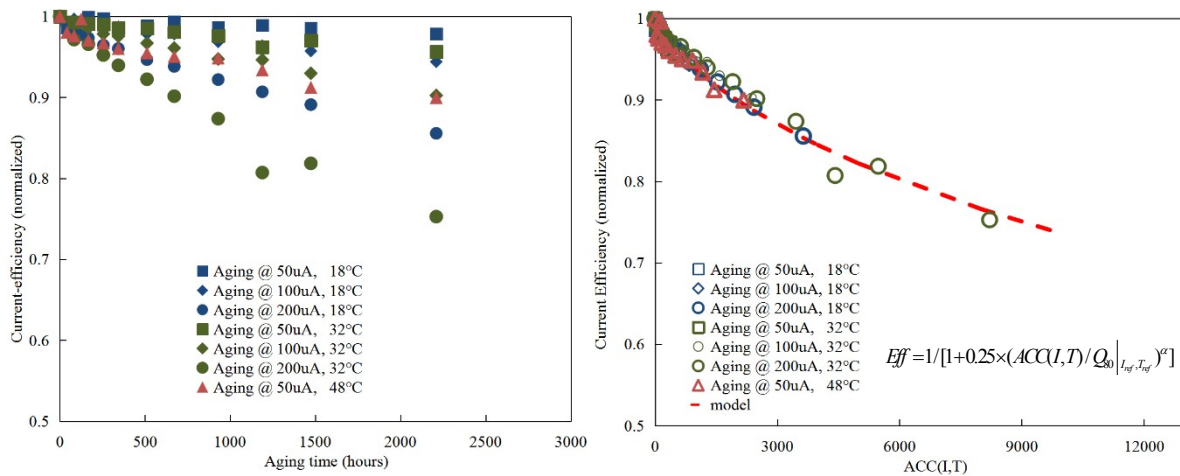


Figure 4-9 Multiple decay curves for OLED stressed under multiple driving conditions in experiment (left); unified degradation profile for multiple driving conditions based on model (right).

### 4.5 Discussion

In this chapter, we proposed a data-counting model for prediction of OLED degradation. In this model, the degradation of current efficiency was analyzed with consideration of the contributions of the coulombic degradation law, current-amplitude and thermal acceleration effects. A degradation model with a unified profile is finally established. Based on the model, the decay scale in current efficiency can be determined by counting the accumulation stress on devices. This approach provides a feasible means to quantify the degradation in operation, and supports prediction under multiple driving conditions. The pixel-wise compensation based on the model can be further implemented for AMOLED display.

Nevertheless, the decay profile depends on the operation point. Multiple decay profiles are needed for various operation points in a display system. This would not be an issue for the digital driving scheme due to fixed operation point, but in the analog driving scheme it should be concerned.

Besides that, an error accumulation may also occur during compensation. The accumulation stress on a pixel is counted in operation, and a deviation of data counting may be then accumulated with the operation time. In the long term, there would be an accumulation error for predicting degradation, resulting in a lower quality of compensation.

In chapter 5, an electro-optical model will be introduced, which could solve the OP in further.

A correlation model will be presented in chapter 6. This model can evaluate the decay of current efficiency with measurable electrical value. It may eliminate the issue of error accumulation.



## 5 Electro-optical Model

To interpret and predict the device performance in the aging process, a specific model for OLED degradation is critical. In chapter 4, a data-counting model for degradation has been introduced. The empirical model provides a unified decay profile, considering the impact of driving conditions, including various current amplitudes and ambient temperature. Through calculation of accumulation stress in operation, the decay scale of device can be quantitatively derived from the decay profile. As mentioned before, however, one challenge is that the degradation depends on the operation point, which make multiple decay lines required for different operation points in a display system (under the analog driving scheme, especially). In this chapter, an electro-optical model will be discussed. The model comprises an equivalent circuit and the electrical-optical characteristic for OLED. The efficiency decay at different operation points can be determined based on the equivalent circuit and its aging parameters. If the data-counting model is seen as a black-box model, in which the prediction for decay is solely based on empirical measurement data; then, the electro-optical model would be as a grey-box model, which is based on the internal equivalent structure of device. The merit of the electro-optical model is that the device performance at any operation condition (e.g. OP or even operation temperature) can be predicted in the aging process. Through determining the aging parameters in the model with calculation or measure, the efficiency decay of OLED device at any operation point can be derived. The electro-optical approach has been presented in publication [Jiang2018].

### 5.1 Structure and equivalent circuit

Generally, the charge injection into organic semiconductor is considered as thermionic emission across the energy barrier [Haldi2008]. The crossed energy barriers could be formed between electrode and organic layer, or two organic layers in the multi-layer structure. The current flow across such energy barrier could be modeled by the typical diode equation [Temp2014],  $I = I_S \left( e^{\frac{V_D}{nV_T}} - 1 \right)$ .  $I_S$  is the saturation current,  $V_D$  is the voltage applied on the

## 5. Electro-optical Model

diode,  $V_T$  is the thermal voltage (equal to  $kT/q$ ).  $n$  is the ideality factor (also called as the emission coefficient).

Figure 5-1 shows the structure and equivalent circuit of an OLED device. OLED device contains multiple organic layers and non-ohmic contacts for the electrode. The layers may be the electron and hole injection layer, the electron and hole transport layer, as well as the emission layer. Electrically, it can be seen as a serial circuit of three or even more diodes depending on the structure of the OLED [Zhao2012]. Serial diodes just impact the electrical characteristic (I-V), but not the optical characteristic (Eff-V). For simplicity, two or more series diodes (e.g. EIL|ETL|HTL|HIL) are merged into one serial diode (seen in Appendix 9-5), symbolized by  $D_{ser}$  in figure 5-1. The OLED device has resistance in each layer which is summed to the resistance  $R$ . For the emission layer, it is modeled by three elements, namely  $D_{emit}$ ,  $D_{non}$  and  $R_{leak}$ .

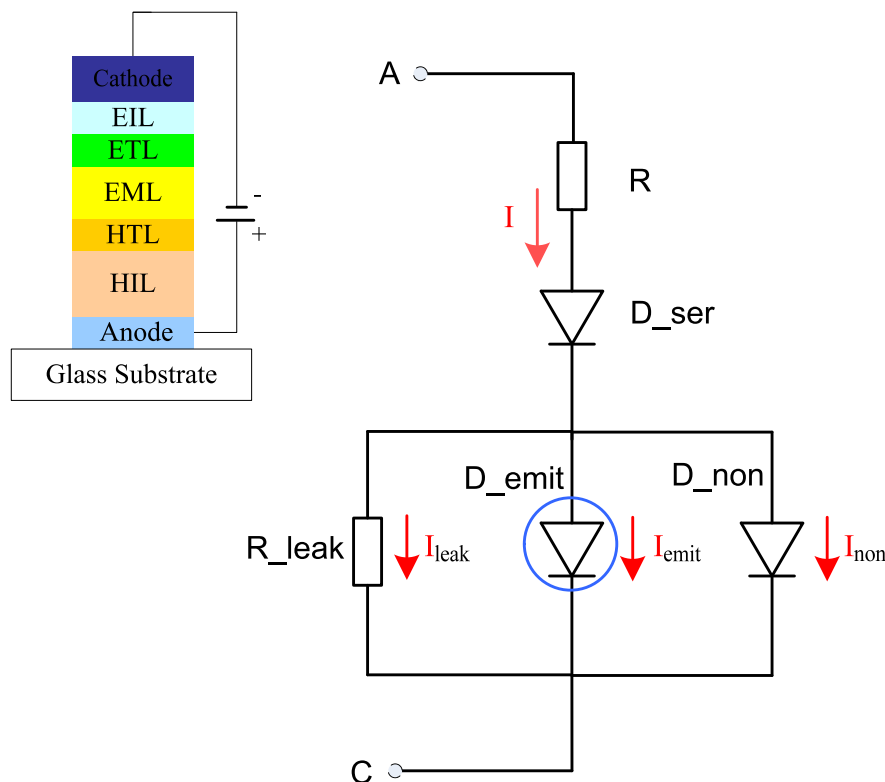


Figure 5-1 Structure and equivalent circuit of an OLED device.

OLED current is therefore split into three branches in the emission layer, as equation 5.1 shows.

$$I = I_{leak} + I_{emit} + I_{non} \quad (5.1)$$

The leakage resistance just has an influence at the very lower operation voltage. The current flowing through  $D_{emit}$  ( $I_{emit}$ ) generates visible light, whereas non-emissive current flow ( $I_{non}$ ) through  $D_{non}$  without generation of any light. It is attributed to the fact that the pair of electron and hole annihilates in the form of both radiative and non-radiative recombination. Both diodes ( $D_{emit}$ ,  $D_{non}$ ) have different parameters, so that current distribution between these two diodes is not constant, but depends on the voltage or current. The intrinsic radiative efficiency  $\eta_{int}$  as the property of  $D_{emit}$  (ratio between the luminance and  $I_{emit}$ ) is assumed to be constant in operation in our model. The effective current efficiency  $Eff$  for entire device is thus as equation 5.2 shows. The formula indicates that the current-flow distribution contributes to the operational dependency of current efficiency.

$$Eff = \frac{I_{emit}}{I} \times \eta_{int} = \frac{I_{emit}}{I_{leak} + I_{emit} + I_{non}} \times \eta_{int} \quad (5.2)$$

Consequently, the effective current efficiency depends on the internal current distribution, which varies with operation point. A dependency of current efficiency on operation point is shown in figure 5-2. This phenomenon has been identified in IVL measurements in chapter 3.

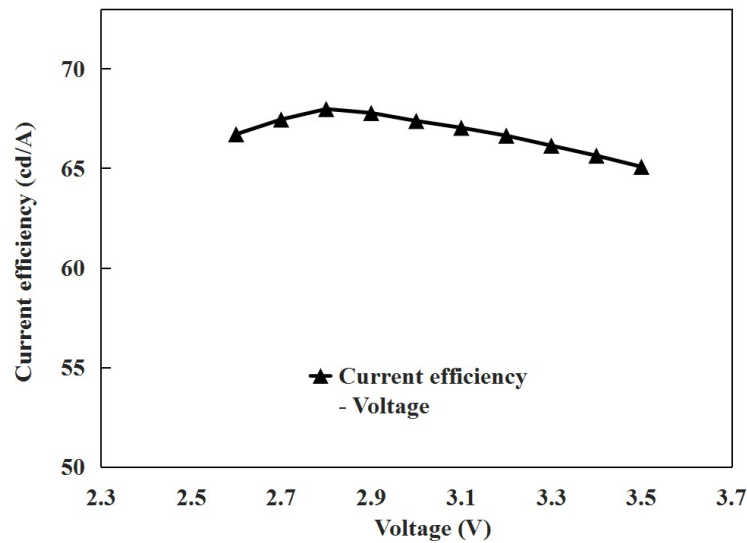


Figure 5-2 Dependency of current efficiency on operation point. Merck green OLED samples.

## 5.2 Electrical and optical characteristic

### A. Electrical Characteristic

The current-voltage characteristic (I-V) of an OLED is shown as figure 5-3 (a). The electrical curve successively presents three different behaviors: the leakage region at low voltage, the recombination region with sharply rising current flow, and the high operation region with rectification behavior.

The low leakage region is dominated by  $R_{leak}$ . It is related to a leakage current flow originating from the fact that in crossbar architecture there is an additional parasitic pathway [Nowy2010]. In theory, just one kind charge (the hole) is injected into the device in this stage and accumulated at the interface of HTL/EML. The majority of charge would not form current flow due to energy barrier and absence of electrons; whereas a small portion of holes will reach the cathode, forming a leakage current flow. Here, the leakage resistance is generally around  $G \Omega$ . It is worth mentioning that the leakage path in this equivalent circuit might also be described by a thermionic emission diode, instead of the leakage resistor  $R_{leak}$ . In reference [Kim2011], a diode equation was introduced to interpret the current flow in the low-voltage regime (before turn-on voltage). In our case, the leakage resistor is adopted in the equivalent circuit for simplicity, which has negligible impacts on the characteristic of the emitting stage we concerned (turn-on range).

In the recombination region, the two parallel diodes, emitting diode  $D_{emit}$  and non-emitting diode  $D_{non}$ , dominate the I-V behavior. It exhibits a sharp rise in current flow in this stage. In fact, with increasing voltage (after turn-on) the electrons are gradually injected into organic layers; meanwhile, the recombination of the pairs of hole and electron induces the dramatically increasing current flow through device. The recombination current flow is twofold: the radiative recombination which generates photons, and the non-radiative recombination which would not emit the visible light. In the model, the  $D_{emit}$  and  $D_{non}$  denote the emitting and non-emitting path, respectively. The parameters for them may be extracted from the I-V characteristic in the corresponding region.

In the high operation region, the serial diode  $D_{ser}$  and resistance  $R$  have a dominating influence on the current flow. It refers to the rectification effect which originates from non-

Ohmic and Ohmic conduction in/between multiple serial layers. The parameters for  $D_{ser}$  and  $R$  can be extracted from this region.

### **B. Optical Characteristic**

Figure 5-3 (b) shows the current efficiency of an OLED in the operation range. The identical optical characteristic of OLEDs was also presented by other researchers [So2010, Mahm2012]. In the curve, three regions are included: the dark region, the climbing region and the so-called Roll-off region.

In the dark region, there is no light emitted from the device, which is corresponding to the leakage region at low operation points of electrical behavior in figure 5-3 (a). It is due to the absence of recombination of dual charge carrier in this stage. In the model, since the threshold voltage of emission  $D_{emit}$  is not surpassed, the recombination current is zero and subsequently, no light is emitted. Therefore the current efficiency of the entire device is zero.

With higher operation voltage, the efficiency curve enters into a steeply climbing stage (until reaching a peak), which is synchronous to the recombination stage in electrical behavior. The significantly elevated efficiency is attributed to the improvement of charge balance of dual charge carrier (holes & electrons)—electrons are gradually injected after build-in potential. Corresponding to the equivalent circuit,  $D_{emit}$  starts to conduct and emits light beginning from this stage. Since the diode current is described by an exponential function, the current through  $D_{emit}$  and  $D_{non}$  increases steeply after turn-on, contributing to the sharp rise on the entire OLED current. Whereas, the leakage current through  $R_{leak}$  gradually become just a negligible share in the whole of the current flow.

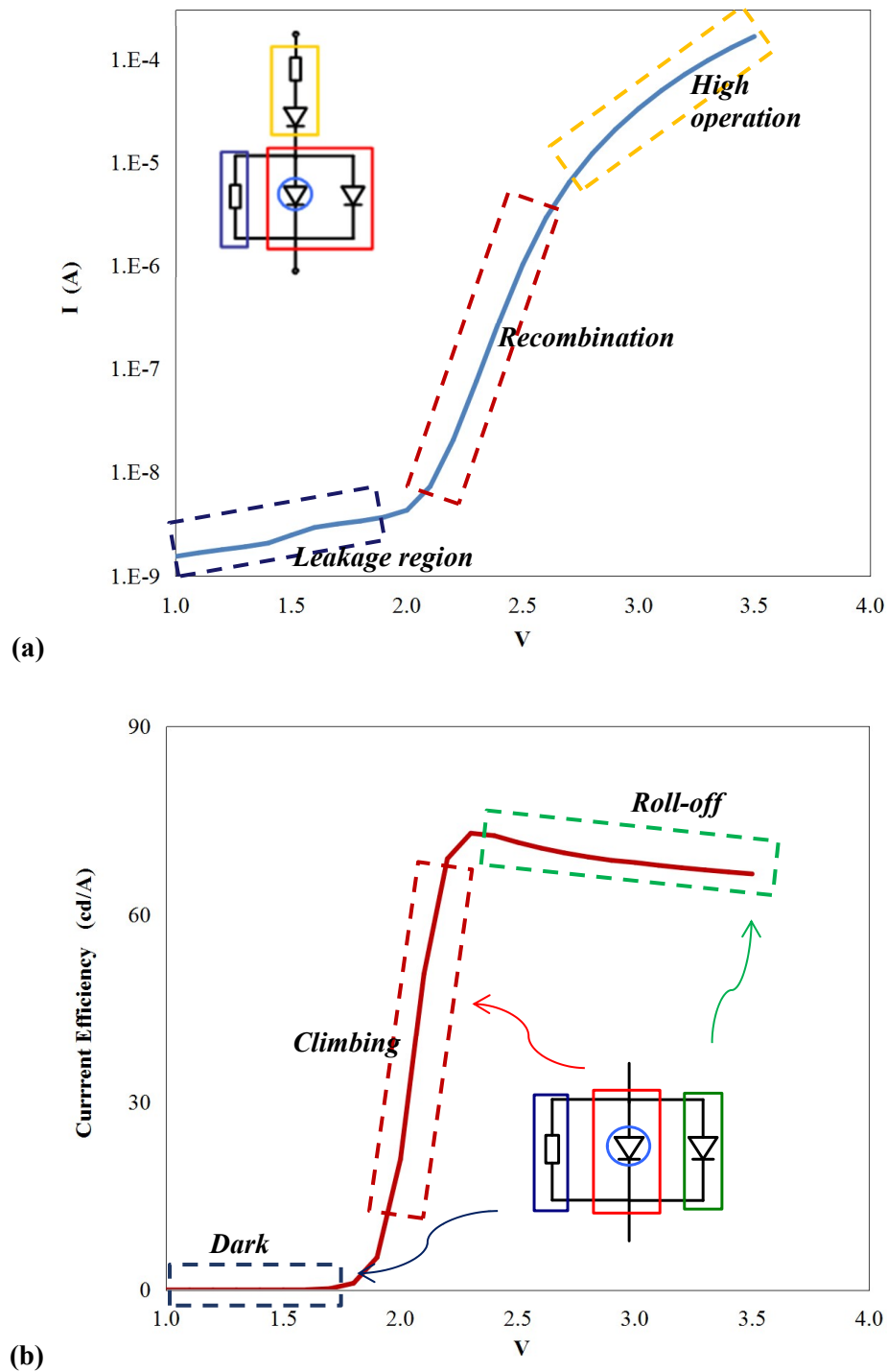


Figure 5-3 Electrical-optical characteristic of an OLED (a) Current-voltage (I-V) curve in semi-log (b) Current efficiency vs voltage curve (Eff-V).

In high operation range, OLEDs enter into the well-known Roll-off stage (after reaching the peak). The Roll-off behavior is generally observed at high operation points, as described in

many publications [Kali2002, Rein2007, Gieb2008, and Wehr2015]. The internal physical mechanism of the charge-balance decline or the exciton quenching (e.g. TTA) may be responsible for this phenomenon. In the model, the non-emitting diode  $D_{non}$  has a lower emission coefficient than  $D_{emit}$ , so that the share of  $D_{non}$  increases with higher voltage, resulting in a decrease of efficiency at the higher voltage. It is worth mentioning that the peak presents transition of predominated effects between the climbing stage and the roll-off stage, and is simulated by model elements  $D_{emit}$  and  $D_{non}$ .

With the equivalent circuit, the electrical-optical characteristic of OLED was simulated as shown figure 5-4 shows, including the current–voltage and current efficiency versus voltage curve. A good agreement between measurement data and simulation results has been achieved.

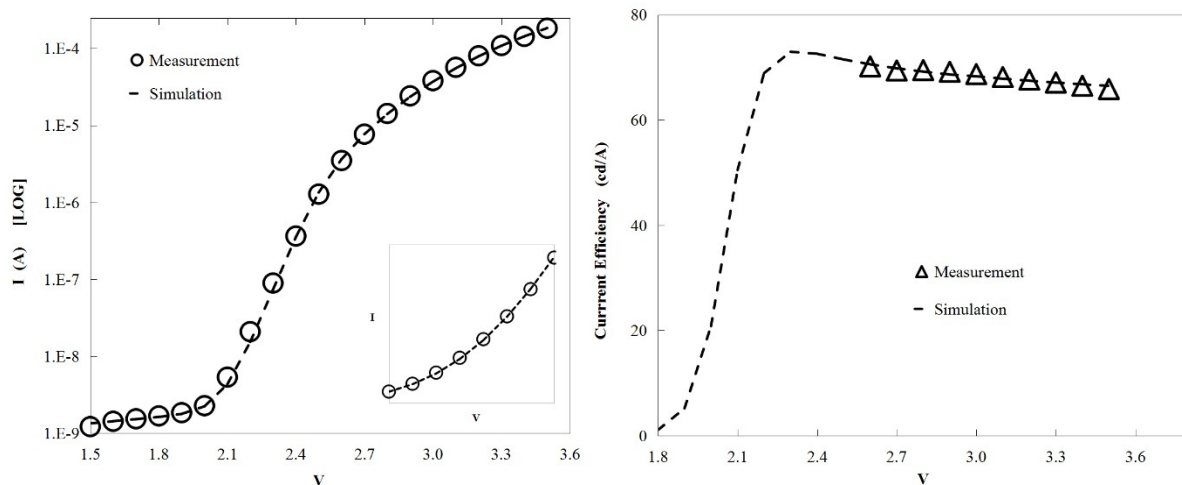


Figure 5-4 Simulation of the electrical-optical characteristic of OLED (a) Current-voltage curve in semi-log (b) Current efficiency vs voltage curve.

The parameters in the model have their individual dominating/sensitive regions in I-V and Eff-V curve, and thus can be extracted from the corresponding regimes from both curves in turn. The extraction for  $D_{emit}$  and  $D_{non}$  considers the recombination region in I-V as well as the roll-off stage in Eff-V. The extraction for  $D_{ser}$  and  $R$  mainly considers the rectification region of I-V, in high operation range. The  $R_{leak}$  is extracted from the leakage region of I-V and dark region of Eff-V, in low operation range. The model parameters are finally determined by an iterative optimization process with a combination of both the electrical and optical measurement data.

### 5.3 Modeling of degradation behaviors

The electrical and optical characteristic of OLED are properly described with the equivalent circuit, as discussed in the previous section. Each element in the circuit shows its corresponding domination region in the Current-voltage and Current Efficiency-voltage curves. Parameters are extracted from the experimental data in turn. In chapter 3, we learned that both electrical and optical properties experience a significant decay during operation in the experiments. The electrical-optical performance in the aging process can be simulated with the equivalent circuit and corresponding parameters. The decay in electrical-optical characteristic due to internal degradation mechanisms, are modeled by the drifting parameters in the equivalent model. Determining deteriorated parameters in the equivalent circuit will help to evaluate the electrical-optical performance of the device in aging.

For each specific aging state, a set of parameters are extracted from the I-V-L measurement. Good agreement between measurement and simulation is achieved, as shown in figure 5-5. The electrical characteristic of OLED devices dramatically decays during operation. Figure 5-5 (a) shows the I-V curve at the pristine and an aged state. I-V curves of samples substantially drift in the aging process. In higher operation range, the current through device drops with the operation time. And the leakage current rises as seen in the low operation range. The interface deterioration or traps formed in serial layer may contribute to the drift in rectification region, which is of particular concern for OLED electrical performance (the current drop in the digital driving scheme; and voltage rise in the analog driving scheme.) The drift in the rectification region is simulated with a variation of parameters of the serial diode  $D_{ser}$  and resistance  $R$ .

Figure 5-5 (b) shows the current efficiency versus voltage at the pristine state and aged state. The current efficiency curve drifts in the aging process, with dependency on operation point. The degradation mechanisms such as non-radiative recombination center (Trap-assisted recombination TAR) or the enhanced exciton quenching (trap-induced TPQ) may contribute to the decay of current efficiency. Based on the equivalent circuit, the degradation behavior is interpreted by the aging on the emitting diode  $D_{emit}$ . At very low voltage, the fitting shows a deviation to some extent. There may be two roots: very simple model for the leakage path; and measurement error due to very low current and particularly low luminance. Since OLEDs are generally operated at higher voltages where recombination current is more predominant, a certain discrepancy at low voltages wouldn't be problematic.

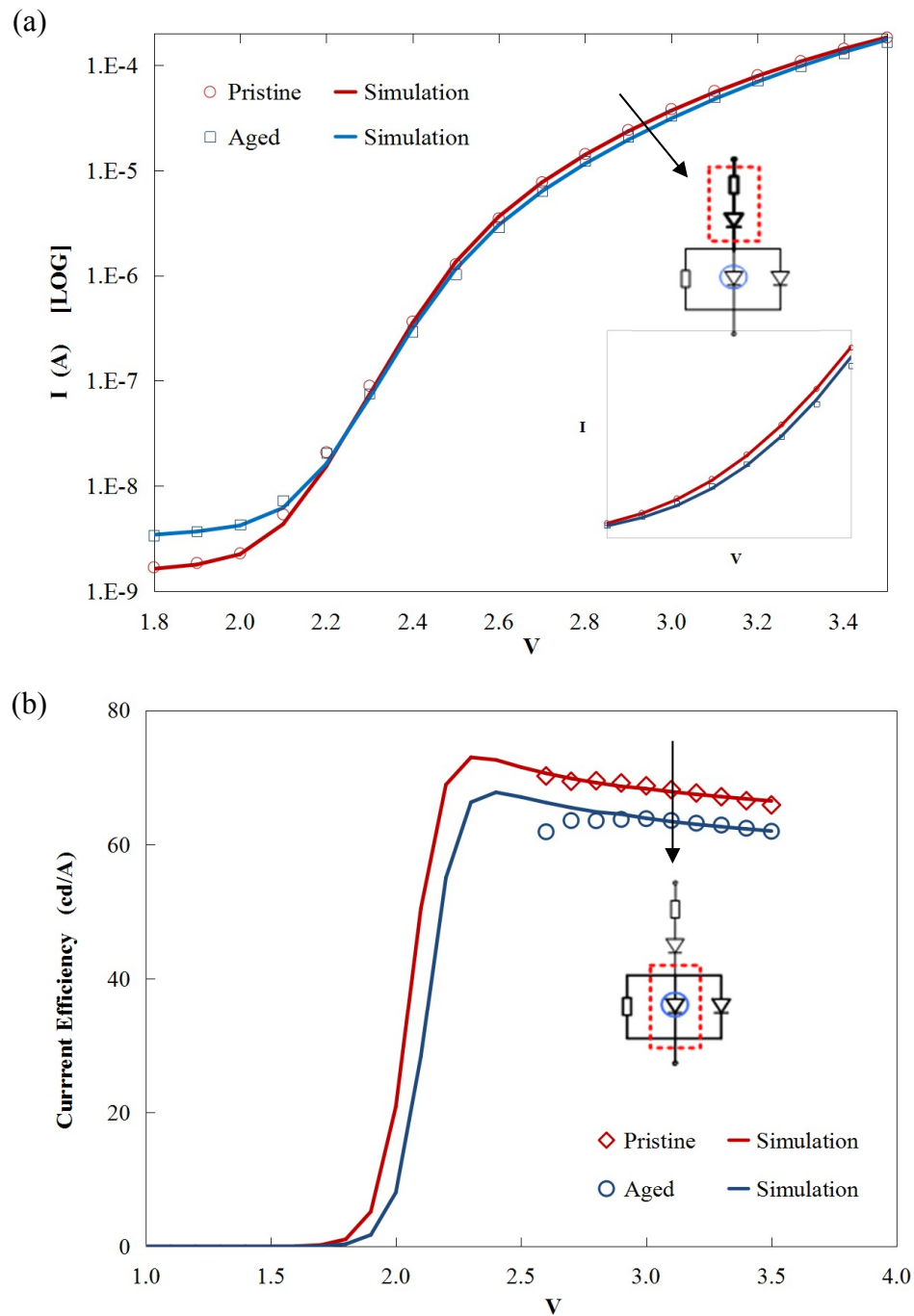


Figure 5-5 Measured and simulated electrical-optical Characteristic at two states in aging process. (a) Semi-log current-voltage curves; (b) current efficiency vs voltage curves. The empty symbols (squares,circles) are experimental data; the solid lines represent the simulations.

### Dependence of model parameters on aging states

The real value for the model is the ability to predict the performance on device in aging, especially the degraded efficiency—it is not directly measured, but predicted with model in

operation. In agreement with intrinsic physical/chemical degradation process, the dominated parameters in the model deteriorate in aging, resulting in the decay behaviors of electrical-optical properties. In this case, it is assumed that the main optical degradation lies in the emissive diode, e.g. due to exciton quenching. For a stringent parameter extraction, just few parameters should drift with the operation time, and the drifting parameters would show a reasonable trend which is consistent with the drift of I-V and Eff-V characteristic.

Figure 5-6 (a) shows the decay of the normalized saturation current of  $D_{emit}$ , which is the most critical parameter in this aging model. The decreasing  $Is_{emit}$  correlates to the drift of current efficiency in figure 5-5 (b). This parameter was extracted at many states during aging test. Consequently, the curve is monotonically decreasing and consistent with the drift in the current efficiency. It implies that the emitting diode gets weaker during the operation, provided the non-emitting diode  $D_{non}$  remains constant in the process. With the parameter  $Is_{emit}$  decreasing, the effective current efficiency according to equation 5.2 gets lower.

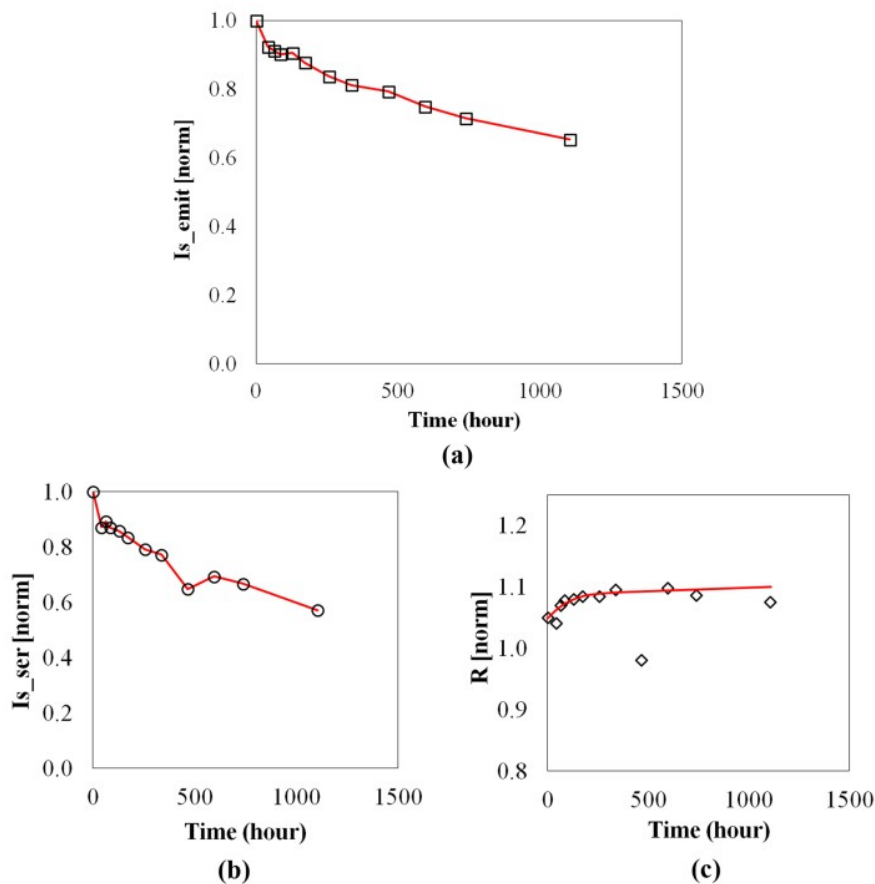


Figure 5-6 Extracted parameters from OLED aging test are plotted with aging time (hours). (a)  $Is_{emit}$  (b)  $Is_{ser}$  (c) serial resistance R.

Figure 5-6 (b) and (c) shows the aging of the normalized saturation current on  $D_{ser}$  and the normalized serial resistance  $R$ . The decreasing  $I_{s\_ser}$  in figure 5-6 (b) corresponds to I-V drift at higher voltage in figure 5-5 (a). The offset of  $R$  at the very beginning is due to the known jump of I-V characteristic in the aging process. Further increase of  $R$  in figure 5-6 (c) correlates with the decrease in the slope at very high voltage in figure 5-5 (a). The variation of the two parameters represents the decay in the serial layers. Injection-barrier rise or conduction decline mainly contribute to the degradation, as analyzed in chapter 2. The decay in serial layers is responsible for the drift of electrical characteristic, but has no impacts on efficiency decay.

The simulation based on the equivalent model and aging parameters is in high agreement with experimental electrical-optical behaviors in operation. This confirms to a certain extent that the degradation in electrical and optical properties can be correlated with the deterioration of parameters in the model. The aging parameters extracted from OLEDs also gives us an internal inspection for degradation. The values of the model parameters on green OLED samples are given in Table I.

Table 5-1 Parameters of Model (pristine)

Parameter	Value	Parameter	Value
<b>R</b>	1.213K $\Omega$ *	<b>R_leak</b>	1.962G $\Omega$ *
<b>I<sub>s_ser</sub></b>	7.745E-6 A *	<b>N_ser</b>	6.208
<b>I<sub>s_emit</sub></b>	8.450E-25 A *	<b>N_emit</b>	2.368
<b>I<sub>s_non</sub></b>	7.536e-26 A	<b>N_non</b>	2.277
<b><math>\eta_{int}</math></b>	109.536cd/A		

\* marks the drifting parameters in aging

In the aging process, the parameter  $R$  and  $I_{s\_ser}$  are mainly responsible for the drift of electrical characteristic, and  $I_{s\_emit}$  contributes to the deterioration in optical characteristic. The influence of  $R_{leak}$  has been neglected. It's worth mentioning that the emission coefficients of an OLED are substantially higher than that of a silicon p-n diode which is close to unity. In this case, it is indeed around 2, implying the strong physical background. This value is also consistent with the

result reported by other group [Kim2011]. The value of  $N_{ser}$  is the sum of multiple serial layers and each layer is also around 2.

### Dependency on driving conditions

Indeed, the decay scale on devices depends on the driving conditions, especially the drive current (initial luminance) and ambient temperature, as discussed in section 3.3. In the data-counting model presented in chapter 4, the effects of driving conditions were considered and evaluated for prediction of the current efficiency decay. In the electro-optical model, whereas, the dependency of device degradation on driving conditions is evaluated with internal aging parameters in the equivalent circuit. The similar approach in the data-counting model could be used to estimate the aging parameters in the equivalent model. Thus, through the calculation of accumulation stress on internal aging parameters, the current efficiency decay in quantity can be calculated, and its decay in multiple operation points can also be derived.

Figure 5-7 (a) shows the decay curves of parameter  $Is_{emit}$  under various driving conditions in the aging tests. It shows that the aging of parameters depends on driving conditions. To practically predict the decay scale, a unified decay profile for the aging parameter is derived (with merging the multiple decay curves), as shown in figure 5-7 (b). The result shows the high consistency for various driving conditions. For other aging parameters, unified prediction line could also be achieved with the same approach as discussed above.

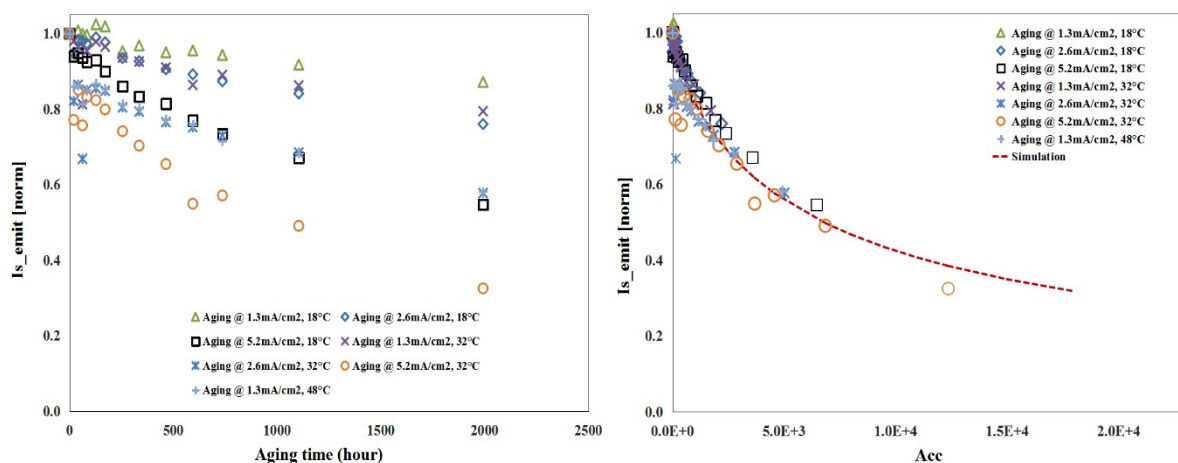


Figure 5-7 (a) Multiple decay curves for  $Is_{emit}$  at various driving conditions (b) an unified decay profile for  $Is_{emit}$  at various driving conditions.

## 5.4 Analysis with simulation

### Simulation of OLED characteristic

The effective current efficiency depends on the internal current distribution, as presented in section 5.1. In figure 5-8, the simulation for internal current-flow distribution has been made based on the equivalent circuit, including leakage current flow, the emissive and non-emissive current flow. Each current flow was normalized to the entire current flow through the device. It shows that the simulation for internal emissive current flow is consistent with the behavior of current efficiency in experiments—it subsequently enters into the dark, climbing and Roll-off stage with increase in the operation voltage. In the low voltage range, the leakage path dominates the entire current flow, and no emissive recombination current flows through the device (no visible light). It identifies that in the low operation range (before turn-on), only single-polar carriers (holes) are injected into organic layers, without forming bipolar recombination. With higher voltage, the emissive and non-emissive path are conducting, and recombination current through them steeply increases. Meanwhile, the leakage current share rapidly falls until as a negligible effect in high operation range. Because the luminance is proportional to emissive current flow, the emitting light from device will thus dramatically rise. The recombination effect indeed dominates this stage. In the high voltage range, the emissive current flow distribution gradually rolls off (after reaching a peak), due to continuously increasing flow in non-emissive recombination path. In the model, it is attributed to the smaller value of ideal factor  $N_{non}$ , compared to  $N_{emit}$ . In physical theory, the internal degradation mechanisms such as charge-balance decline or exciton quenching (e.g. TTA) are responsible for this behavior.

In figure 5-9, simulation of internal voltage distribution was made for analyzing the electrical characteristic, including voltage applied on serial layer ( $D_{ser}$  and  $R$ ), as well as on the emission layer ( $D_{emit}$ ). The voltages on them are normalized to the entire voltage supply on device. It obviously shows that the serial layer exerts a dramatic limitation on the current flow through device in the high operation range, which is consistent with the rectification behavior of I-V characteristic in figure 5-3 (a). In fact, the limitation on current flow commonly occurs in high voltage range due to the lower mobility of holes. In the low operation range, the emission layer dominates the entire voltage, due to no limitation in serial layer in this stage.

## 5. Electro-optical Model

Both emissive layer and serial layer contribute to current flow in high operation voltage, indicating a partial correlation between the electrical degradation and optical degradation.

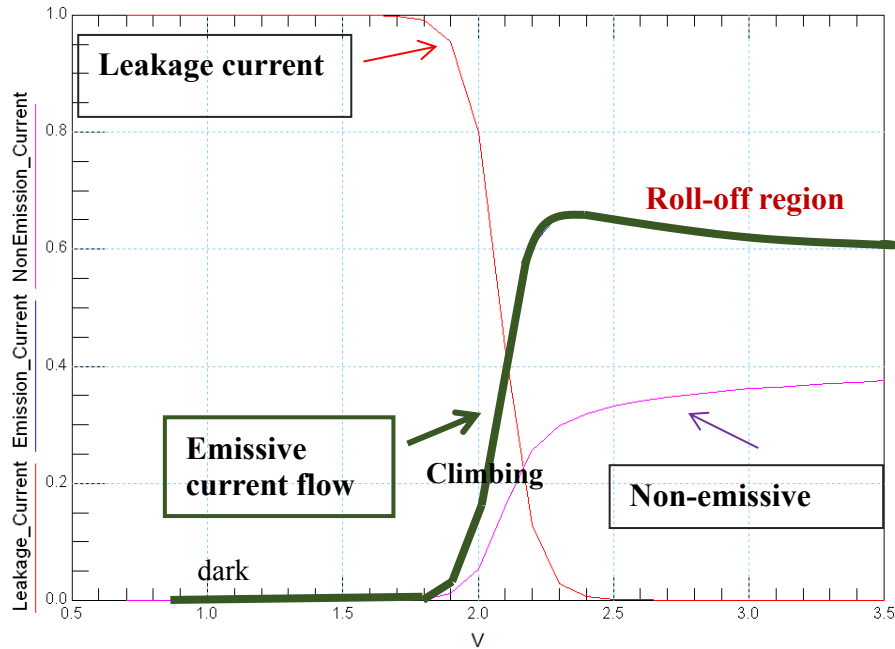


Figure 5-8 Internal current-flow distribution over operation range: the leakage current flow (red solid line), the emissive current flow (green solid line), and the non-emissive current flow (purple solid line). Data from Green Merck OLEDs.

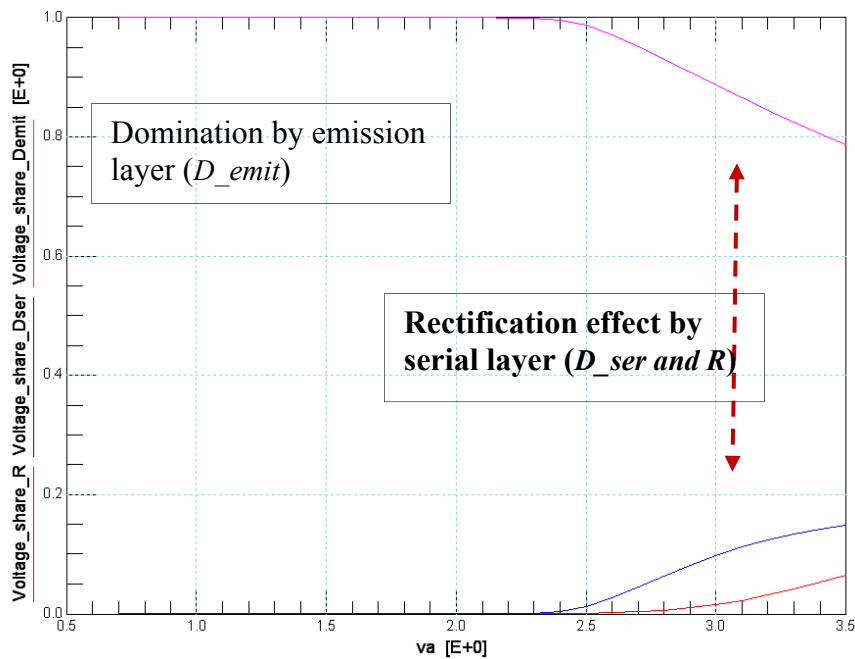


Figure 5-9 Internal voltage distribution over operation range: voltage on emission layer (purple solid line), on serial resistance R (red solid line), and on serial diode (blue solid line).

### Simulation of degradation

Figure 5-10 shows the simulation of emissive flow distribution with parameter  $I_{s\_emit}$  changing in the aging process. The result shows that internal emissive current-flow distribution drops with deterioration of parameter  $I_{s\_emit}$ —the corresponding effective current efficiency decays with the aging parameter. This identifies the theory that the decay in electrical-optical characteristic can be modeled by the drifting parameters based on the equivalent circuit, as presented in the previous section. It provides a feasible means to quantify the current efficiency decay on device during operation.

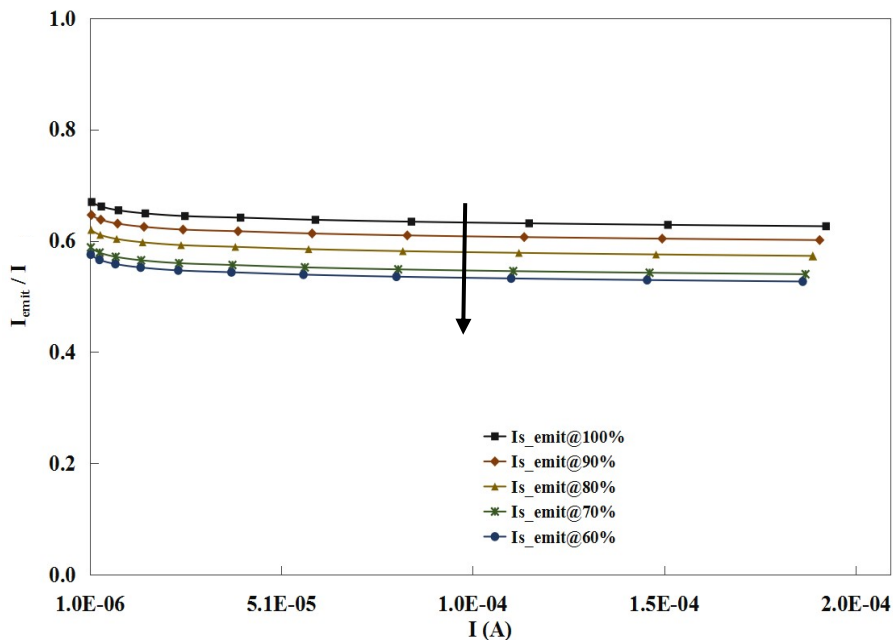


Figure 5-10 The simulation of emissive flow distribution with deterioration of parameter  $I_{s\_emit}$  in the aging process.

## 5.5 Conclusion

An electro-optical model has been presented in this chapter. The model is built based on an equivalent circuit, considering the internal multi-layer structure and the emitting process. In operation, the current flow through device is split into the internal leakage, radiative and non-radiative recombination flow. The effective current efficiency is thus attributed to internal current-flow distribution with the dependency on operation point. The electrical and optical characteristic can be simulated with the equivalent circuit. In further, the degradation behaviors

in characteristic originated from internal degradation mechanisms, are simulated by the drifting parameters in the equivalent model. Through calculating the deteriorated parameters in the equivalent circuit, the electrical-optical performance at any operation point can be quantitatively evaluated during operation. The result shows that the electro-optical model is reliable to simulate the electrical-optical characteristic and degradation behavior for OLEDs.

In chapter 7, the prediction and compensation based on the electro-optical model will be implemented on OLED devices and AMOLED display.

## 6 Correlation Model

Besides the models above, an additional feasible approach to quantitatively evaluate the efficiency decay is called correlation model. This method is intended to derive a correlation between the current efficiency decay and measurable electrical value. Through measuring the change of electrical characteristic of an OLED in operation (e.g. current variation), the relative efficiency decay can be calculated based on the correlation. Then, the corresponding compensation can be implemented to alleviate image sticking artifact. Compared with the data-counting model in chapter 4, the correlation model may prevent error accumulation in the long-term operation, and deliver a more reliable result in strongly aged states. Furthermore, combined with the equivalent circuit in chapter 5, the estimation of decay of current efficiency at any operation point could be feasible.

In the correlation model, the current flow is as a sensitive factor to evaluate the efficiency decay. Some research groups also presented other potential measurable electrical values for correlation. Chen et al. proposed a capacitance-based method for degradation [Chen2012]. Chaji et al. introduced a method of correlating the voltage change / capacitance variation to the luminance loss on pixels [Ignis2015, 2016]. However, the approach using capacitance as the indicator for decay in optical characteristic is limited. Firstly, the capacitance sensitivity for degradation depends on the device materials and structure. In some OLEDs, the capacitance dramatically varies in the aging process, whereas on some others they may not. Indeed, while the charge accumulation might induce the capacitance variation, the degradation mechanisms such as exciton quenching/chemical reaction are not likely to cause capacitance change. Subsequently, even though capacitance shows sensitivity for degradation to some extent, detecting the capacitance variation which is related to the optical degradation is a complex issue, because of the multi-layer structure of OLED. For example, the  $C_{\text{geo}}$  as the geometrical capacitance comprises the capacitances in multiple serial layers; but only the variation of capacitance in EML correlates to the efficiency decay. Besides of capacitance, voltage rise as another potential hint to estimate the efficiency decay in the analog driving scheme [Yu2015,

Weon2006]. However, the sensitivity will be quite low, since the voltage rise is modest in the aging process.

### 6.1 Correlation between efficiency decay and current drift

As discussed in chapter 3, the I-V characteristic shift in the aging process. At a given voltage the current flow through device would drift with operation time. The decay in electrical and optical characteristic are fundamentally linked phenomena according to the analysis of degradation mechanisms in chapter 2. Some degradation mechanisms may contribute to both decays. For example, with the accumulation of charge traps in the emission zone, two effects may be induced: formation of non-radiative recombination centers (efficiency decay), and conductivity decline (voltage rise/current decrease). Moreover, the correlation between them can also be analyzed with the equivalent circuit in chapter 5. The deterioration of radiative diode in EML not only plays a role in the efficiency decay but also in the current flow drop. A correlation between the efficiency decay and current drift can be assumed.

Figure 6-1 shows a correlation between the efficiency decay and current drift in the aging test. The Merck blue OLEDs were stressed at 1200 nits for approx. 1600 hours. I-V-L measurement was taken at each interval during aging. The value of current and efficiency at the pristine stage is as the origin (point [1, 1]). The current flow and efficiency at each aged states were normalized to its pristine stage. With aging time, both efficiency and current flow gradually decrease. The correlation is then extracted, as shown in the figure. The result demonstrated that there is a correlation between the efficiency decay and current drift. The optical characteristic deteriorates with electrical characteristic simultaneously. Additionally, the correlation shifts with operation point to some extent (i.e. 3.2-4.0V). The experimental result for other samples could be found in Appendix 9-6. The efficiency decay correlates with the current drift as discussed above.

A pixel-wise current measurement can be easily implemented for an AMOLED module by inserting a measure unit in external power supply. The method has been developed by Pascal Volkert and described in his thesis [Volk2017]. The pixel circuit and interconnects of the AMOLED glass do not need to be modified, so that the manufacturing complexity and cost of the AMOLED glass are not increased.

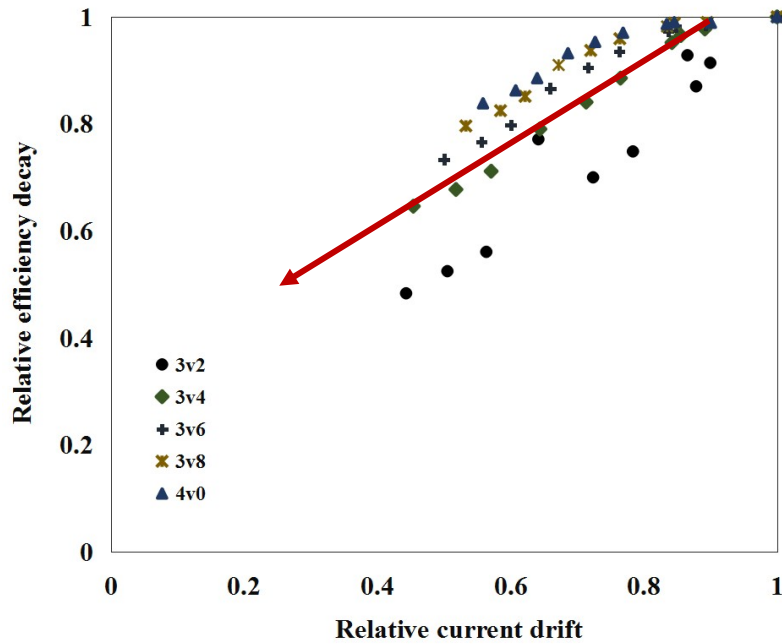


Figure 6-1 Correlation between the efficiency decay and current drift in the aging process. Data from Merck blue OLEDs.

## 6.2 Linear correlation profile

As analyzed above, the efficiency decay can be correlated with current drift in the aging process. It implies that the pixel current is a sensitive measurable value to calculate the efficiency decay based on the correlation profile. A linear correlation profile between the efficiency decay and current drift can be feasibly applied for the compensation of degradation in long-term operation, as the following equation formed approximately,

$$\frac{Eff}{Eff_{pristine}} = k \times \frac{I}{I_{pristine}} + d \quad (6.1)$$

$k$  is the proportional factor,  $d$  is offset. Both depend on the operation voltage. The offset may be due to the interface deterioration in OLEDs at the beginning of aging process.

In figure 6-2, the correlations of the efficiency decay and current drift at various operation points were fitted with linear formula 6.1. A linear relationship has been extracted with the measurement data. Also, the line slope increases with decrease in the operation voltage.

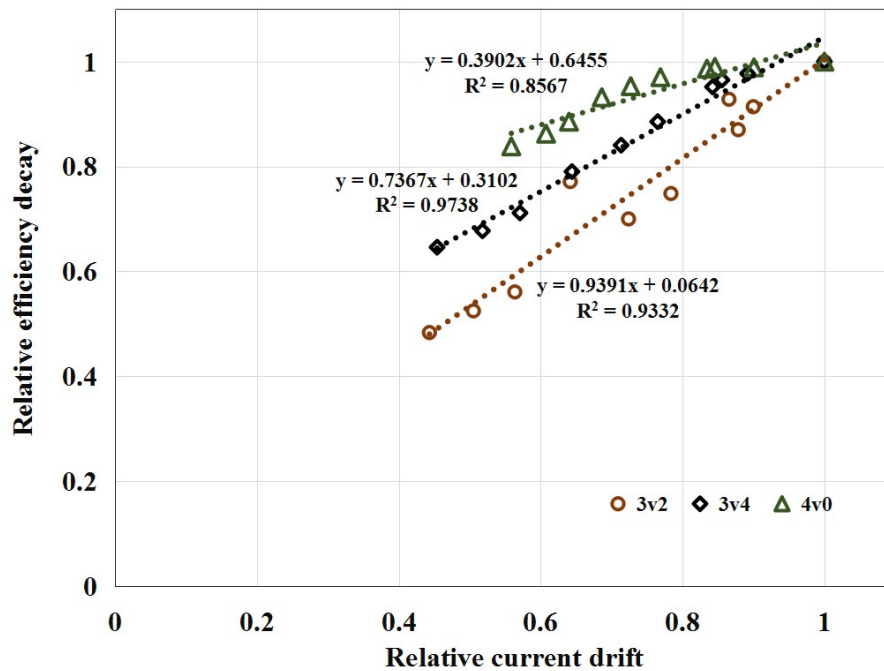


Figure 6-2 Relative linear correlation between the efficiency decay and current drift.

It is also possible to fit with a non-linear function to achieve more accuracy correlation to evaluate the efficiency decay quantitatively.

### 6.3 Partial correlation

Even though there is a strong relation between the efficiency decay and current drift, the correlation is not 100%. Indeed, the decays in the electrical and optical characteristic are partially correlated. Some degradation mechanisms may contribute to both of them, whereas some others only impact one of them. As mentioned before, the accumulation of charge trap in EML may induce both voltage rise and non-radiative recombination center. The exciton quenching plays a role in optical degradation. The deteriorations of injection interface and charge transport are mainly responsible for decay in electrical characteristic.

In figure 6-3, the correlation with dependence on operation point is shown. The curve at lower voltage point (i.e. 3.2V) is well fitted with a linear formula, and the curves at higher points (i.e. 3.6, 4.6V) are fitted with a non-linear function in high quality. At the high voltage point, the current flow drifts more sharply than the efficiency decay, especially in the beginning phase of

aging—efficiency is relatively stable while the current flow significantly decrease. It implies that the correlation at higher operation point is weaker, in comparison to the lower operation points.

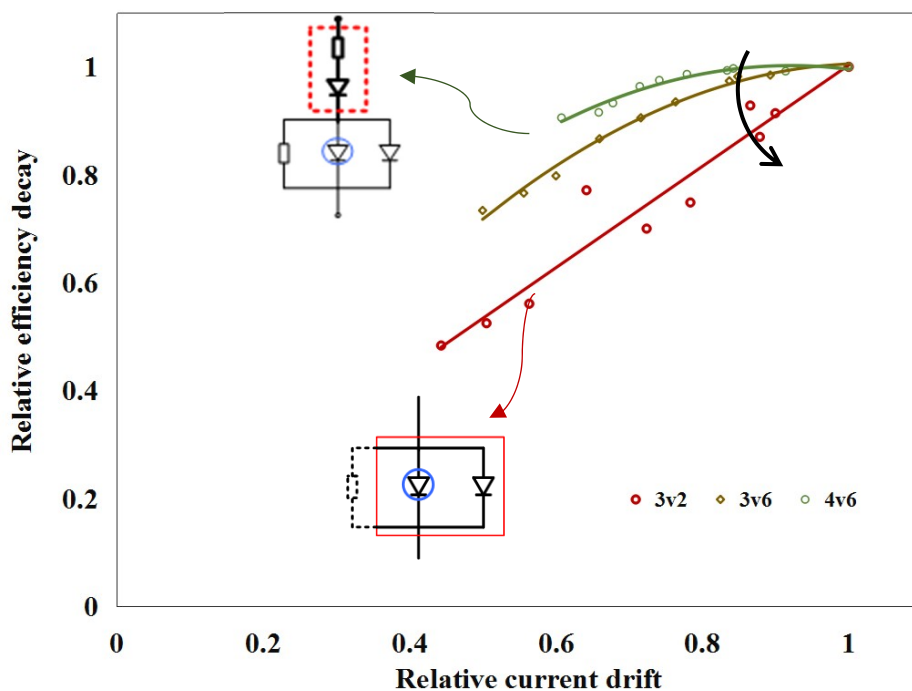


Figure 6-3 Correlation depends on operation point.

Based on the equivalent circuit in chapter 5, the partial correlation between electrical and optical degradation can be analyzed and identified. For the electrical characteristic, the serial elements (serial diode, resistance) and parallel elements (radiative, non-radiative, leakage) contribute to the current flow on device. For the optical characteristic, whereas, the current efficiency is determined by parallel elements (internal current-flow distribution).

At higher operation points (e.g. 4.6V), the serial layers exert a dramatic rectification on current flow. The deterioration of serial elements then plays a primary role in current drift, beside the drift caused by parallel elements. The current drift is therefore partially correlated with the efficiency decay. And even more, it is observed that these two changes are unrelated at the very beginning phase (e.g. the beginning 10% loss on current). In applications, the pre-aging may be applied on the OLEDs to solve this issue.

At a lower point (e.g. 3.2V), the rectification effect caused by serial elements is negligible. Both the current drift and efficiency decay are common attributed to deterioration in parallel elements. Therefore, there is a full correlation between the efficiency decay and current drift in this operation region. The efficiency decay is approximately linearly proportional to the current drift. Indeed, the influence from leakage branch is also negligible in the emitting state (after turn on). Thus, the radiative and non-radiative diodes in parallel circuit dominate the electrical and optical behaviors.

### 6.4 Correlation for aging parameter

The correlation model is aimed to derive the efficiency decay with the measurable electrical value. As discussed above, however, the correlation between efficiency decay and current drift depends on operation point. In higher operation voltage, they are partial correlation. But in a lower operation point (after turn on, before rectification), they can be fully correlated. The challenge is that the decays at higher operation points should be more concerned. The main emitting points (luminance output) are generally in higher operation range. Therefore, how to evaluate the efficiency decay at higher operation point and in a wide range, becomes the key. In section 6.2, some linear correlation curves at various operation point have been extracted for compensation. However, it is still insufficient. The correlation gradually becomes less related at higher operation voltage. The multiple correlation profiles for various operation points are also needed in compensation, increasing the complexity of implementation.

To solve this issue, the correlation model may be combined with the equivalent circuit. In aging, the efficiency decay is attributed to the deterioration of parameter on radiative diode ( $I_{s\_emit}$ ). At the lower operation point, the aging radiative diode is solely responsible for the current drift and efficiency decay, behaving in a fully linear correlation. Inversely, according to the full correlation at lower point, the aging parameter can be calculated exclusively. In further, the efficiency decay at each given operation can be evaluated based on the equivalent circuit, especially for the higher emitting range. It should be noted that in higher operation range, the aging parameter responsible for the efficiency decay cannot be calculated properly. It is due to the drift of other parameters from serial layers meanwhile, which only contributes to the decay in the electrical property.

### Evaluating aging parameter with correlation profile

To calculate the efficiency decay in a wide operation range, the aging parameter ( $I_{s\_emit}$ ) should be determined according to full correlation at a lower point. The full correlation profile can be extracted from a number of OLED samples in the previous aging tests. According to the extracted correlation profile, the efficiency decay scale at a lower point (e.g. 3.2V) can be calculated, through measuring current drift. The aging parameter can be then derived based on the measured current drift and calculated efficiency decay (at the given low point), as the following equation shows.

$$\frac{I_{s\_emit'}}{I_{s\_emit0}} = \frac{I'}{I_0} \Big|_{V_{low}} * \frac{Eff'}{Eff_0} \Big|_{V_{low}} \quad (6.2)$$

Here,  $I_{s\_emit0}$  denotes the initial saturation current on radiative diode. The  $I_0$  and  $Eff_0$  are the initial current flow and current efficiency at a given low point  $V_{low}$ . The  $I'_{s\_emit}$ ,  $I'$  and  $Eff'$  denote the values in the aging stage. It has to be noted that the measurement point  $V_{low}$  should not be too low than turn-on voltage. Otherwise, the leakage branch will influence the correlation.

After evaluating the aging parameter, the efficiency decay at higher operation points and in a wide range can be calculated according to the equivalent circuit. The parameters for equivalent circuit have been extracted in the previous tests, including the stable parameters for the serial and parallel elements.

### Unified degradation correlation for various driving conditions

As presented before, the degradation of OLED is dramatically influenced by driving conditions such as luminance level and ambient temperature. The electrical and optical characteristic decay asynchronously, due to partial correlation. The correlation curve therefore depends on the driving conditions, especially in higher operation points.

However, in the lower operation range, the current drift and efficiency decay share the identical degradation mechanism—deterioration of radiative diode. Therefore, the two decays are synchronous, and the correlation is in linear profile. Because of identical cause for both decays at a lower operation point, the correlation does not shift with driving conditions, but as a single unified profile. Figure 6-4 shows the unified degradation correlation profile at lower operation



for the higher emitting range) may be derived from the equivalent circuit and its aging parameters.

The correlation model provides an approach using measurable electrical value to evaluate the efficiency decay. It can prevent error accumulation in the long-term operation, and deliver a more reliable result in strongly aged states. Based on the equivalent circuit and the correlation for the aging parameters, the efficiency decay at each given operation can be derived during operation.



## 7 Prediction and Compensation

Three feasible modelling approaches for OLED degradation has been introduced in the previous chapters, including the data-counting model, electro-optical model, as well as the correlation model. Based on these models, the prediction and compensation for degradation can be implemented. Before validation for models, the parameters of models has been extracted from numbers of OLED samples in the previous aging tests. To predict efficiency loss, the operation history such as time, driven currents as well as ambient temperature are recorded for the data-counting model; internal aged parameters of equivalent circuit are evaluated for the electro-optical model; and the measurable electrical value is detected in the correlation model. Based on the quantified efficiency loss in the models, the corresponding compensation can be made by adjusting the gray value of pixels on AMOLED display (duty-cycle time on OLED devices). The validation is firstly made on OLED devices— analog single OLED pixel. Thereafter, the validation is implemented on the matrix in AMOLED display.

### 7.1 Validation on OLED devices

#### 7.1.1 Data-counting model

Figure 7-1 shows the unified degradation prediction profile of the data-counting model, as described in section 4.4. During operation, the luminance on an OLED will gradually degrade, with continuous current flow. In operation, the driven current, together with ambient temperature as well as operation time are recorded to evaluate the accumulated stress on OLED. Based on the unified degradation prediction line, a current efficiency loss can be thus quantitatively calculated with the accumulation stress during operation. The operation conditions are considered in the model for prediction, such as the current amplitude (initial luminance level) and ambient temperature. The model parameters have been extracted from numbers of OLED samples in the previous aging tests.

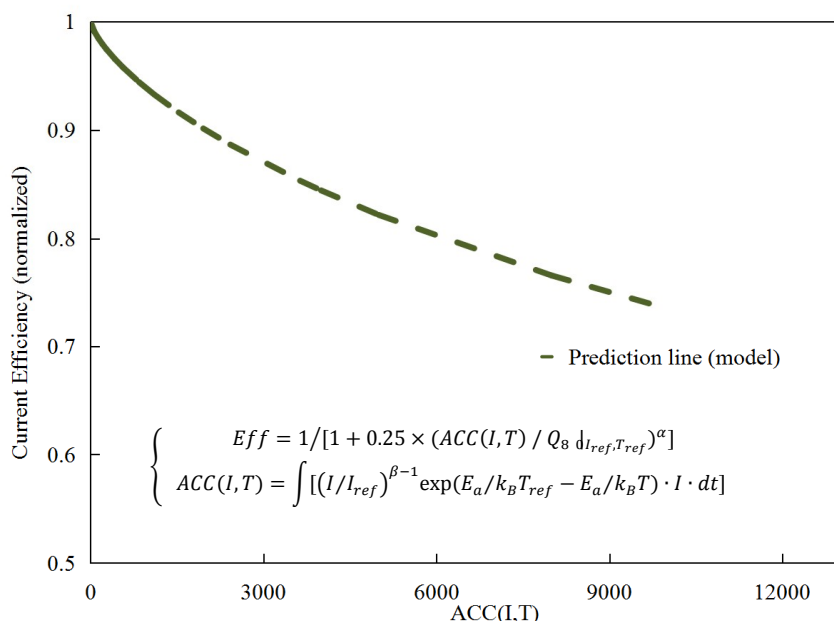


Figure 7-1 Unified degradation prediction profile for multi-operation conditions in the data-counting model. Merck green OLED devices:  $\alpha = 0.7926$ ,  $\beta = 2.122$  and  $E_a = 0.62$ .

### Compensation

In the digital driving scheme, pulse AC voltage is applied on OLED devices. The voltage amplitude is fixed (constant), and controlled with PWM signal. The output emitting light (brightness level  $L$ ) is thus determined by current flow, current efficiency, as well as duty cycle, as shown in equation 7.1.  $L$  denotes the emitting luminance level.  $L_0$  is the initial luminance (at DC).  $I_0$  and  $Eff_0$  are the initial current flow and initial current efficiency, respectively.

$$L = L_0 \times D_{utyCycle} = I_0 \times Eff_0 \times D_{utyCycle} \quad (7.1)$$

As learned in the previous chapters, both electrical and optical characteristic experience degradation in aging. That means, the current flow  $I_0$  and current efficiency  $Eff_0$  at a given voltage will drop with operation time, and both contribute to the luminance loss on device.

$$D_{utyCycle} = D_0 \times CF = D_0 \times \frac{1}{(I/I_0)^\beta \cdot (Eff/Eff_0)} \quad (7.2)$$

To keep the output luminance constant, the duty cycle of PWM control signal is adjusted (increased) and compensates the luminance loss, as shown in equation 7.2. Here,  $D_0$  denotes the duty cycle at initial state, which is given by image data.  $CF$  is the compensation factor. It depends on decays originated from both electrical and optical degradation. The current drop at a given voltage can be directly measured and calculated. For the efficiency decay, the model is employed to quantitatively evaluate decay scale. It has to be noted that in the analog driving scheme, the compensation factor is solely attributed to the efficiency decay due to current-source driving. In the display system, the gray value of a pixel is an adjustable value.

The luminance loss can be calculated and compensated at any aging time point in theory. In fact, the compensation factor is demanded to be adjusted once after a while operation. It is because on display, there is approx. 3-5% the tolerance for human eyes. Additionally, the compensation intervals could be fixed or gradually extended during operation.

The accuracy in calculating the accumulation stress in the digital driving scheme is required for more considerations. In the digital driving scheme, the current amplitude at a given voltage point gradually declines with operation time, as shown in figure 7-2. The accumulation stress should be calculated, considering varying current amplitude due to the amplitude scaling effect in aging. The driven current in the analog driving scheme, whereas, is at fixed values. The drop in current flow in the digital driving scheme can be compensated with measure, to maintain constant quantity of injection charge as the analog driving scheme. However, the amplitude scaling effect should still be considered due to the variation of current amplitude, according to accumulation stress formula in equation 4.7 of section 4.2.

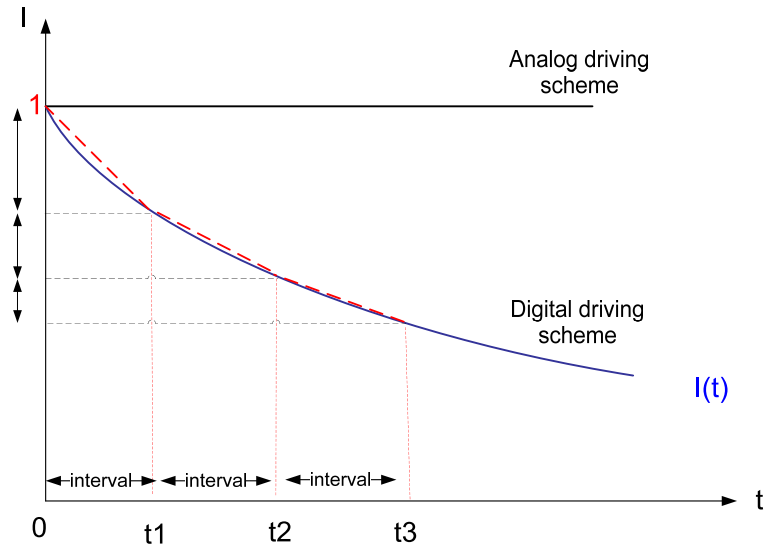


Figure 7-2 The current amplitude (DC) decreases with aging time in the digital driving scheme.

At each time point of compensation, the accumulation stress  $ACC$  in operation period is calculated. The duty cycle of control signal is then adjusted according to the evaluated decay scale. The procedure is as follows,

$$0 : D_{utyCycle} = D_0$$

$$t_1 : ACC_{t_1} = \int_0^{t_1} f(I(t), T) \cdot dt, D_{utyCycle} = D_0 \times \frac{1}{(I_{t1}/I_0)^* (Eff_{t1}/Eff_0)}$$

$$t_2 : ACC_{t_2} = ACC_{t_1} + \int_{t_1}^{t_2} f(I(t), T) \cdot dt, D_{utyCycle} = D_0 \times \frac{1}{(I_{t2}/I_0)^* (Eff_{t2}/Eff_0)}$$

.....

The decline profile of  $I(t)$  is non-linear. For simplicity, the nonlinear profile can be approximately as linear decline profile at each interval. The additional accumulation stress due to the previous compensation should be also considered in the compensation period.

## Results

In this validation, Merck green sample was adopted. The device was driven under pulse AC voltage with 800 Hz, 3.7 volts ( $L=4600$  nits, DC). The initial duty cycle of PWM on OLED is set at 70%. Thus, there is a 30% margin for compensation of the luminance loss. In the beginning operation phase the ambient working temperature is set at 18°C, and subsequently set at 37°C accelerating the aging process. The test was continuously taken in 300 hours. The driving conditions, such as the driven current, ambient temperature as well as operation time, are recorded during operation. The decay scale of current efficiency was calculated in the unified degradation prediction profile, after determining the accumulations stress on device in operation period.

Figure 7-3 shows a comparison between the experimental current efficiency decay and prediction results with the data-counting model. It shows a good agreement between the measurement and prediction based on the model. The efficiency decreased by nearly 5% after 300 hours. The deviation in prediction for the efficiency decay is only approx. 5% (RMSE).

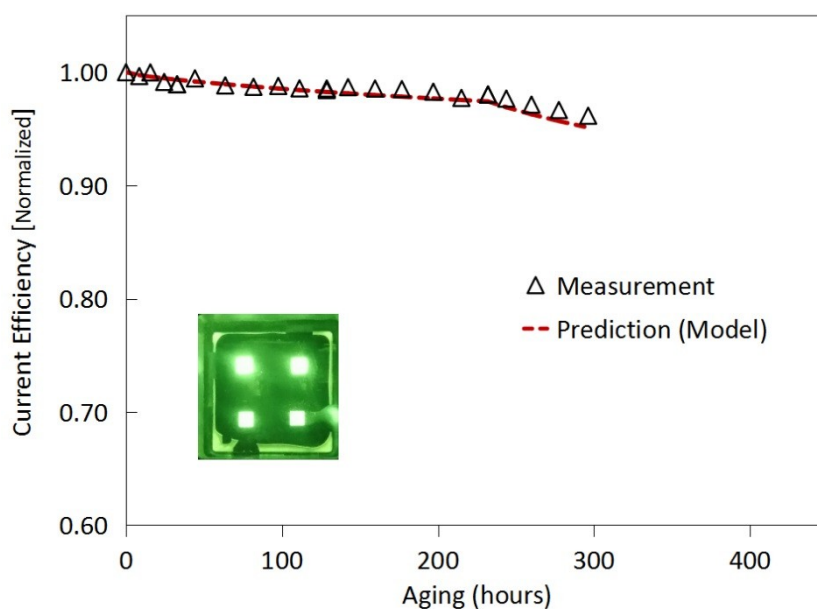


Figure 7-3 Experimental current efficiency decay and prediction results with model on green OLED sample.

The compensation based on the prediction was applied during operation. In this case, the compensation interval is about 100 hours. Figure 7-4 shows compensations applied on OLED device in operation. It shows that the luminance loss has been effectively compensated for OLED during operation. In this case, the total luminance loss is about 15% (compared to its initial value), including the contributions originated from 5% efficiency decay and 11% current drop. The maximum error for compensation is just 8%, far from human sensitivity (3-5%). The compensation can make output luminance stable during operation.

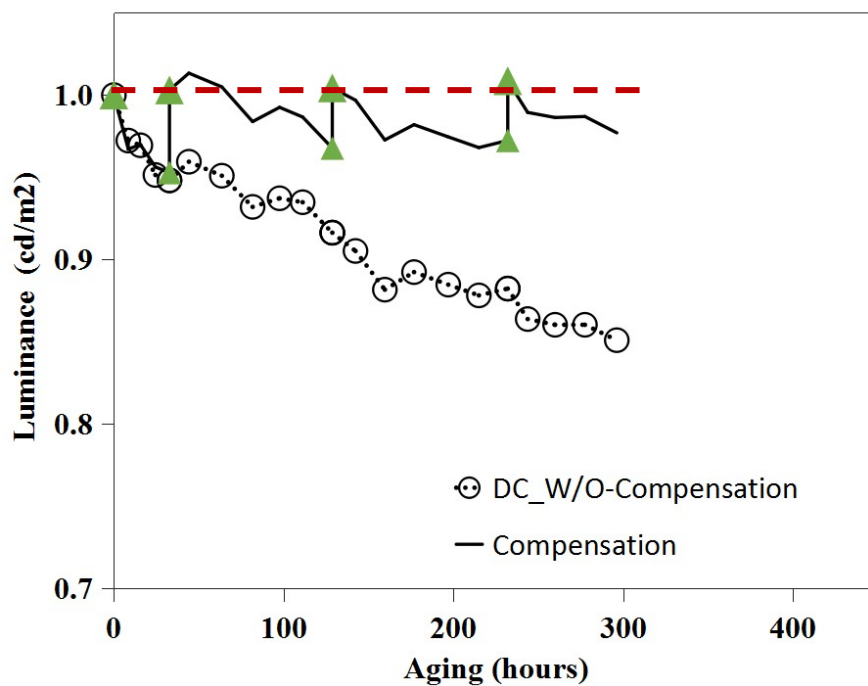


Figure 7-4 Compensations were applied on green OLED device during operation.

The compensation intervals could be managed shorter/ more often for higher-quality compensation. The interval could be flexible—a short time in the beginning stage, and then gradually be extended in the long-term operation, due to the non-linear monotonous decay (sharp decay in the beginning).

### 7.1.2 Electro-optical model

An electro-optical model for OLED has been introduced in chapter 5. The model is built based on an equivalent circuit, and can simulate the electrical-optical degradation behavior during operation. The drifting parameters correlate with efficiency loss in operation. Through

determining the aging parameters in the equivalent circuit, the corresponding efficiency decay at each operation point can be calculated. The drift of parameters in this case can be determined by estimating the accumulated stress (as introduced in the data-counting method). The electro-optical model provides a quantitative approach to calculate the current efficiency decay. The corresponding compensation can then be implemented by adjustable factor (e.g. duty cycle), as presented in the last section. The model parameters have been extracted from numbers of OLED samples in the previous aging tests.

### Prediction

In operation, the OLED device is seen as a gray-box DUT, as shown in figure 7-5. The circuit of multiple diodes with resistance is approximately equivalent to an organic light-emitting diode. Serial elements ( $D_{ser}$ ,  $R$ ) represents the serial layers, and parallel elements ( $R_{leak}$ ,  $D_{emit}$ ,  $D_{non}$ ) are as the emission layer. With the voltage applied, the current flow through device, and meanwhile the light is emitted out, which is function of internal radiative current flow. The current efficiency is determined by internal current distribution in the device.

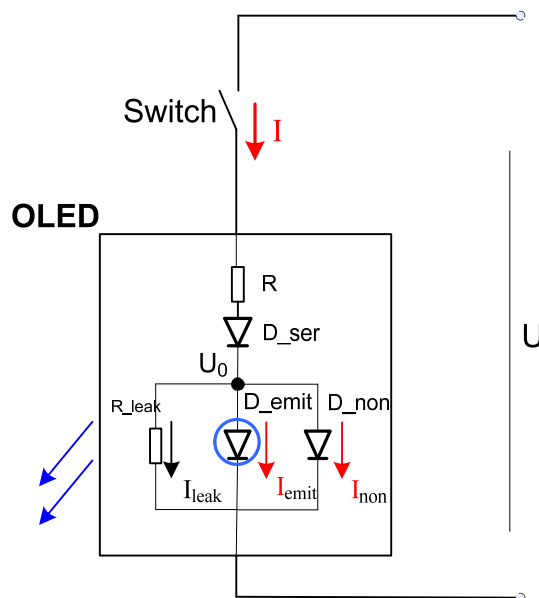


Figure 7-5 OLED as gray-box DUT in operation.

Correspondingly, the equivalent circuit above is described as equation 7.3. The current flow is split into three branches, including leakage current flow  $I_{leak}$ , the emissive flow  $I_{emit}$  and non-emissive flow  $I_{non}$ . The effective current efficiency depends on the internal current distribution.

The intrinsic radiative efficiency  $\eta_{int}$  as the property of  $D_{emit}$  is assumed to be constant in operation in the model. The related discussion could refer to the analysis in chapter 5.

$$\left\{ \begin{array}{l} \text{electrical} \\ \text{Optical} \end{array} \right\} \begin{cases} U = I * R + n_{ser} V_t \cdot \ln \frac{I}{I_{S_{ser}}} + U_0 \\ I = I_{leak} + I_{emit} + I_{non} \\ I_{emit} = I_{S_{emit}} \left[ \exp \frac{U_0}{n_{emit} V_t} - 1 \right] \\ Eff = \frac{L}{I} = \frac{I_{emit} * \eta_{int}}{I} \end{cases} \quad (7.3)$$

In the aging process, the electrical-optical degradation behaviors are determined by the aging parameters, while the most parameters are stable, as discussed before. In this case, the primary aging parameters are  $I_{s\_emit}$  and  $I_{s\_ser}$ . The parameter  $I_{s\_emit}$  is responsible for the current efficiency decay, and  $I_{s\_ser}$  contributes to the current drift. The aging parameters could be evaluated from unified empirical decay profiles ( $f_1, f_2$ ), through estimating the accumulated stress  $Acc$  considering impact factors ( $t, Amp, T$ ). The relation is described the equation 7.4. The empirical decay profiles for the aging parameter  $I_{s\_emit}$  and  $I_{s\_ser}$  are shown as figure 7-6. The related discussion could refer to section 5.3.

$$\left\{ \begin{array}{l} \tilde{I}_{S_{emit}} = f_1(A_{cc}) \\ \tilde{I}_{S_{ser}} = f_2(A_{cc}) \\ A_{cc} = g(t, Amp, T) \end{array} \right. \quad (7.4)$$

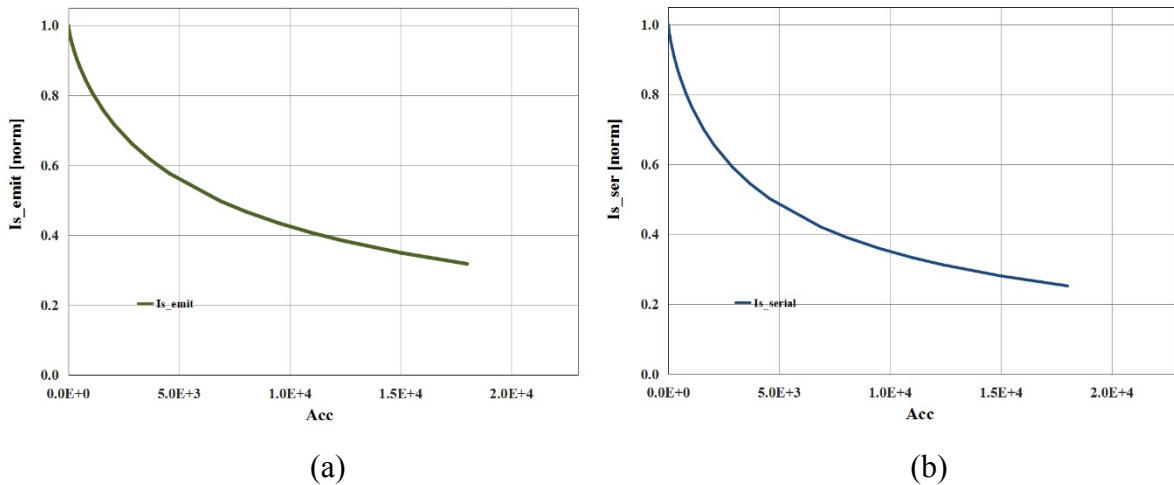


Figure 7-6 (a) unified decay profile  $f_1$  for the aging parameter  $I_{s\_emit}$  (b) unified decay profile  $f_2$  for the aging parameter  $I_{s\_ser}$ .

## Results

The prediction with the electro-optical model is also validated in the same aging tests as presented in the previous section. The parameters in the electro-optical model have been extracted from 9 green OLED samples under multi-operation conditions in the previous aging tests. In the test of validation, the efficiency decay at a given operation point has been calculated during operation, through determining the aging parameters in the equivalent circuit. Figure 7-7 shows the experimental current efficiency decay as well as prediction results based on the electro-optical model as well as the data-counting model. As the figure shows, a good agreement between the measurement and prediction with this model has been achieved. The efficiency decrease by nearly 5% after 300 hours. The deviation in prediction for the efficiency decay is only approx. 2.4 ‰ (RMSE). The accuracy is better than the data-counting model (5‰). It is worth mentioning that the electro-optical model can predict the relative efficiency loss for a wide operation range. The dependence on operation point is crucial, especially for the analog driving scheme on AMOLED displays. The equivalent model allows practical prediction of the performance of aged pixels in a wide operation range, seen as the critical merits.

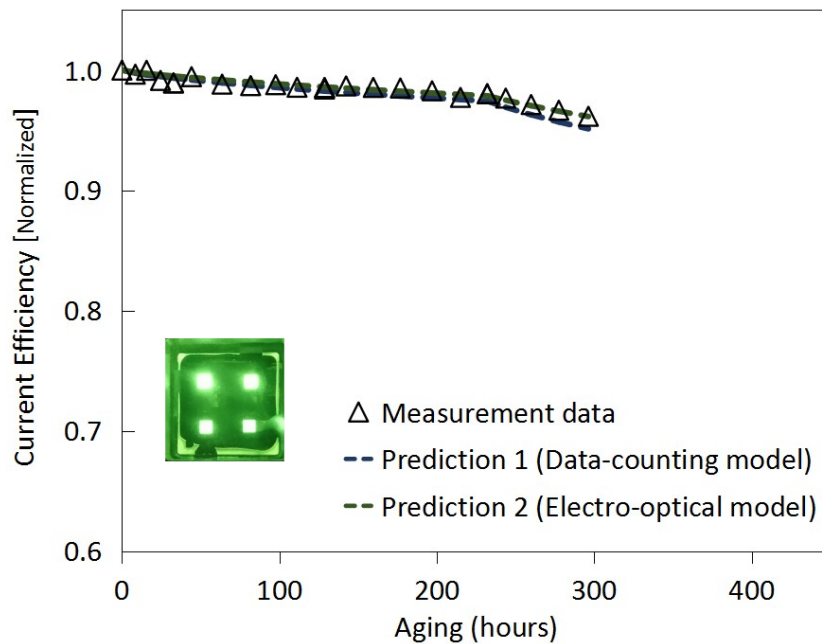


Figure 7-7 Experimental current efficiency decay and prediction results with the electro-optical model and data-counting model on green OLED sample.

### 7.2 Compensation on digital AMOLED display

The image-sticking artifact on AMOLED displays is attributed to the differential aging state on pixels. To alleviate the differential aging, the aging states of all pixels should be calculated and pixel-wise compensated in the display system. In this process, the aging models are demanded to evaluate the decay scale of the current efficiency quantitatively. In the previous chapters of this thesis, three models have been developed. The data-counting model provides an empirical method to predict the efficiency decay, with recording operation history for estimating the accumulated stress under varying driving conditions. The electro-optical model was built based on an equivalent circuit of OLED and can simulate the degradation in electrical-optical performance. Through evaluating the deteriorated parameters in the equivalent circuit, the efficiency decay in operation range can be derived. The correlation model supports the approach to evaluate the efficiency decay with electrical measurable value, which as a feasible feedback method can be integrated in many display systems. The validation of the data-counting and electro-optical model has been made on OLED devices in the last section. In this section, the compensation with the three models will be validated on a digital driving AMOLED display.

#### 7.2.1 Digital AMOLED prototype and test setup

Figure 7-8 shows a digital AMOLED display prototype and test setup for validation. In the digital AMOLED prototype, 2.8" QVGA AMOLED panel from Visionox was adopted, and a digital driving system was implemented with a FPGA board and discrete PCB board [Volk2017]. The image data was input from PC as HDMI signals to the digital driving system, and finally displayed on the AMOLED panel. Besides the display system, the test setup was built for electrical-optical characterization and compensation validation. The ELDIM UMaster camera was used to analyze the luminance distribution before and after aging compensation. The tests were taken in a dark room with constant temperature, in considering of OLED's instability and measurement accuracy under ambient condition.

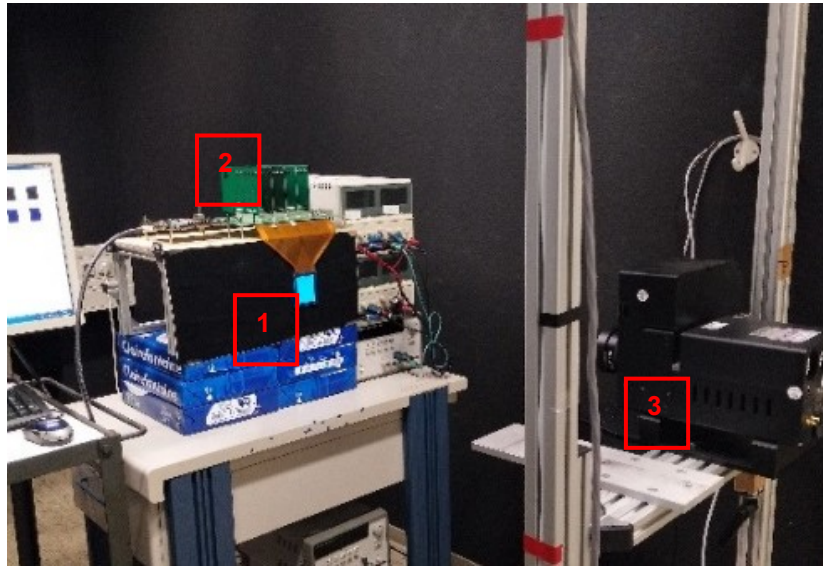


Figure 7-8 Digital AMOLED display prototype and test setup. 1) Visionox 2.8'' QVGA panel 2) Digital driving platform with FPGA + discrete PCB board 3) ELDIM UMaster camera.

### AMOLED panel

In the digital AMOLED display prototype, a display panel manufactured by Visionox was adopted. It is a 2.8 inch panel, with a resolution of 320x240 RGB (141 ppi). The pixel circuit is a simple 2T1C structure. Both transistors in pixel circuit are used as switches in the digital driving scheme. A shift register SR using LTPS PMOS, has been integrated on one side of glass to dynamically scan row pixels. It is worth mentioning that the panel is customized for the digital driving scheme. It can be driven at high operation frequency (up to 600k Hz) for a flicker-free perception. 240 data channels are in parallel into panel, with 1:3 de-multiplexer on each channel for distributing data to subpixels. It enables the frame rates up to 2k Hz. All panel signals, including data signals, SR control signals as well as power supply, are transferred with a FPC (flexible printed circuit). The FPC is connected with discrete board in external driving board. [Volk2014].



Figure 7-9 2.8" QVGA AMOLED panel from Visionox.

The electrical-optical performance of OLEDs on Visionox AMOLED display is described in the table 7-1.

Table 7-1 Performance of OLEDs on Visionox panel

	Color	Area [ $\mu\text{m}^2$ ]	$V_{op}$ [V]	L [ $\text{cd}/\text{m}^2$ ]	Max. Eff [ $\text{cd}/\text{A}$ ]	1931CIE (x, y)	Emission
AMOLED (Visionox)	R	86x30	2~5.4	0~319	6.6	0,66/0,34	FL
	G	86x30	2~5.4	0~328	6.8	0,28/0,65	FL
	B	86x30	2~5.4	0~104	2.5	0,13/0,15	FL

$V_{op}$ =operation voltage, FL= fluorescence

Figure 7-10 shows the chromaticity of Visionox panel in color space, with comparison to Rec.709. The green and red subpixels are sufficient to meet standard Rec.709. For blue subpixels, however, color is in the light blue. Normally, lifetime of light blue OLEDs is better than that of deep blue ones.

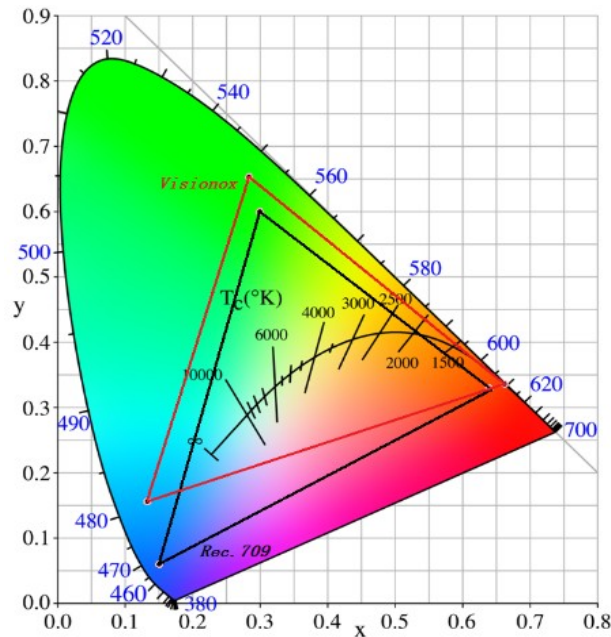


Figure 7-10 Chromaticity of Visionox panel in color space, with comparison to Rec.709.

### External digital driving system

In this display system, the external digital driving system provides all signals for the display panel, including timing control signals, data signals as well as the power supply. It is implemented with FPGA board and discrete PCB board in this case. In practice, the driver system usually integrates TCON and source driver in products, placed on glass (COG) or FPC (COF). In our digital driving system, the pixel pipeline is designed on the FPGA, implementing the digital decomposition, image processing (e.g. gamma correction, white balance), and frame buffer. The image data processed in FPGA are then de-serialize and amplified through discrete PCB board before displayed on the display panel. The discrete PCB board is also responsible for supplying power to the panel. Thus, the whole digital driving system for digital AMOLED display has been established.

### Extraction of model parameters in aging tests

In the previous chapters, models for OLED degradation has been presented. Before implementation compensation in the driving system, the model parameters for Visionox panel should be extracted. In the pre-extraction test, the multiple operation driving conditions were applied on pixels to extract comprehensive parameters.

In this case, the stressing pattern with 9 square areas was displayed on a panel. Each square area contains 625 pixels (25x25). All sub-pixels (RGB) were stressed synchronously. In the aging test, each test square was stressed with their own driven conditions such as brightness level and ambient temperature. The luminance level is in the range of 200 to 900nits, and the temperature is 20-33°C. The localized heating was implemented with thermoelectric module TEC1-12706. The driver TFT in 2T1C was operated with  $V_{gs}$  in the range of 5.49-6.1V.

The measurements were taken in a dark lab. Current-voltage-luminance (IVL) characteristic was measured in every 2 hours in the beginning, and the interval was gradually extended in the long term. Agilent E5270B and SpectraScan PR-740 are used in IVL measurements. The automatic test is implemented by Matlab program on computer. The duration of aging time is approx. 80 hours. The aging parameters were extracted from measurement results.

### 7.2.2 Compensation algorithm

The basic compensation approach on an OLED device (as a single pixel) has been introduced and validated in the previous section. In further, the approach will be applied on all pixels on the display, implementing pixel-wise compensation.

In the digital driving scheme, the luminance is determined by two factors: the current flow and current efficiency. In the aging process, the decays on both factors contribute to the luminance loss, as described in equation 7.5. Due to the dependency of degradation on operation point, the luminance loss here is quantitatively calculated at a given operation voltage, and the same for the current drop and efficiency decay.  $L_0$ ,  $I_0$ , and  $Eff_0$  are the initial luminance, current flow and efficiency of a pixel, respectively.  $L'$ ,  $I'$ , and  $Eff'$  denote the aging states.

$$\frac{L'}{L_0} \Big|_{V=V_0} = \frac{I'}{I_0} \Big|_{V=V_0} * \frac{Eff'}{Eff_0} \Big|_{V=V_0} \quad (7.5)$$

In terms of the decay in electrical property, the current flow through OLED at a given voltage significant drops with operation time. Even though the efficiency of a pixel stays stable, the luminance still suffers a loss due to decreased current flow. Seriously, the electrical characteristic is particularly vulnerable to the degradation than optical characteristic in the aging (a sharp decay in the beginning phase of aging, especially). The decay scale in current

flow is normally twice as much as the efficiency decay. Compared to the digital driving scheme, the decay in electrical property would not be an issue for the analog driving scheme—it does not lead to a luminance loss, due to current-source driving on pixels. Only the voltage rise is observed. From this perspective, it seems like that display with the digital driving scheme suffers more serious degradation issue. Nevertheless, the luminance loss originated current drop can be indeed effectively compensated by directly measuring the pixel current in simple current sensor integrated into displays. Therefore, a similar lifetime like the traditional analog driving scheme can be achieved. In the publication [Volk2017], a current-sensor module has been designed, and compensation for current drop on pixels has been validated.

As we discussed before, the real challenge is the luminance loss originated from the efficiency decay. During operation, OLED pixels inevitably suffer from the efficiency decay, irrespective of the digital driving or analog driving scheme. More importantly, aging models are required to evaluate the efficiency decay, which is an indirectly measurable value on products. Also, the fact that decay with dependence on operation point should also be considered in models. Therefore, several feasible models have been developed, as presented in the previous chapters. Based on these models, the compensation for degradation can be applied, as shown in equation 7.6 and 7.7.

$$CF|_{V=V_0} = \frac{1}{\left(\frac{I}{I_0}\right)|_{V=V_0} * \left(\frac{Eff'}{Eff_0}\right)|_{V=V_0}} \quad (7.6)$$

$$GV_{comp} = GV_{orig} * CF = GV_{orig} * \frac{1}{\left(\frac{I}{I_0}\right) * \left(\frac{Eff'}{Eff_0}\right)} \quad (7.7)$$

To achieve stable output luminance during operation, the compensation factor  $CF$  for aged pixels are applied. It considers operation points and the aging states of pixels, which originated from both the current drop and efficiency decay, as equation 7.6 shows. In the display system, gray value of pixels is adjusted to compensate the decays, as shown in equation 7.7.  $GV_{orig}$  denotes the initial gray value of pixel in pristine state.  $GV_{comp}$  is gray value with compensation on aged pixels. In the digital driving scheme, the time factor is indeed adjusted to implement compensation, since pixel's gray value is coded as the lighting time (on duration). This is

identical with the method presented in section 7.1.1, in which the time factor as the duty cycle is adjusted to compensate the luminance loss of OLED devices.

It is worth mentioning that the compensable margin should be sufficiently reserved for a reasonable decay range. For example, the compensable decay scale is 20% or 30% of the original state, or even 50% in extreme case. In the digital AMOLED prototype, the frame time comprises a program period and light-on period. If it is expected to obtain a wide compensable range, the program period should be as short as possible, raising the requirement for design and manufacture (e.g. TFT on glass). Another possibility to achieve wide compensable range is that pixels are driven at higher operation voltage point with lower initial duty cycle—output luminance is same. But, this will further aggravate the aging scale. Therefore, trade-offs are required in the implementation, considering the compensable decay range, manufacture requirement, luminance performance on display. For the analog driving scheme, the gray value of pixels is coded with current source. To achieve a wider reserved gray value for compensation, higher current flows should be applied on pixels. The challenge would be the evaluation of degradation dependency on operation point, as well as the scaling accelerating decay effect.

### **Image-data flow with compensation**

The compensation algorithm can be integrated into the image-data flow in a digital driving AMOLED system, as figure 7-11 shows.

For the digital driving system without compensation, the image-data flow is as follows: 1) pixel gray value  $GV_{orig}(i,j)$  in a frame is serially inputted to the pixel pipeline; 2) enters into the optimization procedural in pixel pipeline. Pixel's gray value is processed for optimizing display performance, such as Gamma correction or White point; 3) the decomposition procedural. Optimized frame data are decomposed to sub-frame binary value  $B(s)_{ij}$ ; 4) sub-frame buffer. Multiple sub-frames data are stored into the buffer (DRAM); 5) finally, image data together with control signals such as timing  $t_s$  and operation voltage  $[v]$ , are transmitted to the display panel.

To implement the compensation, an additional procedural is integrated into image-data flow between input frame and optimization. In this procedural, the original input gray value on pixels are manipulated, according to the compensation factor  $CF(i,j)$ . The compensation factor is determined by the aging state of a pixel and its operation conditions (e.g. operation point).

The aging state of pixel is attributed to the current drop and efficiency decay. The current drop is calculated by measuring the current flow in sensors; the efficiency decay is evaluated with the models developed in this thesis. The sensors are indeed used as a feedback path in the display system. Several sensors can be integrated for measuring display performance in the current state (current flow of pixels), as well as the working conditions (temperature).

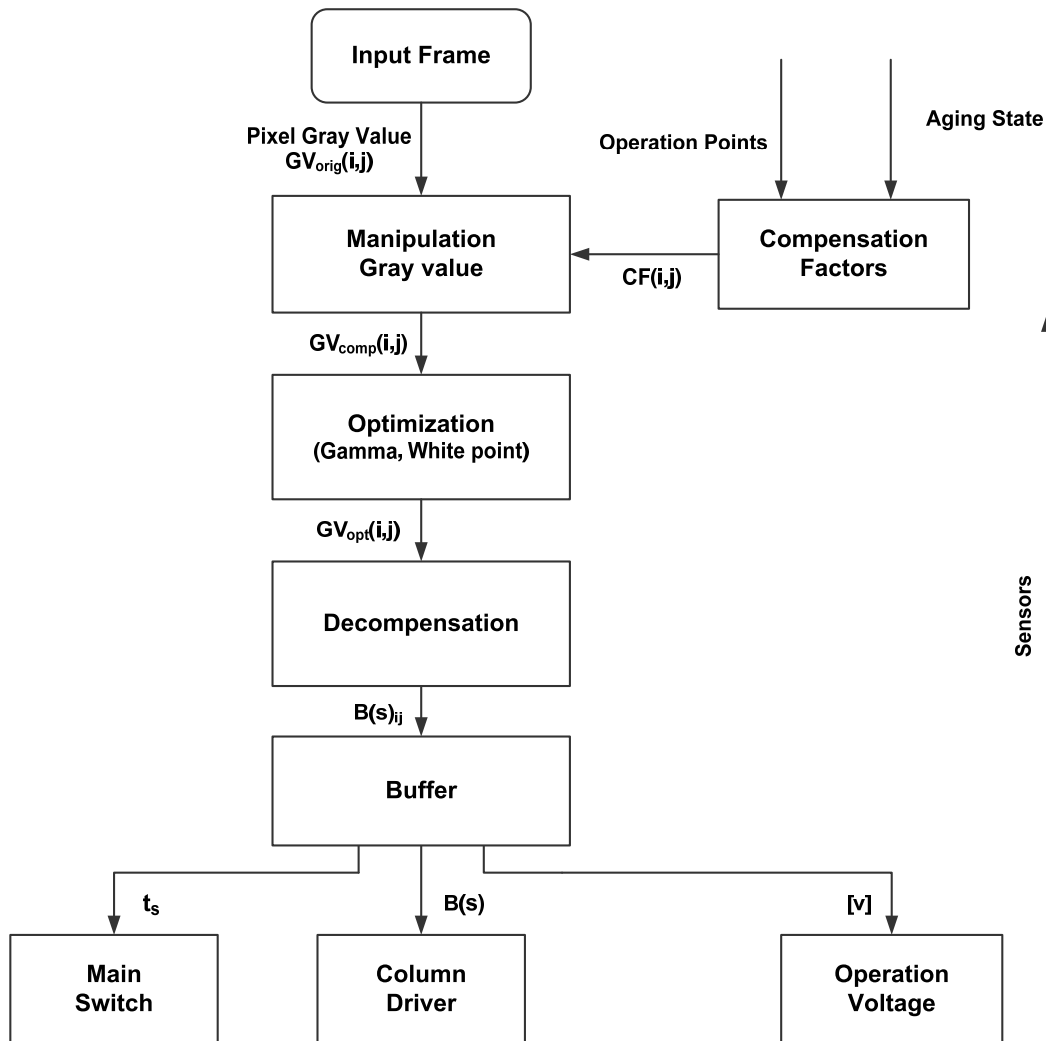


Figure 7-11 Image data flow with compensation in a digital driving AMOLED system.

For the data-counting model, the input pixel data and working conditions are counted to estimate the accumulation stress. The efficiency decay is then quantitatively derived from the degradation prediction profile with accumulation stress. The frame data & working conditions (e.g. data from temperature sensor) are stored in a memory, and module for accumulation stress estimation and unified degradation function are implemented with LUTs in FPGA.

In the correlation model, the efficiency decay is derived from the measurable electrical value, such as the current flow. Through sensor integrated into the display system (e.g. internal circuit or external circuit as current sensor), the currently aging state of pixels can be evaluated. The correlation equations are implemented with LUTs.

In the electro-optical model, the efficiency decay is derived from the equivalent circuit and its aging parameters. Model parameters has been extracted from numbers of samples in the previous test. The currently decay scale of parameters in the equivalent model can be determined by estimating the accumulation stress as in the data-counting method, or using measurable electrical value as in the correlation model.

For the dependency of degradation on operation point, the data-counting model and correlation model would use more LUTs (multiple degradation prediction lines) to accurately predict the efficiency decay. Whereas, in the electro-optical model, the efficiency decay in a wide operation range can be calculated based on the equivalent circuit. If non-uniformity of voltage distribution on the panel is considered, an iterative compensation for sub-frame may also be considered.

The compensation approach above can also be applied to analog driving displays. Through adjusting the pixel gray value through pixel pipeline, pixel-wise compensation can be implemented. However, one challenge is how to accurately predict the degraded performance of OLED at various operation conditions, such as working points in a range or multiple working temperature. The equivalent model may provide a better solution to this issue. It is worth mentioning that the compensation approach with input gray value adjusted, is also feasible to solve non-uniformity caused by variation of TFT, voltage distribution, or temperature distribution on the glass.

### 7.2.3 Validation results

The AMOLED panel was stressed with specific pattern (a square area) to simulate the image burn-in process, which is occurred on a smartphone or TV. Room temperature was set at 20°C. During operation, pixels in the pattern suffered degradation, compared to other pixels on the display panel. With operation time, the image sticking aging artifact happened and became stronger due to the differential aging. Figure 7-12 shows the image sticking on blue color after

10 hours stressing test. The luminance on the pixels in the aged region lost nearly 30% of its initial value. This strong drop may be caused by the digital driving scheme, since the luminance loss for digital AMOLED display comprise contribution originated from both the current drop and efficiency decay. A further root cause may be the limited maturity of the organic materials used in this display prototype.



Figure 7-12 Image sticking on AMOLED display (blue OLEDs).

To suppress the image sticking artifact, the compensation was applied on the aged pixels. The current drift was directly measured and the efficiency decay was calculated with the models. The aged pixels with and without compensation in operation are shown in figure 7-13. It clearly shows that the luminance loss on aged pixels has been effectively compensated, using three approaches—the data-counting model, electro-optical model and correlation model. The deviations in compensation for them are all less than 3.0%, which is free sensitive for human eyes. In this case, the compensable margin for the luminance loss is approx. 30%, which would satisfy the requirement in most applications.

The three models show their effectiveness on prediction of the efficiency decay of aged pixels. With comparison, the data-counting model has less accuracy to some extent than the others (Max. deviation 2.6%). It is more likely due to an accumulation error during operation for the data-counting model, as mentioned before. Through extracting parameters on a large amount of samples, the prediction accuracy for degradation can be improved. For the correlation model, the accuracy compensation depends on the accuracy of electrical value in measurement (e.g. current drift). Measuring the electrical value at a relative constant condition will increase the accuracy for degradation evaluation—the electrical characteristic of OLEDs is quite unstable

under ambient environment (especially for temperature). The real value of electro-optical model is that it can predict the performance (e.g. current efficiency) of OLEDs in a wide operation range (OP) after a period of aging time.

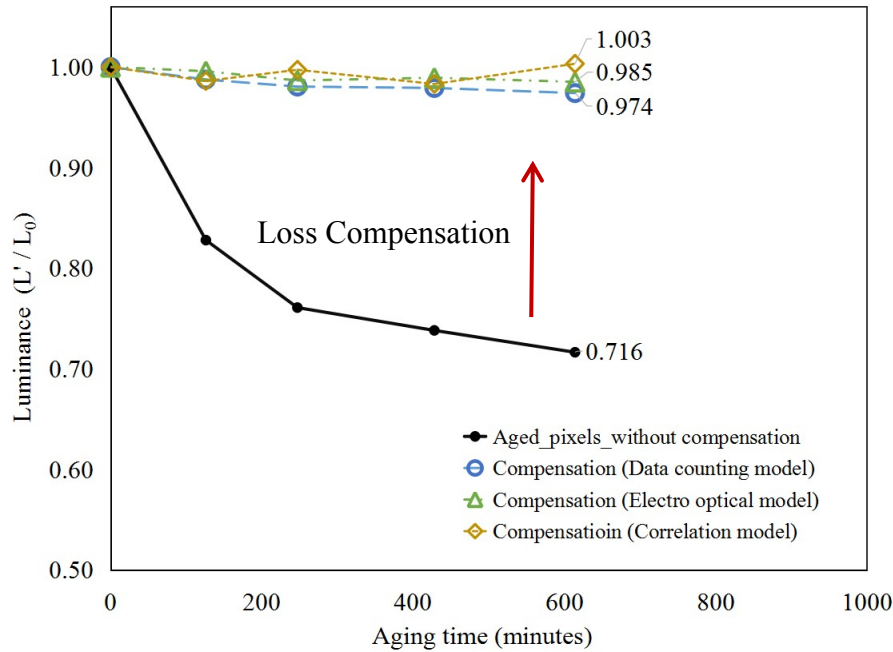


Figure 7-13 Aged pixels with and without compensation.

In the practical application, a combination of three models may deliver more reliability and effectiveness. With the data-counting or correlation approach, the aging parameters can be determined; and then the current efficiency at each operation point can be derived in the equivalent circuit. Furthermore, a combination of the data-counting and electrical measure (correlation) is applied for a long-term aging in the driving system. The data-counting method is used in the beginning phase of aging (e.g. 10, 20% decay), while the electrical measure is responsible for strongly aged phase (e.g. 30%, or even more). It could be applied and validated on more AMOLED panels in future. It is worth mentioning that in driving system, a sufficiency reserved gray value range should be designed to obtain a wide compensable ability. For example, if original image data are in 256 levels, then 384 gray value should be reserved to support 50% compensation ability.

Figure 7-14 shows photographs of uncompensated (left) and compensated (right) display for blue color, taken by a Nikon digital camera. The current drift was directly measured and the efficiency decay was calculated with the data-counting/electro-optical model. It shows that the image sticking aging artifact has been effectively suppressed with compensation.

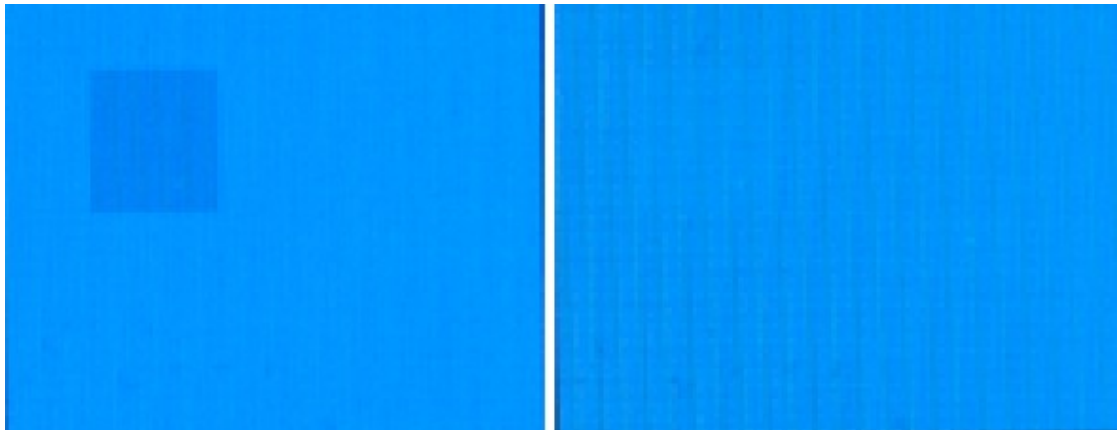


Figure 7-14 Photographs of uncompensated (left) and compensated (right) display for blue color image.

Furthermore, the luminance distribution on the display without and with compensation are compared, as shown in figure 7-15. The luminance distribution was measured by ELDIM UMaster camera. It shows that the non-uniformity due to differential aging has been eliminated. Thus, image sticking artifact was suppressed.

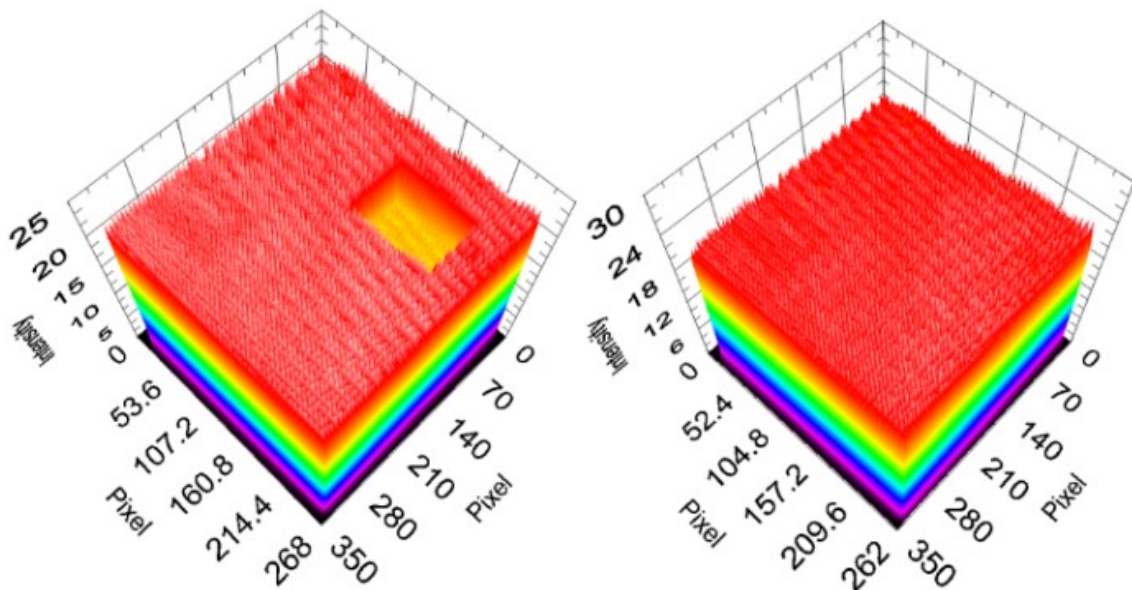


Figure 7-15 Luminance distribution on display without (left) and with applying compensation (right).

The blue OLED is most vulnerable to the degradation in three primary OLEDs. Therefore, compensation was primarily applied on blue OLEDs. Indeed, all three primary channel can be compensated in the driving system. The modeling methods and compensation approach presented in this thesis apply to all three primary subpixels. The non-uniformity due to differential aging in all three primary subpixel can be addressed.

A test image was displayed on panel before and after compensation, as figure 7-16 shows. The current drift was measured and the efficiency decay was derived by a simple correlation model. Luminance loss on each pixel was thus estimated. The result shows image-sticking artifact on AMOLED display was alleviated. It has been discussed in publication by our group [Xu2017].



Figure 7-16 A test image displayed before (left) and after applying compensation (right).

## 8 Conclusion and Outlook

### 8.1 Conclusion

In this thesis, the modeling of OLED degradation has been developed for prediction and compensation of the aging artifact on AMOLED displays. Experiments were carried out to analyze the electrical-optical characteristic and degradation behaviors of OLEDs. Based on these facts, three models have been built, providing us potential/feasible methods to evaluate the decay in current efficiency. Prediction and compensation with these models were finally implemented. Specifically, the contribution of this thesis can be categorized in the following areas:

#### **OLED characteristic and degradation behaviors in experiments**

OLED devices from Merck and Novaled were adopted as test samples in experiments. Fluorescence blue and phosphorescence green organic light-emitting diodes were mainly investigated. Through IVL measurement on devices, the electrical and optical characteristic have been analyzed. Results show that the current efficiency of an OLED depends on the operation point (voltage or current). When the applied voltage increasing, OLED will experience various operation regimes, identifying the facts, such as the hole-electron recombination, rectification effect, and roll-off effect. Furthermore, the electrical-optical curves shift with temperature degree, indicating the thermal instability of organic light-emitting diodes. The electrical property is indeed more vulnerable to the ambient temperature than optical property.

In the aging tests, a number of OLED samples were stressed for thousands of hours. Various driving conditions, such as current flow, temperature and AC/DC, were applied on samples. It shows that the electrical (I-V) and optical (Eff-V) characteristic dramatically drift in the aging process. Multiple degradation mechanisms (e.g. interface deterioration or exciton quenching) may contribute to the degradation behaviors. At a given operation voltage, the current flow and current efficiency gradually decreased with aging time (sharply in the beginning). Additionally,

the decay of current efficiency depends on the operation point. The efficiency at lower voltage decays more strongly, compared to a higher operation point. Besides that, the driving condition also impacts the decay scale of OLEDs, significantly. The higher current/temperature is applied to OLED devices, the stronger decay they would suffer. For AC condition, it is observed to apply a positive influence on I-V drift, but little impact on the efficiency decay. For the OLED chromaticity in aging, it shows that color shifts with aging time. Regarding the blue fluorescence and green phosphorescence devices, they exhibit similar electrical-optical characteristic and degradation behaviors in experiments.

### **Modeling: Data-counting model, Electro-optical model, and Correlation model**

- a) The data-counting model provides a feasible method for evaluating the degradation during operation quantitatively. In this model, the contributions of coulombic degradation law, current-amplitude and thermal acceleration effects on the efficiency decay are considered for the accumulation stress on OLED in aging. A unified degradation profile was extracted. Through counting the accumulation stress on OLED, the corresponding efficiency decay can be derived from the degradation profile. Compensation based on the model can be further implemented. The model parameters are extracted from numbers of samples. It also allows predicting the efficiency decay under various driving conditions. In the display system, the accumulation stress is proportional to the gray values (GV) ever displayed on a pixel. Thus, the method is called as data counting.
- b) The electro-optical model is based on an equivalent circuit. Multiple diodes with resistance are approximately equivalent to the OLED, in considering the multi-layer structure and emitting process. The current flow through the device is split into internal leakage flow, radiative and non-radiative recombination flow. The effective current efficiency is then attributed to internal current-flow distribution, with the dependency on operation point. The equivalent circuit simulates the electrical-optical characteristic of OLED, as observed in experiments (e.g. the rectification effect, roll-off effect). Based on the equivalent circuit, the degradation behaviors in electrical-optical characteristic are modeled by the drifting parameters. The efficiency decay in the operation range is simulated with the equivalent model. For prediction and compensation, through determining the deteriorated parameters

in the equivalent circuit, the electrical-optical performance in aging, with the dependence on operation point, can be quantitatively derived.

- c) The correlation model is aimed to derive the current efficiency decay with the measurable electrical value. The correlation between efficiency decay and current drift was analyzed and identified with the experiment results. A simple linear correlation profile was firstly extracted. Furthermore, the correlation depends on operation point, indicating partial correlation between optical degradation and electrical degradation. The correlation at higher voltage is indeed weaker than at low operation point. To evaluate the degraded efficiency in wide operation range, the correlation model is combined with the equivalent circuit. From the full correlation profile at a low operation point, the aging parameter responsible for the efficiency decay can be determined. Thereafter, the efficiency decay at each operation point can be derived with the equivalent circuit (especially, for the higher emitting range).

Three models presented in the thesis, provide the potential and feasible approach to determine the degradation in quantity during operation. However, they have their own strength and weakness in the practical applications. For the data-counting model, the efficiency decay is evaluated from a degradation profile through counting the accumulation stress on OLED. Nevertheless, an error accumulation may occur in compensation. The accumulation stress on OLED is counted during operation, and a deviation may accumulate in long-term operation, resulting in an accumulation error for degradation prediction and compensation. Besides that, the decay profile depends on the operation point. Multiple decay profiles are needed for various operation points in the display system. This may not be an issue for the digital driving scheme (fixed voltage), but should be of more concern in an analog driving system. In comparison to the data-counting model, the correlation model delivers evaluation of the efficiency decay with measurable electrical value, seen as a feedback approach. It can overcome the issue of error accumulation in the data-counting model, and deliver more reliable result in strongly aged states. The real value of the electro-optical model is that the electrical-optical performance in a wide operation range can be quantitatively derived after a period of aging, by evaluating the aging parameters in the equivalent circuit. The equivalent circuit considers OLED multi-layer structure and the emitting process (OLED as grey-box device).

### **Prediction and compensation**

Based on the developed models, the prediction and compensation of degradation have been implemented on OLED devices and the digital AMOLED display. The parameters of models were extracted from numbers of OLED samples in the previous aging test. To predict the efficiency decay, the driving factors such as operation time, driven currents as well as ambient temperature were recorded for the data-counting model; the internal aging parameters of equivalent circuit were evaluated for the electro-optical model; and the current drift was measured in the correlation model. The luminance loss is attributed to the decays in current flow and efficiency in the digital driving system. The efficiency decay was derived from models, while the current drop was directly measured. Based on the quantified degradation in operation, the corresponding compensation has been finally implemented by adjusting the gray value of pixels on display (and the duty-cycle time on OLED devices). The results show that the models effectively predict the efficiency decay during operation. The luminance loss is compensated with a low deviation. The non-uniformity due to differential aging states is eliminated. Image sticking artifact on AMOLED display has been thus suppressed with free sensitivity in human eyes.

The compensation approach not just applies to the digital driving system, but also the analog driving display system. During operation, the OLED aging states are evaluated, and then the compensation factors are determined for all pixels. Through adjusting the grey value in pixel pipeline, pixel-wise compensation can be finally implemented, addressing the aging artifact on AMOLED display. Due to a wide range of operation points, the dependency of compensation on operation point should be more concerned in the analog driving scheme.

In the practical applications, a combination of three models in the driving system may deliver more reliability and effectiveness to derive the degradation on OLED. On one side, a combination of the data-counting model and correlation model can be applied for a long-term aging. The data-counting method is used in the beginning phase of aging (e.g. 10, 20% decay), while the correlation approach (electrical measure) is responsible for strongly aged phase (e.g. 30%, or even more). On another side, the electro-optical model could be combined with the data counting & correlation model. The aging parameters are determined by the counted accumulation stress or measurable electrical value. The efficiency decay at each operation point is then derived by the equivalent circuit.

## 8.2 Outlook

Research at OLED degradation is an ongoing effort. Due to time constraints, more research could not be explored, and presented in this thesis. Here, we outline the potential research points as future work.

AC condition and reverse bias also play roles in the OLED degradation. In this thesis, these conditions are fixed in the digital driving scheme. To achieve more effectiveness, these impact factors may be considered in the accumulation stress formula of data-counting model.

The equivalent model is worth to be further improved, especially for lower operation range. The leakage branch also experiences decay in aging, influencing the efficiency decay at a very low operation point. In the analog driving scheme, it may require more attention. Replacing the leakage resistance with diode may make the simulation more effective.

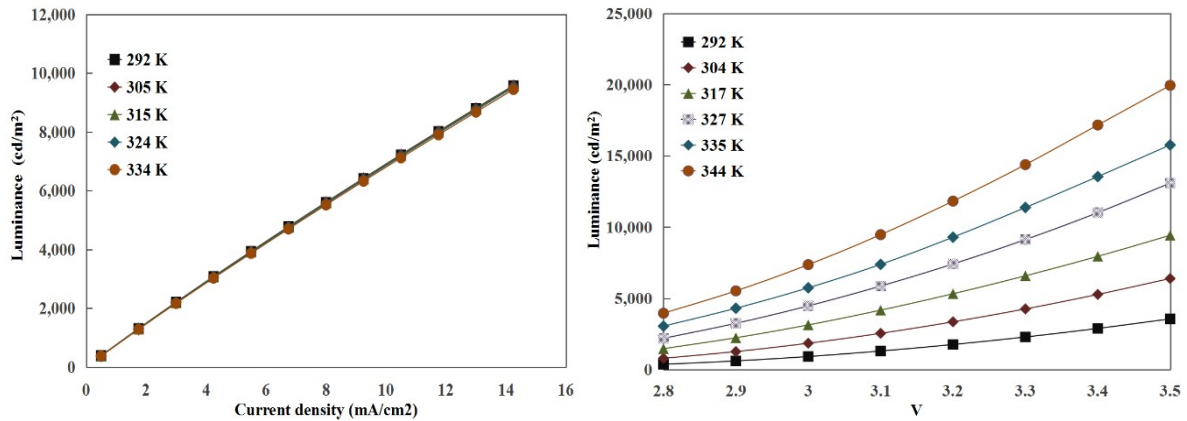
Regarding the evaluation of aging parameter in the correlation method, the challenge is to detect the suitable operation point, at which a full correlation between the efficiency decay and current drift is formed. More OLED samples are needed to be tested.

For the implementation of compensation on products, a combination of three models may deliver more reliability and effectiveness for deriving OLED degradation, in considering the model's strength and weakness. Besides that, compensation algorithm with all three primary channels may be necessary for AMOLED panels. The sensing circuit and algorithm might be integrated into the driving system (on-chip/glass).

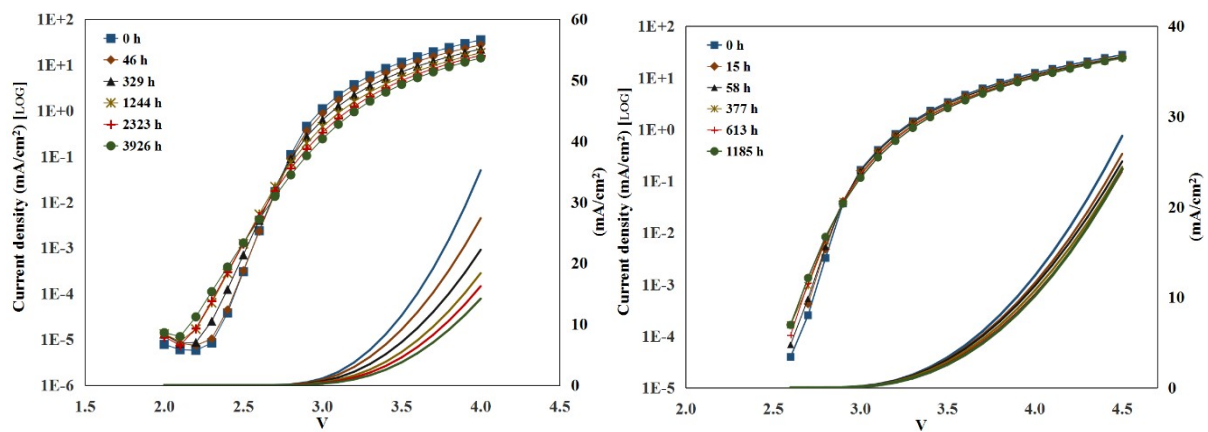
Aging compensation may mitigate the main weakness of AMOLEDs and significantly extend their lifetime. The AMOLEDs with longer lifetime can dominate more potential markets and fulfill the high expectations for the new generation display.



## 9 Appendix

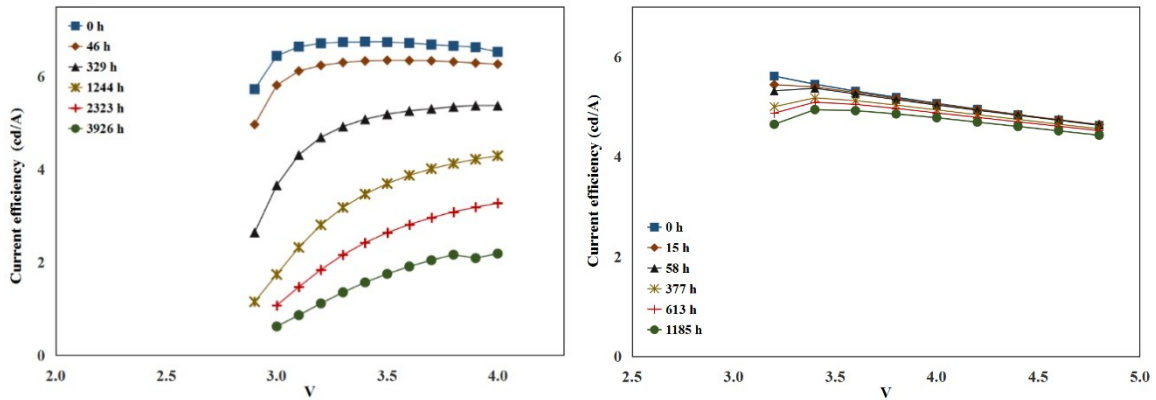


9-1 Luminance versus operation points at various temperature: Luminance-current curves for the analog driving scheme (left) and Luminance-voltage curves for the digital driving scheme (right).



9-2 Current-Voltage (I-V) curve drift with aging time. Novaled fluorescence blue (left); Merck fluorescence blue (right).

## 9. Appendix



9-3 Current Efficiency-Voltage (Eff-V) curve drift with aging time. Novald fluorescence blue (left); Merck fluorescence blue (right).

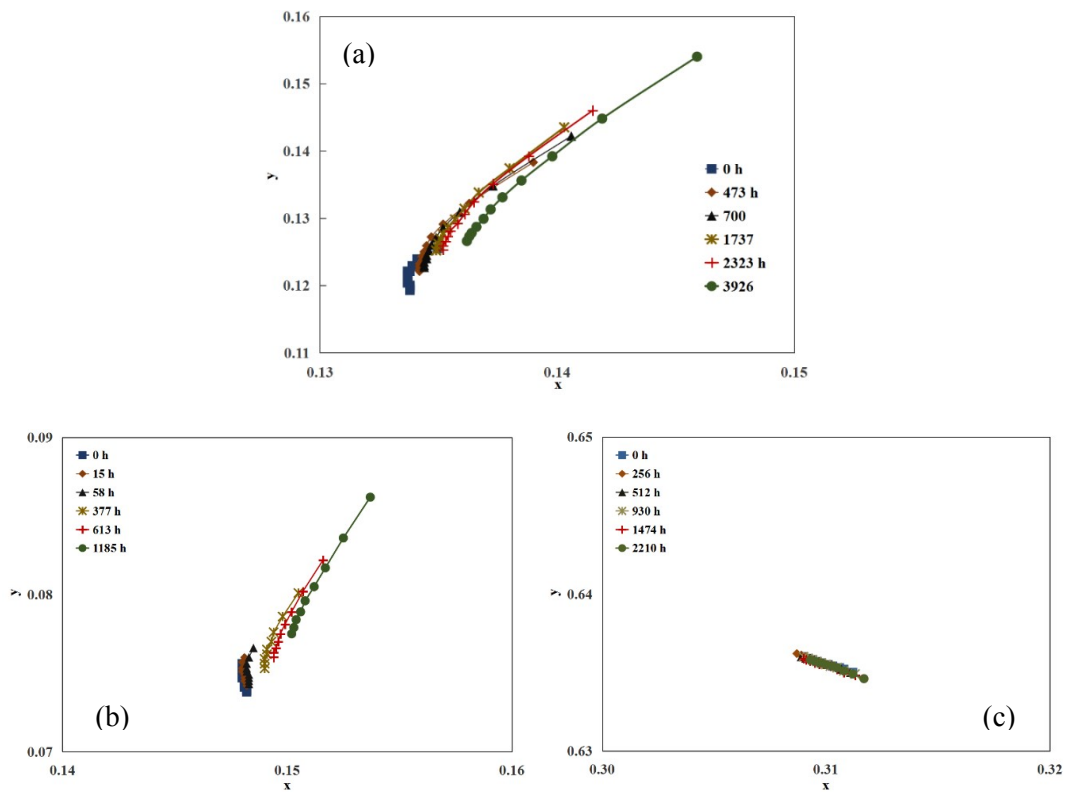
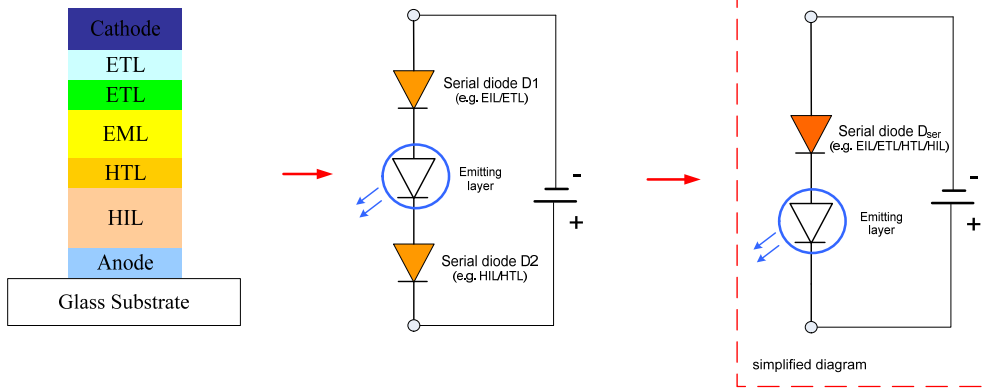
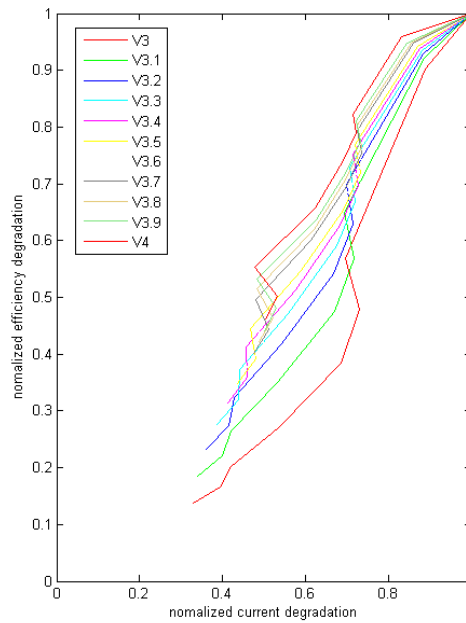


Figure 9-4 Color shift with aging time (in operation range). (a) Novald blue OLED samples (b) Merck blue OLEDs (c) Merck green OLED samples.



$$\left\{ \begin{array}{l} I_{ser} = I_{S_{ser}} \left[ \exp \frac{U_{ser}}{n_{ser} V_t} - 1 \right] \\ n_{ser} = n_1 + n_2 \\ I_{S_{ser}} = I_{S_1}^{n_1/(n_1+n_2)} * I_{S_2}^{n_2/(n_1+n_2)} \end{array} \right.$$

9-5 In the equivalent circuit of multi-layer OLED device, two serial diodes can be merged into one serial diode.



9-6 Correlation between the efficiency decay and current drift in the aging process. Data from Novaled blue OLEDs.



## 10 List of abbreviations

<b>AMOLED</b>	Active Matrix Organic Light Emitting Diode
<b>ASIC</b>	Application Specific Integrated Circuit
<b>CIE</b>	Commission Internationale de l'éclairage
<b>COF</b>	Chip On Film
<b>COG</b>	Chip On Glass
<b>CMOS</b>	Complementary Metal Oxide Semiconductor
<b>DAC</b>	Digital to Analog Converter
<b>DC</b>	Direct Current power supply
<b>DRAM</b>	Dynamic Random-Access Memory
<b>EQE</b>	External Quantum Efficiency
<b>FPC</b>	Flexible Printed Circuit
<b>FPGA</b>	Field Programmable Gate Array
<b>HDMI</b>	High Definition Multimedia Interface
<b>HUD</b>	Head Up Display
<b>HMD</b>	Head Mounted Display
<b>IQE</b>	Internal Quantum Efficiency
<b>IC</b>	Integrated Circuit
<b>ITO</b>	Indium Tin Oxide

## 10. List of abbreviations

---

<b>OP</b>	Operation point
<b>LCD</b>	Liquid Crystal Display
<b>LTPS</b>	Low Temperature Polycrystalline Silicon
<b>LUT</b>	Look-Up Table
<b>OLED</b>	Organic Light Emitting Diode
<b>OP</b>	Operation Point
<b>PCB</b>	Printed Circuit Board
<b>PCM</b>	Pulse Code Modulation
<b>PDM</b>	Pulse Density Modulation
<b>PDP</b>	Plasma Display Panel
<b>PMOLED</b>	Passive Matrix Organic Light Emitting Diode
<b>PMOS</b>	P-Channel Metal Oxide Semiconductor
<b>PWM</b>	Pulse Width Modulation
<b>QVGA</b>	Quarter Video Graphics Array
<b>SID</b>	Society for Information Display
<b>SMOLED</b>	Small Molecular OLED
<b>TFT</b>	Thin Film Transistor
<b>TV</b>	Television
<b>UART</b>	Universal Asynchronous Receiver Transceiver

## 11 List of figures

Figure 1-1 OLED display applications including mobile phones, TVs, autos, VR/AR. (Photos from reuters, OLED-info, and engadget.com).....	2
Figure 1-2 Lifetime improvement of OLEDs over the last decades: (a) fluorescent and (b) phosphorescent, including red, green, blue, and white OLEDs [Scholz2015].....	3
Figure 1-3 The differential aging of pixels on OLED panel. Red dots denote aged pixels (more stressed), and gray dots are as pristine pixels (or less stressed).....	4
Figure 1-4 Image sticking artifact on Samsung Galaxy S6 (left) and on Visionox AMOLED panel (right).....	4
Figure 2-1 (a) Basic sandwich structure of OLED device; (b) Simplified diagram of OLED device operation.....	8
Figure 2-2 Energy level and energy conversion process diagram of an organic molecule [Schm2013].....	9
Figure 2-3 An example of multi-layer structure (left) and schematic energy level (right) for OLED devices. (Based on [Tsuji2017]).....	10
Figure 2-4 Schematic illustration of the light emission process and key factors for the external quantum efficiency of organic light-emitting diodes. (Based on [Schm2013, Tsuji2017])....	11
Figure 2-5 Active-matrix OLED display (AMOLED) [Wik.D2018].....	17
Figure 2-6 (a) 2T1C Pixel circuit [Ko2011] (b) analog driving scheme (c) digital driving scheme.....	18
Figure 2-7 An image is decomposed into several subframes in the digital driving scheme [Xu2012].....	18

## 11. List of figures

---

Figure 3-1 Photos of OLED devices from Novaled and Merck.....	22
Figure 3-2 (a) The schematic diagram of measurement setup for OLED devices.....	23
Figure 3-2 (b) the photos of measurement setup for OLED devices.....	24
Figure 3-3 Current-voltage (I-V) curve in semi-log at room temperature. Data from Merck green OLED devices.....	25
Figure 3-4 (a) Luminance-voltage (L-V) curve at room temperature (b) Current efficiency-voltage (Eff-V) characteristic. Merck green OLED devices.....	26
Figure 3-5 Experimental IVL (left) and current efficiency (right) curves for Merck and Novaled OLED samples.....	29
Figure 3-6 The chromaticity of OLEDs (Merck and Novaled) in CIE1931.....	30
Figure 3-7 CIE coordinates of OLEDs at various operation points.....	31
Figure 3-8 I-V curve shift with temperature (left); current flow at given operation points increases with temperature (right). Data from Merck green OLED devices.....	32
Figure 3-9 (a) Current efficiency versus current density curve shift with temperature (b) the current efficiency at given operation points decreases with temperature (c) Current efficiency versus voltage curve shift with temperature. Merck green OLED devices.....	34
Figure 3-10 color shift with variation of temperature. Data from Merck green OLED devices.....	35
Figure 3-11 Current-voltage (I-V) curve drift with aging time. Primary axis in semi-log, and secondary axis in linear scale. Merck Green OLED sample is stressed at approx. 2500 nits at 32°C.....	37
Figure 3-12 Current efficiency versus voltage at various aging states.....	38
Figure 3-13 Luminance-voltage (L-V) curves at various aging states.....	39

Figure 3-14 (a) Current efficiency of OLEDs decays with aging time under various driving current flows (b) current efficiency decays with aging time under various ambient driving temperature.....	40
Figure 3-14 (c) current efficiency decays with aging time under multiple driving conditions. Data from Merck green OLED devices.....	41
Figure 3-15 (a) Current decreases with aging time under DC and AC driven conditions (b) Current efficiency decreases with aging time under DC and AC driven conditions. Data from Merck green OLED devices.....	42
Figure 3-16 Color shifts with aging time. Novaled blue OLED samples.....	43
Figure 4-1 The luminance decays with operation time.....	46
Figure 4-2 A simple schematic diagram that charge are injected into the device, which induces the OLED decay with accumulation in this process .....	48
Figure 4-3 Current efficiency decay (normalized) versus total injected charge (Q) into devices at various stressing current amplitudes. Decay exponent $\alpha=0.7926$ .....	49
Figure 4-4 $Q_{80}$ versus Current amplitude in log scale.....	51
Figure 4-5 Current efficiency decay vs Q for OLEDs aged under various ambient temperature (18, 32, 48 °C). Decay exponent $\alpha=0.7926$ .....	52
Figure 4-6 $Q_{80}$ versus temperature with $E_a = 0.62$ eV.....	54
Figure 4-7 Multiple decay curves for OLEDs stressed under various drive currents in experiment (left); unified decay profile for various drive currents based on derivation in the model (right).....	56
Figure 4-8 Multiple decay curves for OLEDs stressed under various ambient temperatures in experiment (left); unified decay profile for various ambient temperature based on derivation in the model (right).....	56

## 11. List of figures

---

Figure 4-9 Multiple decay curves for OLED stressed under multiple driving conditions in experiment (left); unified degradation profile for multiple driving conditions based on model (right).....	58
Figure 5-1 Structure and equivalent circuit of an OLED device.....	62
Figure 5-2 Dependency of current efficiency on operation point. Merck green OLED sample.	63
Figure 5-3 Electrical-optical characteristic of an OLED (a) Current-voltage (I-V) curve in semi-log (b) Current efficiency vs voltage curve (Eff-V).....	66
Figure 5-4 Simulation of the electrical-optical characteristic of OLED (a) Current-voltage curve in semi-log (b) Current efficiency vs voltage curve .....	67
Figure 5-5 Measured and simulated electrical-optical Characteristic at two states in the aging process. (a) Semi-log current-voltage curves; (b) current efficiency vs voltage curves. The empty symbols (squares, circles) are experimental data; the solid lines represent the simulations.....	69
Figure 5-6 Extracted parameters from OLED aging test are plotted with aging time (hours). (a) $I_{s\_emit}$ (b) $I_{s\_ser}$ (c) serial resistance R .....	70
Figure 5-7 (a) Multiple decay curves for $I_{s\_emit}$ at various driving conditions (b) an unified decay profile for $I_{s\_emit}$ at various driving conditions.....	72
Figure 5-8 Internal current-flow distribution over operation range: leakage current flow (red solid line), emissive current flow (green solid line), and non-emissive current flow (purple solid line). Data from Green Merck OLEDs.....	74
Figure 5-9 Internal voltage distribution over operation range: voltage on emission layer (purple solid line), on serial resistance R (red solid line), and on serial diode (blue solid line).....	74
Figure 5-10 The simulation of emissive flow distribution with deterioration of parameter $I_{s\_emit}$ in the aging process .....	75

---

Figure 6-1 Correlation between the efficiency decay and current drift in the aging process. Data from Merck blue OLEDs.....	79
Figure 6-2 Relative linear correlation between the efficiency decay and current drift.....	80
Figure 6-3 Correlation depends on operation point.....	81
Figure 6-4 Unified degradation correlation for various driving conditions. At lower operation point (i.e. 3.2V).....	84
Figure 7-1 Unified degradation prediction profile for multi-operation conditions in the data-counting model. Merck green OLED devices: $\alpha = 0.7926$ , $\beta = 2.122$ and $E_a = 0.62$ .....	88
Figure 7-2 The current amplitude (DC) decreases with aging time in the digital driving scheme.....	90
Figure 7-3 Experimental current efficiency decay and prediction results with model on green OLED sample.....	91
Figure 7-4 Compensations were applied on green OLED device during operation.....	92
Figure 7-5 OLED as gray-box DUT in operation.....	93
Figure 7-6 (a) unified decay profile $f_1$ for the aging parameter $I_{s\_emit}$ (b) unified decay profile $f_2$ for the aging parameter $I_{s\_ser}$ .....	94
Figure 7-7 Experimental current efficiency decay and prediction results with the electro-optical model and data-counting model on green OLED sample.....	95
Figure 7-8 Digital AMOLED display prototype and test setup. 1) Visionox 2.8" QVGA panel 2) Digital driving platform with FPGA + discrete PCB board 3) ELDIM UMaster camera.....	97
Figure 7-9 The 2.8" QVGA AMOLED panel from Visionox.....	98
Figure 7-10 Chromaticity of Visionox panel in color space, with comparison to Rec.709.....	99
Figure 7-11 Image data flow with compensation in a digital driving AMOLED system.....	103

## 11. List of figures

---

Figure 7-12 Image sticking on AMOLED display (blue OLEDs).....	105
Figure 7-13 Aged pixels with and without compensation.....	106
Figure 7-14 Photographs of uncompensated (left) and compensated (right) display for blue color image).....	107
Figure 7-15 Luminance distribution on display without (left) and with applying compensation (right).....	107
Figure 7-16 A test image displayed before (left) and after applying compensation (right).....	108

## 12 References

**Anton2004** D. Antonio-Torres, P. F. Lister, P. Newbury. “Modelling of a Compensation Scheme for OLED Degradation”. *SID Symposium Digest* 35(1), 1124-1127, 2004.

**Anton2005** D. Antonio-Torres, P. F. Lister, P. Newbury. “LUT-based compensation model for OLED degradation”. *Journal of the SID* 13(5), 435-441, 2005.

**Aziz2002** H. Aziz, Z. D. Popovic, N. Hu. “Organic light emitting devices with enhanced operational stability at elevated temperatures”. *Appl. Phys. Lett.* 81, 370, 2002.

**Baiju2011** M.R. Baiju. “Organic Light Emitting Diodes: Device Physics and Effect of Ambience on Performance Parameters”. In: *Optoelectronics-Devices and Applications*, 2011.

**Chen2012** X. Chen, B. Liu, Y. Chen, M. Zhao, C.J. Xue. X. Guo. “Active Compensation Technique for the Thin-Film Transistor Variations and OLED Aging of Mobile Device Displays”. *IEEE/ACM international conference on computer-aided design* 516-522, 2012.

**Fan2017** R. Fan, X. Zhang, Z. Tu, T. Hwang, J. H. Fu, P. Lu, M. Jou. “Equivalent Lifetime Method to Improve OLED Luminance Degradation”. *SID Symposium Digest* 48(1), 1999-2002, 2017.

**Fery2005** C. Fery, B. Racine, D. Vaufrey, H. Doyeux, and S. Cinà. “Physical mechanism responsible for the stretched exponential decay behavior of aging organic light-emitting diodes”. *Appl. Phys. Lett.* 87, 213502, 2005.

**Gasp2015** D. J. Gaspar and E. Polikarpov. “OLED Fundamentals”. CRC Press, ISBN: 978-1466515185, 2015.

**Gieb2008** N. C. Giebink and S. R. Forrest. “Quantum efficiency roll-off at high brightness in fluorescent and phosphorescent organic light emitting diodes”. *Phys. Rev. B* 77, 235215, 2008.

**Haldi2008** A. Haldi, A. Sharma, W. J. Potscavage Jr., B. Kippelen. “Equivalent circuit model for organic single-layer diodes”. *Journal of Applied Physics* 104, 064503, 2008.

**Ignis2015** A. Nathan and G. Chaji. “OLED Luminance Degradation Compensation”. US Patent 9,125,278, 2015.

**Ignis2016** G. Chaji, J. M. Dionne, Y. Azizi, J. Jaffari, A. Hormati, T. Liu, V. Muravin, J. Soni, N. Zahirovic, and S. Alexander. “Display System with Compensation Techniques and/or Shared Level Resources”. US Patent 2016/0027382A1, 2016.

**Ishii2002** M. Ishii and Y. Taga. “Influence of temperature and drive current on degradation mechanisms in organic light-emitting diodes”. *Appl. Phys. Lett.* 80, 3430, 2002.

**Jiang2015** X.Jiang, P.Volkert and C.Xu. “Degradation Behavior of blue OLEDs”. *Proceedings, SID Eurodisplay 46(S1)*, 62, 2015.

**Jiang2016** X.Jiang and C.Xu. “Data-counting Model or Empirical Prediction of OLED Degradation”. *Proceeding, IDW, OLED1-3*, 2016.

**Jiang2018** X. Jiang and C. Xu. “An Electro-optical OLED Model for Prediction and Compensation of AMOLED Aging Artifacts”. *SID Symposium Digest* 49(1), 441-444, 2018.

**Kana2016** S.P. Kanakasundaram. “Characterization and Compensation of Temperature Related Image Artifacts in a Digitally Driven AMOLED Display System”. Master Thesis, Saarland University, 2016.

**Kali2002** J. Kalinowski, W. Stampor, J. Męzyk, M. Cocchi, D. Virgili, V. Fattori, P. D. Marco. “Quenching effects in organic electrophosphorescence”. *Phys. Rev. B* 66, 235321, 2002.

**Kim2011** C.H. Kim, O. Yaghmazadeh, Y. Bonnassieux, and G. Horowitz. “Modeling the low-voltage regime of organic diodes: Origin of the ideality factor”. *Journal of Applied Physics* 110, 093722, 2011.

**Kim.H2007** H. Kim<sup>1</sup>, S. Kim, S. W. Chang, D. Lee<sup>2</sup>, D. Jeong, H. K. Chung, Y. Hong. “Frequency Dependence of OLED Voltage Shift Degradation”. *Digest of IMID* 38(3), 1108-1111, 2007.

**Kim.H2012** H. Kim, S. Kim, Y. Hong. “Frequency Dependency of Multi-layer OLED Current Density-voltage Shift and Its Application to Digitally-driving AMOLED”. *Journal of the Optical Society of Korea* 16(2), 181-184, 2012.

**Kobrin2003** P. Kobrin, E. Boehmer, P. King, R. Fisher, S. Robinson, P. Green. “Time Dependence of OLED Luminance”. *SID Symposium Digest* 34(1), 539-541, 2003.

**Ko2011** S. H. Ko. “Organic Light Emitting Diode: Material, Process and Devices”. INTECH Open Access Publisher, ISBN: 9533072733, 9789533072739, 2011.

**Kuik2012** M. Kuik, J. A. Kostera, A. G. Dijkstrab, G. A. H. Wetzelaera, P.W.M.Blom. “Non-radiative recombination losses in polymer light-emitting Diode”. *Organic Electronics* 13(6), 969-974, 2012.

**Lee2014** K-Yu. Lee, Y-P. Hsu, P. C. P. Chao, W-D. Chen. “A New Compensation Method for Emission Degradation in an AMOLED Display via an External Algorithm, New Pixel Circuit, and Models of Prior Measurements”. *Journal of Display Technology* 10(3), 189-197, 2014.

**Mahm2012** A. Mahmoud, F. Jaiser, S. Bagnich, T. Unger, J. Blakesley, A. Wilke, D. Neher. “Electrical and Optical Simulations of a Polymer-Based Phosphorescent Organic Light-Emitting Diode with High Efficiency”. *Journal of Polymer science* 50(22), 1567-1576, 2012.

**Mats2008** Y. Matsueda, D-Y. Shin, H-K. Chung. “AMOLED Technologies for Uniform Image and Sufficient Lifetime of Image Sticking”. *SID Symposium Digest* 39(1), 9-12, 2008.

**Meer2006** R. Meerheim, K. Walzera, M. Pfeiffer, K. Leo. “Ultrastable and efficient red organic light emitting diodes with doped transport layers”. *Appl. Phys. Lett.* 89, 061111, 2006.

**Moraes2015** I. R. Moraes, S. Scholz, M. Hermenau, M. L. Tietze, T. Schwaba, S. Hofmanna, M. C. Gathera1, K. Leo. “Impact of temperature on the efficiency of organic light emitting diodes”. *Organic Electronics* 26,158-163, 2015.

**Naka2014** H. Nakanotani, T. Higuchi, T. Furukawa, K. Masui, K. Morimoto, M. Numata, H. Tanaka, Y. Sagara, T. Yasuda, C. Adachi. “High-efficiency organic light-emitting diodes with fluorescent emitters”. *Nature Communications* 5:4016, 2014.

**Niu2016** Q. Niu, A. H. Wetzelaer, P. W. M. Blom, N. I. Craciun. “Modeling of Electrical Characteristics of Degraded Polymer Light-Emitting Diodes”. *Advance Electronic Materials* 2(8), 2016.

**Niu2017** Quan Niu. “Electrical Degradation of Polymer Light-Emitting Diodes”. Dissertation, Max-Planck Institute for Polymer Research, Johannes Gutenberg University, 2017.

**Nowy2009** S. Nowy, W. Ren, J. Wagner, J. A. Weber, W. Brütting. “Impedance spectroscopy of organic hetero-layer OLEDs as a probe for charge carrier injection and device degradation”. *Proceedings of SPIE* 7415, 2009.

**Nowy2010** S. Nowy, W. Ren, A. Elschner, Wi. Lövenich, W. Brütting. “Impedance spectroscopy as a probe for the degradation of organic light-emitting diodes”. *Journal of Applied Physics* 107, 054501, 2010.

**Oh2015** K. Oh, S-K. Hong, O-K. Kwon. “Lifetime Extension Method for Active Matrix Organic Light-Emitting Diode Displays Using a Modified Stretched Exponential Decay Model”. *IEEE Electron Device Letters* 36(3), 277-279, 2015.

**Parker1999** I. D. Parker and Y. Cao. “Lifetime and degradation effects in polymer light-emitting diodes”. *Journal of Applied Physics* 85, 2441, 1999.

**Rein2007** S. Reineke, K. Walzer and K. Leo. “Triplet-exciton quenching in organic phosphorescent light-emitting diodes with Ir-based emitters”. *Phys. Rev. B* 75, 125328, 2007.

**Scholz2015** S. Scholz, D. Kondakov, B. Lüssem, K. Leo. “Degradation Mechanisms and Reactions in Organic Light-Emitting Devices”. *Chem. Rev.* 115 (16), 8449–8503, 2015.

**Schm2013** T. Schmidt. “Photophysics of organic Light-Emitting diodes-Device efficiency and degradation processes”. Dissertation, Universität Augsburg, 2013.

**Schm2015** T. Schmidt, L. Jäger<sup>1</sup>, Y. Noguchi, H. Ishii, W. Brütting<sup>1</sup>. “Analyzing degradation effects of organic light-emitting diodes via transient optical and electrical measurements”. *Journal of Applied Physics* 117, 215502, 2015.

- So2010** F. So and D. Kondakov. “Degradation Mechanisms in Small-Molecule and Polymer Organic Light-Emitting Diodes”. *Advanced Materials* 22(34), 3762-3777, 2010.
- Soh2006** Soh, Chihao Xu. “Dependence of OLED Display Degradation on Driving Conditions”. *SID MID Europe*, 2006.
- Suo2008** Fan Suo, J. S. Yu, W.Z. Li, S. L. Lou, D. Jing, Y. D. Jiang. “Study on temperature characteristics of organic light-emitting diodes based on tris-(8-hydroxylquinoline)-aluminum”. *Chinese Science Bulletin* 53(4), 624-631, 2008.
- Tang1987** C. W. Tang and S. A. Van Slyke. “Organic electroluminescent diodes”. *Appl. Phys. Lett.* 51, 913, 1987.
- Temp2014**, F. Templier. “OLED Microdisplays: Technology and Applications”. WILEY, ISBN: 978-1-848-21575-7, 2014.
- Tsuji2017** T. Tsujimura. “OLED Display Fundamentals and Applications”. WILEY, ISBN: 9781119187318, 2017.
- Van1996** S. A. Van Slyke, C. H. Chen, C. W. Tang. “Organic electroluminescent devices with improved stability”. *Appl. Phys. Lett.* 69, 2160-2162, 1996.
- Volk2014** P. Volkert and C. Xu. “Principle and validation of digital driving for active matrix organic light emitting diodes displays”. *Journal of the SID* 22(1), 43-54, 2014.
- Volk2015** P. Volkert, X.T. Jiang and C. Xu. “Characterization and compensation of OLED aging in a digital AMOLED system”. *Journal of the SID* 23(12), 570-579, 2015.
- Volk2017** P. Volkert. “Digital gesteuertes AMOLED-System: Konzeption, Entwicklung und Realisierung”. *Dissertation, Saarland University*, 2017.
- Weon2006** B. M. Weon, S. Y. Kim, J-L. Lee. “Evolution of luminance by voltage in organic light-emitting diodes”. *Appl. Phys. Lett.* 88, 013503, 2006.
- Wehr2015** S. Wehrmeister, L. Jäger, T. Wehlius, A. F. Rausch, T. C. G. Reusch, T. D. Schmidt, W. Brütting. “Combined Electrical and Optical Analysis of the Efficiency Roll-Off in Phosphorescent Organic Light-Emitting Diodes”. *Phys. Rev. Applied* 3, 024008, 2015.

- Wik2018** “OLED”, Wikipedia.org. <https://en.wikipedia.org/wiki/OLED>, 2018.
- Wik.A2018** “Arrhenius equation”, Wikipedia.org. [https://en.wikipedia.org/wiki/Arrhenius\\_equation](https://en.wikipedia.org/wiki/Arrhenius_equation), 2018.
- Wik.C2018** “Chromaticity”, Wikipedia.org. <https://en.wikipedia.org/wiki/Chromaticity>, 2018.
- Wik.D2018** “AMOLED”, Wikipedia.org. <https://en.wikipedia.org/wiki/AMOLED>, 2018.
- Wik.E2018** “Energy level”, Wikipedia.org. [https://en.wikipedia.org/wiki/Energy\\_level](https://en.wikipedia.org/wiki/Energy_level), 2018.
- Wik.L2018** “Luminance”, Wikipedia.org. <https://en.wikipedia.org/wiki/Luminance>, 2018.
- Wik.M2018** “Active matrix”, Wikipedia.org. [https://en.wikipedia.org/wiki/Active\\_matrix](https://en.wikipedia.org/wiki/Active_matrix), 2018.
- Xu2012** C.Xu, Y. Dobrev. “Digital Driving Method Utilizing Image Decomposition for Nonuniformity Compensation of AMOLED Display”. *IMID Digest* 63 (1), 475-476, 2012.
- Xu2017** C. Xu, P. Volkert, X.T. Jiang. “Acquiring longer AMOLED Lifetime with Digital Aging Compensation”. *SID Symposium Digest* 48(1), 207-210, 2017.
- Yahi2000** M. Yahiro, D. Zou, T. Tsutsui. “Recoverable degradation phenomena of quantum efficiency in organic EL devices”. *Synthetic Metals*, 111–112, 237–240, 2000.
- Yu2015** M-H. Yu, T-H. Tran, Y. P. Hsu, Paul C-P. Chao, K-Y. Lee, Y-H. Kao. “A new prediction model on the luminance of OLEDs subjected to different reverse biases for alleviating degradation in AMOLED displays”. *Microsystem Technologies* 21(12), 2771–2776, 2015.
- Zhao2012** B. Zhao, R. Huang, J. Bu, Y. Lu, Y. Wang, F. Ma, G. Xie, Z. Zhang, H. Du, J. Luo. “A new OLED SPICE model for pixel circuit simulation in OLED-on-silicon microdisplay design”. *Journal of Semiconductors* 33(7), 2012.
- Zoran2003** Zoran. D. Popovic, G. Vamvounis, H. Aziz, N-X. Hu. “OLEDs with enhanced high temperature operational stability”. *Proceedings of SPIE* 4800, 2003.

## 13 Publications

- [1] X. T. Jiang, P. Volkert, C. Xu. “Degradation Behavior of blue OLEDs”. Proceedings of SID Eurodisplay 46(S1), 62, 2015.
  
- [2] P. Volkert, X. T. Jiang, C. Xu. “Characterization and compensation of OLED aging in a digital AMOLED system”. Journal of the Society for Information Display 23(12), 570-579, 2015.
  
- [3] X. T. Jiang and C. Xu. “Data-counting Model for Empirical Prediction of OLED Degradation”. Proceedings of IDW, OLED1-3, 2016.
  
- [4] C. Xu, P. Volkert, X. T. Jiang. “Acquiring longer AMOLED Lifetime with Digital Aging Compensation”. SID Symposium Digest 48(1), 207-210, 2017.
  
- [5] X. T. Jiang and C. Xu. “An Electro-optical OLED Model for Prediction and Compensation of AMOLED Aging Artifacts”. SID Symposium Digest 49(1), 441-444, 2018.